NRL Report 8205

Liquid Surface Levitation Holography

Part 1 — Theoretical Analysis

ALFRED V. CLARK, JR.

Structural Mechanics Branch
Marine Technology Division

August 11, 1980

REPORT DOCUMENTATION PAGE		READ INSTRUCTIONS BEFORE COMPLETING FORM
1. REPORT NUMBER NRL Report 8205	2. GOVT ACCESSION NO. AD-A088 418	3. RECIPIENT'S CATALOG NUMBER
4. TITLE (and Subtitle) LIQUID SURFACE LEVITATION HOLOGRAPHY. PART 1 — THEORETICAL ANALYSIS		5. TYPE OF REPORT & PERIOD COVERED Interim Report on a continuing NRL Problem.
		6. PERFORMING ORG. REPORT NUMBER
7. AUTHOR(s) Alfred V. Clark, Jr.		8. CONTRACT OR GRANT NUMBER(s)
9. PERFORMING ORGANIZATION NAME AND ADDRESS Naval Research Laboratory Washington, D.C. 20375		10. PROGRAM ELEMENT, PROJECT, TASK AREA & WORK UNIT NUMBERS NRL Problem F01-25 Project RR023-03-45
11. CONTROLLING OFFICE NAME AND ADDRESS Office of Naval Research Arlington, VA 22217		12. REPORT DATE August 11, 1980
		13. NUMBER OF PAGES 108
14. MONITORING AGENCY NAME & ADDRESS(if different from Controlling Office)		15. SECURITY CLASS. (of this report) Unclassified
		15a. DECLASSIFICATION/DOWNGRADING SCHEDULE

16. DISTRIBUTION STATEMENT (of this Report)

Approved for public release; distribution unlimited.

17. DISTRIBUTION STATEMENT (of the abstract entered in Block 20, if different from Report)

18. SUPPLEMENTARY NOTES

19. KEY WORDS (Continue on reverse side if necessary and identify by block number)

Acoustic holography
Acoustic imaging
Surface properties

Nondestructive testing
Transfer functions

20. ABSTRACT (Continue on reverse side if necessary and identify by block number)

   The liquid surface levitation holography system has been analyzed, paralleling analyses by previous investigators but treating several new areas. Depth of focus and depth of field of the acoustic lens system are considered, accounting for differences in the acoustic properties of the imaging and object-tank fluids. The mechanical properties of the minitank membrane are shown to have three significant effects: multiple internal reflections of acoustic waves are enhanced

(Continued)

DD FORM 1473 EDITION OF 1 NOV 65 IS OBSOLETE
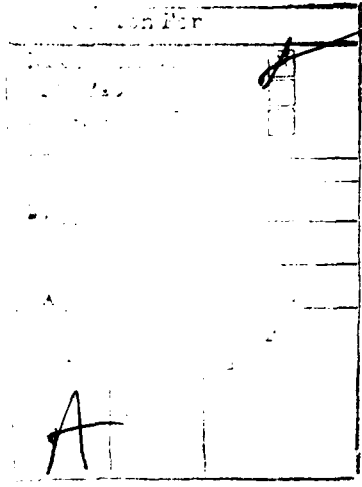1 JAN 73
S/N 0102-014-6601

i

20. ABSTRACT (Continued)

in the minitank, which causes the minitank transfer function to become oscillatory for large imaging-fluid depths; deformation of the membrane can degrade the focused acoustic image; and coupling between motions of the membrane and of the liquid surface occurs at low spatial frequencies. Possible coupling between the acoustic field quantities (pressure, density, and velocity) and the surface levitation field is shown to be negligible for a typical system. The low-spatial-frequency deformation (bulge) of the liquid surface is calculated for typical system parameters. The natural frequencies of oscillation of the surface are much less than the rate at which the surface is excited. Consequently the bulge builds up to a steady-state value.

CONTENTS

LIQUID SURFACE LEVITATION HOLOGRAPHY
PART 1 — THEORETICAL ANALYSIS

1. INTRODUCTION

Acoustic holography is an area of active research which finds application in such varied fields as imaging of organs of the human body and nondestructive testing. There are several methods of recording the acoustic image by holographic means; one of the more promising is to use the surface of a liquid as the recording medium. This method has the advantage of recording the entire field of view of the system and displaying the image in visual form in real time.

Liquid surface acoustic holography has been analyzed by a number of authors. Probably the most thorough analyses to date have been by Pille [1] and by Pille and Hildebrand [2]. A comprehensive treatment of the subject is given by Brenden [3]. The present work is a rigorous analysis of a typical liquid surface holography system and is a natural extension of the work of Pille and Hildebrand. It will for continuity repeat some of their major results, and it will also consider some interesting effects which have not been treated elsewhere.

The system to be analyzed is shown in Fig. 1. The object to be imaged is immersed in an acoustic fluid (usually water) contained in a large tank called the object tank. The object is insonified by a transducer, and the sound transmitted through the object is imaged by an acoustic lens system onto the surface of a smaller tank called a minitank that contains an imaging fluid. The imaging fluid is usually other than water. A second (reference) transducer emits an acoustic wave which enters the small tank and forms an interference pattern with the focused acoustic image at the liquid surface. The interference pattern levitates the liquid surface.

The surface is in effect a phase hologram, which is reconstructed with laser light. The light reflected from the surface is phase modulated due to the levitation and passes through an optical system consisting of lenses and a spatial filter. The optical system focuses the reconstructed image onto a ground-glass viewing screen.

The system consists of five subsystems and processes:

The acoustic lens system,

The minitank,

The interference of the acoustic image with the acoustic reference beam,

The response of the liquid surface,

The optical system.

1

SPATIAL FILTER   LENS   LASER

LIQUID SURFACE HOLOGRAM

REFLECTOR

OBJECT

OBJECT
TRANSDUCER   ACOUSTIC LENSES   REFERENCE
TRANSDUCER
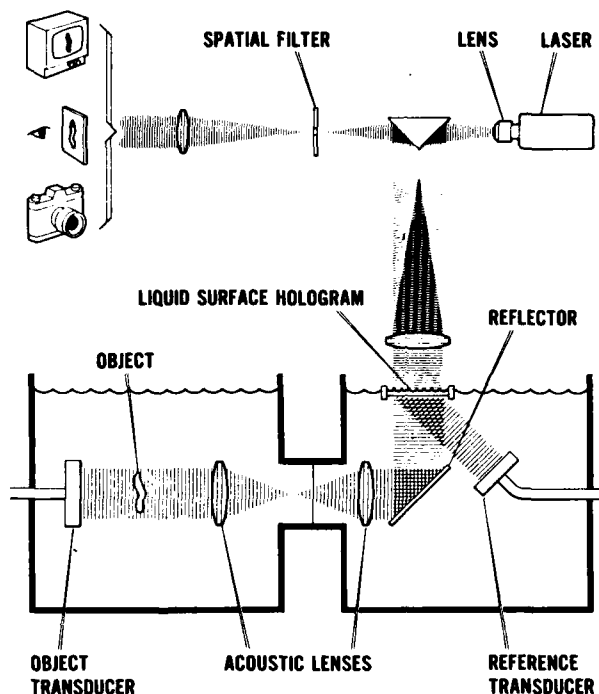
Fig. 1 — A typical system for liquid
surface acoustic holography

Following this introductory section are five main sections, each devoted to one of these five subsystems. The transfer function for each subsystem is derived, along with the conditions necessary for good imagery.

In the first main section (section 2) the input to the acoustic lens system is the distribution of acoustic sources which represents the object being imaged. The output is the velocity potential in the acoustic image at the liquid surface of the minitank. This ignores internal reflections in the minitank and the mechanical properties of the thin membrane which is at the bottom of the minitank and separates the two fluids. The transfer function does account for defocusing.

In section 3 the input is the velocity potential in the focused acoustic image. The output is the corresponding acoustic particle velocity at the liquid surface of the minitank. Now multiple internal reflections in the minitank as well as the effect of the membrane are taken into account.

In section 4 the interference generated by the reference transducer and the focused image is considered. The interference upshifts the spatial frequencies in the velocity field associated with the acoustic image and acts as a driving pressure to levitate the liquid surface.

The interference pattern arises because of the momentum flux per unit area, which is a nonlinear effect. Accordingly section 5 begins with a brief review of some aspects of nonlinear

acoustics. It is the vertical component of the steady momentum flux per unit area, called the radiation pressure, which acts as a driving pressure for the levitation of the surface. The transfer function for the liquid surface is derived, with the input being a pulse of radiation pressure and the output being the levitation of the liquid surface.

The transfer function is time dependent. After the pulse of radiation pressure excites the surface, there is a time t_s when the transfer function is constant over the bandwidth of spatial frequencies associated with the focused image. The laser samples the liquid surface at this time. Because the imaging fluid has viscosity, the levitation caused by the interference of the acoustic image and reference beam decays. When the levitation has become small, another pulse of radiation pressure excites the surface, and after another delay of duration t_s the laser again samples the surface. This process is repeated rapidly enough to form a flicker-free optical reconstruction.

The reflected laser light is shown to consist of a multiplicity of beams (diffracted orders). The purpose of the optical train is to spatially filter the reflected light and thus extract the beam carrying information about the acoustic image and to focus this beam into an image suitable for observation by eye.

In section 6 the transfer function for the optical reconstruction is derived. The input is the height of the liquid surface, and the output is the optical disturbance.

The transfer functions for the various subsystems have been derived in Refs. 1 and 2. To maintain continuity, it is necessary to repeat some of the results of these previous analyses. The present work also considers the following topics, which have not been treated elsewhere in any detail:

● Defocusing and depth of field of the acoustic lens system are considered, accounting for difference in the minitank and object-tank fluids. It is found that the depth of field is typically a few acoustic wavelengths. The criterion for negligible defocusing is derived.

● The effects of the mechanical properties of the thin membrane separating the minitank from the object tank are considered. Three major effects are of interest here:

— The first is the effect of the membrane on the transmission and reflection coefficients appropriate to the interface between the imaging and object-tank fluids. These coefficients are used in calculating the transfer function for the minitank. For certain ratios of minitank depth to acoustic wavelength constructive (and destructive) interference can occur due to multiple internal reflections. This causes loss of fidelity in recording the acoustic image. Such interference is enhanced by the presence of the membrane. Furthermore the use of identical imaging and object-tank fluids causes the interference to become even more pronounced when the effect of the membrane is significant.

— The second interesting effect of the membrane is the possibility of coupling of its oscillation with those of the liquid surface. Previous investigations [1,2], have been based on the assumption of a rigid membrane; this is shown to be valid only when this coupling effect is negligible.

— The third effect is degradation of the focused image by membrane displacement. For typical minitank and object-tank fluids the membrane must not be displaced more than a fraction of an acoustic wavelength; otherwise the acoustic image can be distorted. This limitation on membrane displacement places an upper bound on the intensity in the acoustic field, calculated here for a typical system.

● The equations governing the motion of the fluids and the liquid surface are rigorously derived here from mass and momentum conservation. In general the equations are nonlinear. In order that the liquid surface faithfully record the acoustic image, the equation of motion of the surface must be linearized. This places another upper bound on permissible acoustic intensity, which also is calculated.

● Another consequence of the nonlinearity of the mass and momentum conservation equations is the possibility of coupling between the acoustic field and the field generated by motion of the surface. Such a coupling would seriously impair the fidelity of the recording process. It is shown that this coupling is negligible.

● The interference between the focused acoustic image and the reference beam produces a levitation of the surface containing information about the acoustic object; this levitation h_i can be considered "signal". There is an additional low-spatial-frequency "bulge" h_b, which can be thought of as "noise", since it causes an additional phase shift in the reflected light unrelated to the acoustic image. It is shown that for typical system parameters the bulge will reach a steady-state value, unlike the information-bearing levitation. This is unfortunate, since there is no time when the surface can be sampled to avoid the distortion caused by the bulge.

● The question of maximizing the "signal-to-noise" ratio h_i/h_b is also considered. In a typical imaging situation the ratio reaches a maximum when the velocity potential in the focused image equals that in the reference beam. For typical system parameters the ratio is of the order of 10^{-1}.

● The possibility of using several reflected orders of laser light to image phase objects is also explored. Since the optical reconstruction is viewed by eye (an intensity detector), phase objects will be invisible when only one order of reflected light is used in the optical reconstruction. However, by using two or more orders and allowing them to interfere, a fringe pattern is produced with phase shifts corresponding to the outline of the phase object.

2. ACOUSTIC LENS SYSTEM

2.1 Formation of an Acoustic Image

Consider the formation of an acoustic image by the acoustic lens system shown in Fig. 1. The acoustic energy from the object transducer passes into the object to be imaged and is diffracted, internally reflected, and attenuated. This distorted sound field emerges from the object and propagates through the acoustic lens system, which focuses it on the surface of the minitank.

Consider the situation shown in Fig. 2, where an object is placed in the $z' = 0$ plane and insonified by the object transducer. In the volume V, enclosed by the surface σ in the figure, the velocity potential is [4]
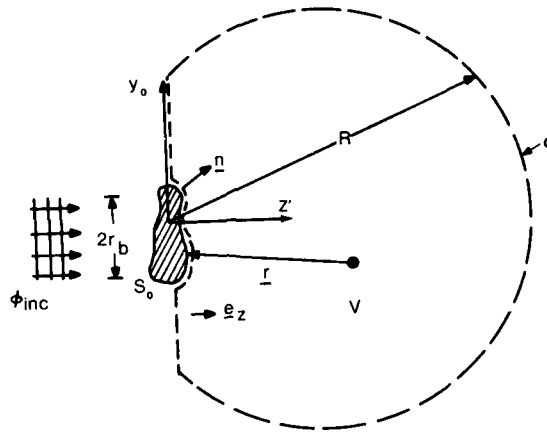
Fig. 2 — Quantities used in calculating the acoustic field due to
the presence of any acoustic object S_o

$$4\pi \phi_o(\mathbf{r}) = \int_\sigma \left[\phi_o(\sigma) \frac{\partial}{\partial n} \left(\frac{e^{ikr}}{r} \right) - \frac{e^{ikr}}{r} \frac{\partial \phi_o(\sigma)}{\partial n} \right] d\sigma. \tag{1}$$

The integration is performed over the surface σ. The quantity r is the magnitude of $\mathbf{r}$, a vector from a point in V to the surface σ, $\mathbf{n}$ is the unit normal vector pointing into V, and $n = |\mathbf{n}|$. A time factor $e^{-i\omega_a t}$ has been suppressed, where ω_a is the transducer frequency (with the subscript a indicating an acoustic quantity). The wavenumber k is given by ω_a/C, with C the sound speed in the object-tank fluid.

The assumptions inherent in (1) are:

- The fluid is inviscid and compressible;

- Body forces (such as gravity) are negligible within the fluid;

- The sound field sets up small perturbations about the equilibrium state of the fluid;

- There are no reflections; the fluid is assumed to be infinite in extent;

- The fluid flow is irrotational; that is, $\mathbf{v}_o = \nabla \phi_o$, where $\mathbf{v}_o$ is the particle velocity.

It can be shown that the integral over the hemispherical surface in Fig. 2 vanishes for large R. Assume that the object is placed in the near field of the transducer and that the transducer emits a beam of radius r_b. Then the region in the $z' = 0$ plane outside a circle of radius r_b does not contribute to the surface integration; only the insonified region contributes to the integral in (1).

As an approximate boundary condition let $\phi_o(\sigma, t) = S_o(\sigma)\phi_{inc}(\sigma, t)$ and $\partial \phi_o/\partial n = S_o(\partial \phi_{inc}/\partial n)$, where S_o is the object transmission function and ϕ_{inc} is the velocity potential in the incident beam. S_o accounts for any changes in amplitude and phase due to internal flaws, voids, changes in acoustic path lengths, etc. in the object.

5

Let r be much greater than λ_a, the acoustic wavelength. Then in (1),

$$\frac{\partial}{\partial n}\left(\frac{e^{ikr}}{r}\right) \cong ik\,\frac{\partial r}{\partial n}\,\frac{e^{ikr}}{r}.\tag{2a}$$

Furthermore, for an incident plane wave of the form $\phi_{inc} = A(x, y)\,e^{ikz}\,e^{-i\omega_a t}$,

$$\frac{\partial \phi_o(\sigma)}{\partial n} \cong ik\,\frac{\partial z}{\partial n}\,S_o(\sigma)\,\phi_{inc}(\sigma).\tag{2b}$$

Using these results in (1) gives

$$\phi_o = ik \int S_o(\sigma)\,\phi_{inc}(\sigma,\,t)\left(\frac{\partial r}{\partial n} - \frac{\partial z}{\partial n}\right)\frac{e^{ikr}}{4\pi r}\,d\sigma.\tag{3}$$

This shows that the field transmitted by the object is a superposition of secondary sources of strength $S_o\,\phi_{inc}$, with directivity pattern $\partial r/\partial n - \partial z/\partial n$, distributed over that part of the object surface insonified by the incident beam.

Equation (3) is difficult to deal with in the most general case, so the following simplifications are made. First the object is assumed planar, so that $\partial z/\partial n = 1$. Then attention is restricted to the field at points lying near the z' axis, so that $\partial r/\partial n \cong -1$. This reduces (3) to

$$\phi_o = \frac{-i}{\lambda_a} \int \psi_o(\sigma,\,t)\,\frac{e^{ikr}}{r}\,d\sigma,\tag{4}$$

where the source strength is ψ_o.

The sound field represented by (4) propagates from left to right through the acoustic lens system shown in Fig. 3. The lenses L_1 and L_2 are placed a distance $f_1 + f_2$ apart, where f_1 is the focal length of L_1, and f_2 is the focal length of L_2. For simplicity two-dimensional propagation will be considered; that is, the object is assumed to lie in the y_o plane, and L_1 and L_2 are cylindrical lenses. Generalizing to three dimensions would increase the complexity of calculations and add no physical insight.
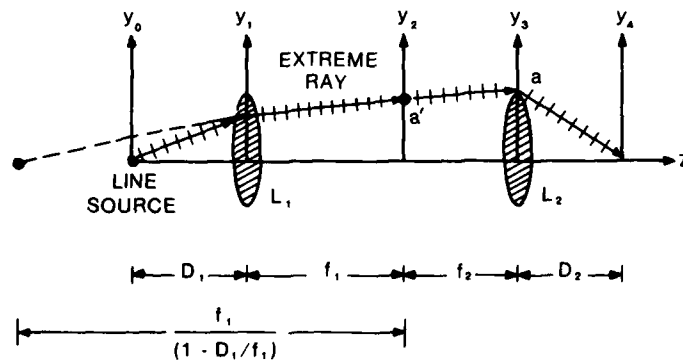

Fig. 3 — Acoustic lens system

For two-dimensional propagation, integrating (4) in the x direction (out of the plane of the paper in Fig. 2) gives [4]

$$\phi_o(y, z) = \frac{e^{-\pi i/4}}{2\sqrt{\lambda_a}} \int \frac{\psi_o(y_o) e^{ikr} dy_o}{\sqrt{r}}, \qquad r >> \lambda_a. \tag{5}$$

Assume that the sound field emerges from the object in the $z' = 0$ plane and denote the field incident on L_1 by $\phi_o^-(y_1)$. Equation (5) can be used to compute $\phi_o^-(y_1)$; the source points now lie on the y_o plane ($z' = 0$), and the field points lie on the y_1 plane ($z' = D_1$). The lens thickness is assumed negligible here. Let both source and field points lie near the z' axis of the lens system. Then

$$r = \sqrt{D_1^2 + (y_o - y_1)^2} \cong D_1 + (y_o - y_1)^2/2D_1, \tag{6}$$

since higher order terms in $(y_o - y_1)^2/2D_1$ are negligible. The cylindrical wave $e^{ikr}/\sqrt{r}$ is approximated by

$$\frac{e^{ikr}}{\sqrt{r}} \cong \frac{e^{ikD_1}}{\sqrt{D_1}} e^{ik(y_o-y_1)^2/2D_1}, \tag{7}$$

which is a two-dimensional paraxial approximation [4]. Equation (5) becomes

$$\phi_o^-(y_1) = \frac{e^{ikD_1}}{2\sqrt{D_1\lambda_a}} e^{-\pi i/4} \int \psi_o(y_o) e^{ik(y_o-y_1)^2/2D_1} dy_o. \tag{8}$$

Using the symbol $\propto$ for proprotionality and $\overset{s}{\oplus}$ for spatial convolution,

$$\phi_o^-(y_1) \propto \psi_o(y_o) \overset{s}{\oplus} e^{iky_o^2/2D_1}. \tag{9}$$

Assume that lens L_1 is aberration free and multiplies $\phi_o^-(y_1)$ by a quadratic phase factor $e^{-ky_1^2/2f_1}$; see for example Ref. 4. This represents a converging cylindrical wave which focuses at a distance f_1 behind the lens. For a lens of width $2a$, the sound field $\phi_o^+(y_1)$ emerging from the lens is

$$\phi_o^+(y_1) = \text{Rect} (y_1/a) e^{-iky_1^2/2f_1} \phi_o^-(y_1), \tag{10}$$

where Rect (y_1/a) is unity for $|y_1| \leqslant a$ and zero otherwise.

Equation (5) is now used to calculate the field in the y_2 plane, the back focal plane of L_1. The source distribution is $\phi_o^+(y_1)$, and the distance r between the source points (in the y_1 plane) and the field points (in the y_2 plane) is approximated by

$$r \cong f_1 + (y_1 - y_2)^2/2f_1. \tag{11}$$

Then

$$\phi_o(y_2) = \frac{e^{-\pi i/4}}{2\sqrt{f_1 \lambda_a}} e^{ikf_1} [\phi_o^+(y_1) \overset{s}{\oplus} e^{iky_1^2/2f_1}] \tag{12}$$

or, by use of (9) and (10),

$$\phi_o(y_2) \propto e^{ik(D_1+f_1)} e^{iky_1^2/2f_1} \overset{s}{\oplus} \{\text{Rect} (y_1/a) e^{-iky_1^2/2f_1} [\psi_o(y_o) \overset{s}{\oplus} e^{iky_o^2/2D_1}]\}. \tag{13}$$

For $a^2 \gg 2D_1/k$ it can be shown that

$$\phi_o(y_2) \propto e^{(iky_2^2/2f_1) (1 - D_1/f_1)} \, \bar{\psi}_o(\eta) \, e^{ik(D_1 + f_1)}, \tag{14}$$

where $\bar{\psi}_o(\eta)$ is the Fourier transform of $\psi_o(y_o)$ and $\eta = y_2/\lambda_a f_1$. Typical values are $D_1 = 14$ cm, $a = 8$ cm, and $k = 120$ rad/cm; thus the inequality $a^2 \gg 2D_1/k$ is easily satisfied. The proof of (14) is fairly straightforward and is carried out in the first section of Appendix A.

Suppose $\psi_o(y_o) \propto \delta(y_o)$; that is, the object is a line source at $y_o = z' = 0$. Then $\bar{\psi}_o(\eta) = 1$ and (14) gives $\phi_o(y_2) \propto e^{iky_2^2(1-D_1/f_1)/2f_1}$. This is the paraxial approximation for a cylindrical wave which converges to a focus at a distance $-f_1/(1 - D_1/f_1)$ to the right of the y_2 plane if $D_1 > f_1$; if $D_1 < f_1$, then the wave diverges from a (virtual) line source a distance $f_1/(1 - D_1/f_1)$ to the left of the y_2 plane. This situation is illustrated in Fig. 3 for the case $D_1 < f_1$. If $D_1 = f_1$, then the virtual source appears to be at $z' = -\infty$; that is, the lens converts the cylindrical wave emitted by the line source into a plane wave.

Due to the finite size of the acoustic lenses, some of the sound field in the y_2 plane may not pass through lens L_2. In fact, Fig. 3 shows that if $f_1 > D_1$, the extreme ray (which strikes the rim of L_2) passes through $y_2 = a'$, where $a' < a$. Thus, in calculating the propagation of the sound field from the y_2 plane to L_2, the y_2 integration extends from $-a' \leqslant y_2 \leqslant a'$.

Also note that typically the lens width $2a$ and the distances D_1, f_1, f_2, and D_2 are the same order of magnitude. This implies that the paraxial approximation cannot be rigorously used in this calculation. The theory of Fourier analysis indicates that if the object distribution ψ_o extends only over a small region $|y_o| \leqslant b$, and $b \ll a$, then $\bar{\psi}_o(\eta)$ will extend over a large region of the y_2 plane. Since $\bar{\psi}_o(\eta)$ does not necessarily lie close to the z' axis of the lens system, the paraxial approximation is, strictly speaking, invalid when propagation from the y_2 plane to L_2 is considered. This difficulty is avoided (at least mathematically) by assuming that the acoustic lenses are corrected so that the result of the breakdown of the paraxial approximation (resulting in aberrations) is compensated for. This requires, for instance, that an incident plane wave be diffracted by the lens into a cylindrical wave which focuses in the back focal plane of the lens.

With this assumption about lens quality, the acoustic field incident on L_2 is

$$\phi_o^-(y_3) \propto e^{ikf_2} \{ e^{iky_2^2/2f_2} \overset{s}{\oplus} [\text{Rect } (y_2/a') \, \phi_o(y_2)] \}, \tag{15}$$

and the emergent field is just

$$\phi_o^+(y_3) = \text{Rect } (y_3/a) \, \phi_o^-(y_3) \, e^{-iky_3^2/2f_2}. \tag{16}$$

The field in the y_4 plane is

$$\phi_o(y_4) \propto e^{ikD_2} [e^{iky_3^2/2D_2} \overset{s}{\oplus} \phi_o^+(y_3)]. \tag{17}$$

As shown in detail in Appendix A, the operations indicated by the above are simplified by assuming that $a^2 \gg D_2/k$ and that

$$1/f_1 + 1/f_2 = D_1/f_1^2 + D_2/f_2^2. \tag{18}$$

8

which is the focusing condition for the lens system. Then, if $L = D_1 + f_1 + f_2 + D_2$,

$$\phi_o(y_4) \propto e^{ikL}(f_1/f_2) \, \psi_o \left[\frac{-y_4 f_1}{f_2} \right] \overset{s}{\oplus} \text{sinc} \left(\frac{2\pi a' y_4}{\lambda_a f_2} \right), \tag{19}$$

where $\text{sinc } x \equiv (\sin x)/x$.

The relation (19) is a scaled, inverted image of the object distribution ψ_o convolved with $\text{sinc } (2\pi ya'/\lambda_a f_2)$, the impulse response of the lens system. The impulse response is the output of the lens system due to a line source at $y_o = z' = 0$. The relation (19) holds only if the distances D_1 and D_2 are related through the focusing condition (18). The y_o and y_4 planes are said to be conjugate planes; an object placed in one plane will be imaged in the other.

At this point it is necessary to use some geometrical acoustics to determine a'. For the line source $\psi_o = \delta(y_o)$ in Fig. 3 the extreme ray intercepted by lens L_2 (at $y_3 = a$) passes through $y_2 = a'$, and $a' < a$ for $D_1 < f_1$. The extreme ray appears to come from a virtual source a distance $f_1/(1 - D_1/f_1)$ to the left of the y_2 plane. From similar triangles

$$\frac{a'}{f_1} = \frac{a}{f_1 + (1 - D_1/f_1) \, f_2}, \tag{20}$$

and using this equation in conjunction with the focusing condition leads to $a'/f_2 = a/D_2$. If $D_1 > f_1$, then L_1 becomes the limiting aperture of the lens system, and $a'/f_2 = (a/D_1)(f_1/f_2)$. Hence the impulse response of the lens system is $\text{sinc } (2\pi y_4 a/\lambda_a D_2)$, which is convolved with the (scaled) input ψ_o:

$$\phi_o(y_4) \propto e^{ikL} \, (f_1/f_2) \, \psi_o \left[\frac{-y_4 f_1}{f_2} \right] \overset{s}{\oplus} \text{sinc} \left(\frac{2\pi \, y_4 a}{\lambda_a D_2} \right). \tag{21}$$

The image will be demagnified if $f_2 < f_1$, which increases the acoustic intensity at the liquid surface; the surface is assumed to be the y_4 plane here. However, it will be seen that this is obtained at the expense of increasing the range of spatial frequencies that must be faithfully recorded by the surface.

When the convolution theorem of Fourier analysis is used, the field in the image plane becomes

$$\phi_o(y_4) \propto e^{ikL} \int_{-\infty}^{\infty} \text{Rect} \left[\frac{\eta}{\eta_m} \right] \bar{\psi}_o \left[\frac{-f_2 \eta}{f_1} \right] e^{2\pi i \eta y_4} \, d\eta, \tag{22}$$

with $\eta_m = a'/\lambda_a f_2$. The Fourier transform of $\text{sinc } (2\pi y \eta_m)$ is $\text{Rect } (\eta/\eta_m)$, as shown in, for example, Ref. 4. The factor $\text{Rect } (\eta/\eta_m)$ shows that only components in the spectrum of $\bar{\psi}_o(- f_2\eta/f_1)$ having spatial frequencies $|\eta| < \eta_m f_1/f_2$ will be passed by the lens system.

The field between L_2 and the image plane can be represented as

$$\phi_o(y, z') \propto e^{ikL} \int_{-\infty}^{\infty} \bar{\psi}_o \left[\frac{-f_2 \eta}{f_1} \right] \text{Rect} \left[\frac{\eta}{\eta_m} \right] e^{2\pi i \eta y} \, e^{2\pi i \zeta z} \, e^{-i\omega_a t} \, d\eta \tag{23}$$

for $z' = z + L$. The time factor $e^{-i\omega_a t}$ has been restored here. This equation satisfies the wave equation between the y_3 and y_4 planes, provided that

9

$$\zeta^2 = 1/\lambda_a^2 - \eta^2. \tag{24}$$

Furthermore (23) reduces to (22) on the image plane (y_4 plane), where $z = 0$. Hence the field to the right of L_2 can be thought of as a superposition of plane waves which have the form $\bar{\psi}_o(- f_2\eta/f_1)e^{2\pi i\eta y}e^{2\pi i\zeta z}$ traveling with direction cosines $\lambda_a\zeta$ relative to the z' axis. The factor Rect (η/η_m) shows that only those waves having a spatial frequency in the bandpass $|\eta| \leqslant \eta_m$ will propagate through the lens system. In the y_4 plane these waves combine to produce the acoustic image. Furthermore, if $f_2 < f_1$, then the bandwidth of the object distribution $\bar{\psi}_o$ increases by the factor f_1/f_2.

If $f_1 < f_2$, then the image is magnified in accordance with (21), and from (22) the spatial frequency spectrum of $\bar{\psi}_o$ decreases. However, the function Rect (η/η_m) remains the same, showing that more components of the object spectrum are passed by the lens system. As the lens system accepts more spatial frequencies in $\bar{\psi}_o(-f_2 \eta/f_1)$, less degradation of the image results.

Another method of increasing image quality is to increase η_m, the cutoff of the lens system in the spatial frequency domain. Suppose $D_1 \leqslant f_1$; then $\eta_m = a/\lambda_a D_2$. For a lens of fixed diameter the cutoff can be increased by decreasing D_2 (increasing D_1) until $D_2 = f_2$. The focusing condition (18) shows that if $D_1 = f_1$, then $D_2 = f_2$, so that all rays intercepted by L_1 are captured by L_2, and $\eta_m = a/\lambda_a f_2$. If $D_1 \geqslant f_1$, then lens L_1 becomes the limiting aperture of the lens system and $\eta_m = af_1/\lambda_a f_2 D_1$; in this case, since $f_1 < D_1$, η_m has decreased. Consequently the best image is obtained when the object is placed in the front focal plane of L_1.

Equation (22) shows that the focused image has spatial frequency components

$$\bar{\phi}_o(\eta) \propto \text{Rect}\left[\frac{\eta}{\eta_m}\right]\bar{\psi}_o\left[\frac{-f_2\eta}{f_1}\right]. \tag{25}$$

This is the output of the lens system in the spatial frequency domain, due to input $\bar{\psi}_o(\eta)$, when focusing condition (18) is satisfied. The transfer function, which relates $\bar{\phi}_o(\eta)$ to $\psi_o(\eta')$, is given by the convolution

$$\overset{\eta'}{\oplus} \delta\left[\eta' + \frac{f_2}{f_1}\eta\right],$$

followed by multiplication by Rect (η/η_m).

2.2 Depth of Focus of the Lens System

The acoustic lens system focuses the acoustic image on the air-imaging fluid interface (Fig. 1). In general the imaging fluid will differ from the fluid in which the object is submerged (object-tank fluid). The focusing condition (18) has been derived on the assumption that fluid properties are the same between the y_o plane and the y_4 plane (surface of the imaging fluid). It is of interest to consider what, if any, corrections need to be made to (18) when the minitank fluid is not the same as the object-tank fluid.

The velocity potential for the region between lens L_2 and the bottom of the minitank can be represented by (23), repeated here for convenience:

$$\phi_o(y, z) \propto e^{ikL} \int_{-\infty}^{\infty} \bar{\psi}_o \left[\frac{-f_2 \eta}{f_1} \right] \text{Rect} \left[\frac{\eta}{\eta_m} \right] e^{2\pi i \eta y} e^{2\pi i \zeta z} e^{-i\omega_a t} \, d\eta. \tag{23}$$

If the imaging fluid and object-tank fluid are identical, then on the liquid surface of the minitank, where $z = 0$, the above reduces to (20).

Let the imaging fluid have sound speed c_u and wavelength λ_u, where the subscript u is used because the minitank is the upper tank; then in the minitank

$$\nabla^2 \phi_o = \left[\frac{1}{c_u} \right]^2 \ddot{\phi}_o. \tag{26}$$

The velocity potential in the minitank becomes

$$\phi_o \propto e^{ikL} \int_{-\infty}^{\infty} \bar{\psi}_o \left[\frac{-f_2 \eta}{f_1} \right] \text{Rect} \left[\frac{\eta}{\eta_m} \right] e^{-2\pi i \zeta d} e^{2\pi i \zeta_u (z+d)} e^{2\pi i \eta y} e^{-i\omega_a t} \, d\eta, \tag{27}$$

where

$$2\pi \zeta_u = \sqrt{(\omega_a/c_u)^2 - (2\pi \eta)^2} = \frac{2\pi \cos \theta_2}{\lambda_u} \tag{28}$$

to satisfy the wave equation (26). θ_2 is the angle between the z axis and direction of propagation of the wave in the minitank, and d is the minitank depth. Evaluating (27) at $z = 0$ (the liquid surface) gives

$$\phi_o(y_4) \propto e^{ikL} \int_{-\infty}^{\infty} \bar{\psi}_o \left[\frac{-f_2 \eta}{f_1} \right] \text{Rect} \left[\frac{\eta}{\eta_m} \right] e^{2\pi i (\zeta_u - \zeta)d} e^{2\pi i \eta y_4} e^{-i\omega_a t} \, d\eta. \tag{29}$$

Comparing (29) with (23) shows that an additional phase factor having argument $2\pi i (\zeta_u - \zeta)d$ has appeared. This occurs because the acoustic path lengths of the traveling waves in the integrand have changed due to the difference in sound speed between the imaging and object-tank fluids. The phase factor represents a defocusing effect.

If the depth of focus of the lens system is great enough, then this defocusing can be ignored and the system is diffraction limited; that is, any image degradation is due to the fact that only waves having spatial frequencies in the bandpass $|\eta| \leqslant \eta_m$ are collected by the lens system. To investigate this further, assume small angles of incidence. Then, from (24),

$$\zeta = \sqrt{1/\lambda_l^2 - \eta^2} \cong 1/\lambda_l - \frac{1}{2} \eta^2 \lambda_l, \tag{30}$$

and similarly for ζ_u. Here λ_l is the acoustic wavelength in the object-tank (lower-tank) fluid. This allows (29) to be rewritten as

$$\phi_o(y_4) \propto \int_{-\infty}^{\infty} \bar{\psi}_o \left[\frac{-f_2 \eta}{f_1} \right] \text{Rect} \left[\frac{\eta}{\eta_m} \right] e^{-\pi i (\lambda_u - \lambda_l)\eta^2 d} e^{2\pi i \eta y_4} e^{-i\omega_a t} \, d\eta. \tag{31}$$

Because the factor Rect (η/η_m) is present, the integration will extend only over the region $|\eta| \leqslant \eta_m$. If $\pi |\lambda_u - \lambda_l|\eta^2 d \ll 1$ in this region, then defocusing is negligible. Let the imaging fluid be for example Freon E-5 and let water be the object-tank fluid; then $\lambda_u = 0.47\lambda_l$. Furthermore, let $d \sim O(\lambda_l)$, and $a/D_2 = 0.3$, so that $\pi |\lambda_u - \lambda_l|d\eta_m^2 \sim O(1)$; the notation $d \sim O(\lambda_l)$ means that d and λ_l are the same order of magnitude. For this case, the system is no longer diffraction limited, and defocusing effects are important.

To correct this situation, one possibility is to reposition the lenses; that is, to calculate the correction to the focusing condition (18) necessary to cause the acoustic image to focus on the liquid surface when $\lambda_u \neq \lambda_l$. However, a simple example suffices to show that for large f-number lenses this is rather impractical.

Consider the situation in which the object to be imaged is a line source, so that $\psi_o(y_o) = \delta(y_o)$ and $\bar{\psi}_o(\eta) = 1$. From (31),

$$\phi_o(y_4) \propto \text{sinc}\,(2\pi y_4 \eta_m) \overset{s}{\oplus} e^{-ik_u y_4^2/2\Delta}, \tag{32}$$

where $\Delta = (\lambda_l - \lambda_u)d/\lambda_u$ and $k_u = 2\pi/\lambda_u$; the inverse transform of $e^{-\pi i(\lambda_u - \lambda_l)d\eta^2}$ is $e^{-ik_u y_4^2/2\Delta}$. The quadratic phase factor is the paraxial approximation for the field in the y_4 plane due to a cylindrical wave which focuses at a line $z = \Delta$, which is above the liquid surface. If the previous criterion for negligible defocusing $|\pi(\lambda_l - \lambda_u)d\eta_m^2| \ll 1$ is to be satisfied, then Δ must satisfy

$$\Delta \ll \frac{1}{\pi \lambda_u} \left[\frac{\lambda_l D_2}{a} \right]^2, \tag{33}$$

where it is assumed that $D_1 < f_1$. Using the values that were given for λ_l, λ_u, etc. shows that in this instance $\Delta \ll 6\lambda_l$. Hence for negligible defocusing the lenses must be repositioned so that the defocusing error is reduced below approximately 6 acoustic wavelengths. As the lens width $2a$ increases, the tolerable defocusing error decreases. The criterion (33) can be applied to any focusing error, if Δ is interpreted as the distance from the plane of sharpest focus to the liquid surface.

The focusing condition for the case $\lambda_l \neq \lambda_u$ is

$$\frac{1}{f_1} + \frac{1}{f_2} = \frac{D_1}{f_1^2} + \frac{D_2 - \Delta(\lambda_u/\lambda_l)}{f_2^2}. \tag{34}$$

Here the y_4 plane is required to be the liquid surface. To derive (34), recall that the line source is imaged a distance Δ above the liquid surface; from geometry the distance D_2 between L_2 and the liquid surface must be increased by $\Delta\theta_2/\theta_1$, where θ_1 is the angle of incidence of an acoustic ray in the object tank and θ_2 the corresponding angle in the minitank. Use of Snell's law

$$\frac{\sin\theta_1}{\lambda_l} = \frac{\sin\theta_2}{\lambda_u} \tag{35}$$

for small angles shows that D_2 must increase by $\Delta\lambda_u/\lambda_l = d(1 - \lambda_u/\lambda_l)$.

2.3 Depth of Field of the Lens System

Rather than repositioning the lenses the object can be translated along the z axis (scanned) until it is in the plane giving the sharpest image. To fully use the real-time imaging capabilities of the system, it is desirable that the depth of field be large; this will avoid the need for mechanical scanning devices.

To calculate the depth of field, assume that the object is slightly displaced from the y_o plane. The y_o plane and the y_4 plane (the liquid surface) are now conjugate planes for $\lambda_u \neq \lambda_l$.

That is, an object placed in one plane will be imaged in the other. The locations of these planes are such that (34) is satisfied.

Suppose the object is again a line source and let it be displaced ϵ units in a direction away from L_1. Then the lens system will form the image a distance ϵ' below the liquid surface. Here ϵ' is calculated from

$$\frac{1}{f_1} + \frac{1}{f_2} = \frac{D_1 + \epsilon}{f_1^2} + \frac{D_2' - \epsilon'(\lambda_u/\lambda_l)}{f_2^2} \tag{36}$$

for $D_2' = D_2 - d(1 - \lambda_u/\lambda_l)$. This assumes that $\epsilon' < d$. Since D_2' and D_1 are such that the focusing condition (34) is satisfied, (36) gives $\epsilon' = \epsilon (f_2/f_1)^2 (\lambda_l/\lambda_u)$.

The velocity potential in the y_4 plane will be (for $D_1 < f_1$)

$$\phi_o(y_4) \propto \text{sinc}\left[\frac{2\pi y_4 a}{\lambda_l D_2}\right] \overset{s}{\oplus} e^{ik_u y_4^2/2\epsilon'}, \tag{37}$$

which is a representation of the field due to a line source ϵ' units below the liquid surface, convolved with the impulse response of the lens system. This can also be written as

$$\phi_o(y_4) \propto \int_{-\infty}^{\infty} \text{Rect}\,(\eta/\eta_m)\, e^{\pi i \lambda_u \epsilon' \eta^2}\, e^{2\pi i \eta y_4}\, d\eta. \tag{38}$$

If the principal image degradation is to be due to the finite size of the effective aperture of the lens system, then the argument $\pi\lambda_u\epsilon'\eta^2$ must be much less than 1 in the spatial frequency bandpass $|\eta| \leqslant \eta_m$. Using this criterion and assuming $D_1 < f_1$, the displacement ϵ of the object from the y_o' plane must satisfy

$$\epsilon << \left[\frac{f_1}{f_2}\right]^2 \left[\frac{D_2}{a}\right]^2 \frac{\lambda_l}{\pi}. \tag{39}$$

As a typical example let $f_1/f_2 = 1.4$ and $D_2/a = 3$; then $\epsilon << 6\lambda_l$. Any object placed less than 6 acoustic wavelengths from the y_o' plane will then be within the depth of field of the lens system according to the criterion expressed by (39).

2.4 Transfer Function For the Lens System

For an object described by the distribution $\psi_o(y_o')$ of line sources the velocity potential in the y_4 plane will be

$$\phi_o(y_4) \propto e^{ik_u y_4^2/2\epsilon'} \overset{s}{\oplus} \left[\text{sinc}\,(2\pi y \eta_m) \overset{s}{\oplus} \psi_o\left(\frac{-f_1 y}{f_2}\right)\right]. \tag{40}$$

This has the equivalent Fourier integral representation

$$\phi_o(y_4) \propto \int_{-\infty}^{\infty} \bar{\psi}_o\left(\frac{-f_2 \eta}{f_1}\right) \text{Rect}\left[\frac{\eta}{\eta_m}\right] e^{\pi i \lambda_u \epsilon' \eta^2}\, e^{2\pi i \eta y}\, d\eta. \tag{41}$$

Hence in the spatial frequency domain the transfer function which accounts for displacement of the object a distance ϵ from the y_o' plane is $e^{\pi i \lambda_u \epsilon' \eta^2}$, with $\epsilon' = \epsilon (f_2/f_1)^2 \lambda_l/\lambda_u$. The total transfer function for the cylindrical acoustic lens system is contained by the outer box in Fig. 4.
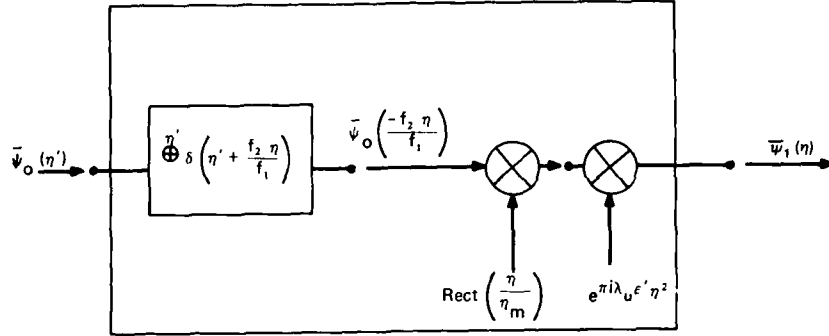
Fig. 4 — Transfer function for the acoustic lens system

3. EFFECT OF THE MINITANK

The preceding section considered the formation of the acoustic image on the liquid surface of the minitank. It was shown that the acoustic image can be thought of as a superposition of plane waves traveling at all spatial frequencies passed by the effective aperture of the acoustic lens system. The effect of the minitank on each of these plane waves will now be considered. It will be shown that multiple internal reflections can occur in the minitank. The effect of the membrane which separates the object-tank fluid from the imaging fluid will also be accounted for. In previous analyses [1,2], it was assumed that the membrane is transparent to ultrasound, and its presence was ignored. It will be shown here that in certain instances the membrane is not transparent and can have significant effects on system performance.

The purpose of the minitank is twofold. It isolates the liquid surface from environmental disturbances due to vibration etc., and it allows the use of a thin film of imaging fluid whose properties are more advantageous than those of the object-tank fluid (typically water). For example, Freon E-5 is often used as an imaging fluid, because its surface tension is less than that of water.

3.1 Transfer Function for the Minitank

To this point the acoustic field has been assumed monochromatic. Previous investigations [1,2] have shown that better image fidelity can be obtained if the object and reference transducers are operated in a pulsed CW mode. The reason for this will be demonstrated in section 5. Let ϕ_{inc} be the magnitude of the velocity potential in the acoustic wave incident on the object S_o, and let $\hat{t} = t - \Delta t$. Let the object transducer emit a quasimonochromatic pulse of duration $2\Delta t$ such that $\omega_a >> 1/\Delta t$. If normal incidence is assumed, the velocity potential at the object is

$$\phi_{inc}(z' = 0) \propto A(y_o)\ \text{Rect}(\hat{t}/\Delta t)\ e^{-i\omega_a t}. \tag{42}$$

Equation (23) gives the acoustic field between lens L_2 and the membrane when the acoustic field is monochromatic and defocusing is negligible. To obtain the quasimonochromatic equivalent, set $\bar{\psi}_o(y_o, \omega) = S_o(y_o)\ \bar{\phi}_{inc}(y_o, \omega)$; then, from (42),

14

$$\bar{\phi}_{inc}(y_o, \omega) \propto A(y_o) \text{ sinc } [(\omega - \omega_a)\Delta t] e^{i(\omega - \omega_a)\Delta t}, \tag{43}$$

and, by setting $S_o' = A(y_o) S_o(y_o)$ and $z = z' - L$,

$$\phi_o(y, z, t) \propto \int_{-\infty}^{\infty} \int_{-\infty}^{\infty} e^{i\omega L/c} [\text{sinc } (\omega - \omega_a)\Delta t] \bar{S}_o' \left[\frac{-f_2\eta}{f_1}\right] \text{Rect} \left[\frac{\eta}{\eta_m}\right]$$

$$\times e^{i(\omega - \omega_a)\Delta t} e^{2\pi i \eta y} e^{2\pi i \zeta z} e^{-i\omega t} d\eta d\omega. \tag{44}$$

This can be integrated over ω; let $\omega' = \omega - \omega_a$, with $\omega' \ll \omega_a$ since the pulse is quasi-monochromatic. Defining

$$2\pi\eta = (\omega_a/c_l) \sin \theta_1 + (\omega'/c_l) \sin \theta_1$$

and

$$2\pi\zeta = (\omega_a/c_l) \cos \theta_1 + (\omega'/c_l) \cos \theta_1$$

allows (44) to be integrated over ω' (since $d\omega = d\omega'$) with the result

$$\phi_o(y, z, t) \propto \int_{-\infty}^{\infty} \text{Rect} \left[\frac{\eta}{\eta_m}\right] \bar{S}_o' \left[\frac{-f_2\eta}{f_1}\right] e^{(i\omega_a/c_l)(y \sin\theta_1 + z \cos\theta_1 - c_l t_L)}$$

$$\times \text{Rect} \left[\frac{t_L - \Delta t - (1/c_l)(y \sin \theta_1 + z \cos \theta_1)}{\Delta t}\right] d\eta, \tag{45}$$

where t_L is the retarded time $t - L/c_l$. This result represents a superposition of plane wave pulses traveling at spatial frequencies $2\pi\eta = \omega_a \sin \theta_1/c_l$.

Let the field of (45) be incident on the membrane, located in the $z = -d$ plane (Fig. 5). In the spatial frequency domain

$$\bar{\phi}_o(\eta, z = -d, t) \propto \bar{\psi}_1(\eta) e^{2\pi i(\eta y - \zeta d)}, \tag{46}$$

where for the moment a time factor has been omitted. $\bar{\psi}_1(\eta)$ represents the diffraction-limited acoustic image $\text{Rect } (\eta/\eta_m) \bar{S}_o'(- f_2\eta/f_1)$.

Obviously, not all waves of form (46) reach the liquid surface together. However, differences in arrival times cannot be distinguished by the liquid surface for small angles of incidence. The field incident on the liquid surface will be

$$\bar{\phi}_o(\eta, 0, t) \propto \bar{T}_{12}(\eta) \bar{\psi}_1(\eta) e^{2\pi i \eta y} e^{2\pi i(\zeta_u - \zeta)d} \text{Rect } (\hat{t}/\Delta t). \tag{47}$$

Here time is shifted so that $t = 0$ when the pulse (47) reaches the liquid surface. The transmission coefficient for the membrane is denoted as $\bar{T}_{12}(\eta)$ and will be calculated in section 3.2. The term $e^{2\pi i(\zeta_u - \zeta)d}$ is the image degradation which results if the focusing correction (34) is not made. If S_o is placed in the y_o' plane, so that the correction has been made, this factor can be dropped. If S_o is displaced a distance ϵ from this plane, the factor which accounts for the resulting image degradation will be absorbed into $\bar{\psi}_1$ for ease of notation:

$$\bar{\psi}_1 = \text{Rect} \left[\frac{\eta}{\eta_m}\right] \bar{S}_o' \left[\frac{-f_2\eta}{f_1}\right] e^{\pi i \lambda_l \epsilon \eta^2 f_2^2/f_1^2}. \tag{48}$$
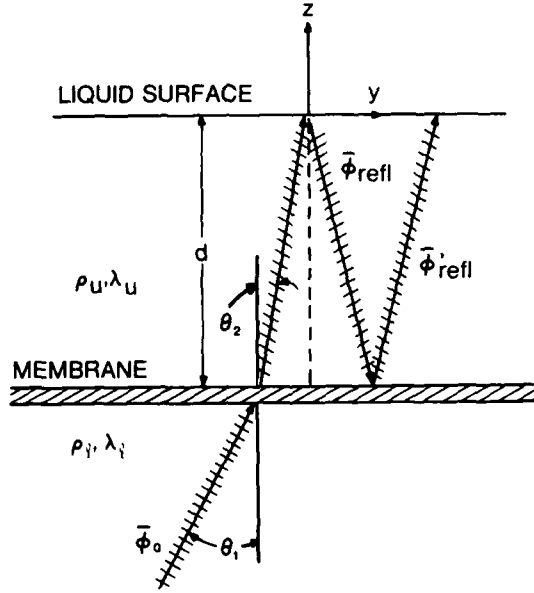
Fig. 5 — Wave incident on the minitank membrane.
Multiple internal reflections are present.

Since the acoustic impedance of air is much smaller than that of the imaging fluid, the reflection coefficient at the liquid surface is -1. Thus the wave reflected from the surface is

$$\bar{\phi}_{refl}(\eta, z, t) \propto -\bar{T}_{12}(\eta) \, \bar{\psi}_1(\eta) \, e^{2\pi i \eta y} e^{-2\pi i \zeta_u z} e^{-i\omega_a t}$$
$$\times \text{Rect}\left[\frac{\hat{t} - (1/c_u) \, (y \sin\theta_2 - z \cos\theta_2)}{\Delta t}\right]. \qquad (49)$$

The particle velocity at the liquid surface in the vertical (z) direction due to the incident and reflected waves is

$$\bar{v}_{oz}(\eta, 0, t) = \frac{\partial}{\partial z} \, (\bar{\phi}_o + \bar{\phi}_{refl})|_{z=0} \qquad (50a)$$

or

$$\bar{v}_{oz}(\eta, 0, t) \propto 4\pi i \zeta_u \bar{T}_{12}(\eta) \, \bar{\psi}_1(\eta) \, e^{2\pi i \eta y} e^{-i\omega_a t} \text{Rect} \, (\hat{t}/\Delta t). \qquad (50b)$$

Here the incident wave strikes the liquid surface at $z = y = 0$ (Fig. 5).

The wave $\bar{\phi}_{refl}$ will reach the membrane at $z = -d$, $y = d \tan\theta_2$, where it will be partially reflected, with reflection coefficient $\bar{R}_{21}(\eta)$. The arrival time at the membrane is $d/(c_u \cos\theta_2)$. If this partially reflected pulse is denoted as $\bar{\phi}'_{refl}$ and a time factor is suppressed, then

$$\bar{\phi}'_{refl}(\eta, z, t) \propto -\bar{T}_{12} \, \bar{R}_{21} \, \bar{\psi}_1(\eta) \, e^{2\pi i \eta y} e^{2\pi i \zeta_u (z+2d)}. \qquad (51)$$

The factor $e^{4\pi i \zeta_u d}$ appears, so that the phase of $\bar{\phi}_{refl}$ and $\bar{\phi}'_{refl}$ are equal at the membrane.

The pulse $\bar{\phi}'_{refl}$ reaches the liquid surface at time $t' = 2d/(c_u \cos \theta_2)$, where t' is the time of the first internal reflection in the minitank. This generates another reflected wave $\bar{\phi}''_{refl}$:

$$\bar{\phi}''_{refl} \propto \bar{R}_{21} \ \bar{T}_{12} \ \bar{\psi}_1(\eta) \ e^{2\pi i \eta y} \ e^{-2\pi i \zeta_u (z-2d)}$$

$$\times \ \text{Rect} \left[\frac{(\hat{t} - t') - (1/c_u)(y \ \sin \theta_2 - z \ \cos \theta_2)}{\Delta t} \right]. \tag{52}$$

Continuing in this fashion would show that the vertical component of velocity at the liquid surface after N internal reflections is [1]

$$\bar{v}_{oz}(\eta, \ 0, \ t) \propto 4\pi i \ \zeta_u \ \bar{T}_{12} \ \bar{\psi}_1(\eta) \ \sum_{n=0}^{N} \left[(-\bar{R}_{21} \ e^{4\pi i \zeta_u d})^n \ \text{Rect} \left(\frac{\hat{t} - t_n}{\Delta t} \right) \right]. \tag{53}$$

The factor $e^{4\pi i \zeta_u d}$ represents a phase shift due to one internal reflection, and t_n is the time of the nth internal reflection:

$$t_n = \frac{2nd}{c_u \cos \theta_2} = nt'. \tag{54}$$

The complicated expression (53) can be simplified if $\Delta t \gg t'$. Typically, the minitank depth d is a few acoustic wavelengths, and Δt is of the order of 10^{-4} s. Then

$$\frac{\Delta t}{t'} = \frac{c_u (\Delta t) \ \cos \theta_2}{2d} \sim O(100), \tag{55}$$

where $\Delta t/t' \sim O(100)$ denotes that the ratio is of the order of 100. In the above, it is assumed that the transducers operate in the megahertz range and that $\cos \theta_2 \sim O(1)$.

Since $\Delta t \gg t'$,

$$\text{Rect} \left(\frac{\hat{t} - t_n}{\Delta t} \right) \cong \text{Rect} \left(\frac{\hat{t}}{\Delta t} \right) \tag{56}$$

unless t_n is large. But if t_n is large, the product $\bar{R}_{21}^n \ \text{Rect} \ [(\hat{t} - t_n)/\Delta t]$ in (53) is small, since $\bar{R}_{21} < 1$. Hence the summation on the right-hand side of (53) extends only over small n, and (56) holds. Furthermore

$$\sum_n (-\bar{R}_{21} \ e^{4\pi i \zeta_u d})^n = \frac{1}{1 + \bar{R}_{21} \ e^{4\pi i \zeta_u d}}, \tag{57}$$

so that, denoting $2\pi/\lambda_u$ by k_u,

$$\bar{v}_{oz}(\eta, \ 0, \ t) \propto 2ik_u \ \bar{g}_1(\eta) \ \text{Rect} \left(\frac{\hat{t}}{\Delta t} \right) \bar{\psi}_1(\eta), \tag{58}$$

where the quantity

$$\bar{g}_1(\eta) = \frac{\bar{T}_{12} \ \cos \theta_2}{1 + \bar{R}_{21} \ e^{4\pi i \zeta_u d}} \tag{59}$$

represents the transfer function for the minitank. It relates the vertical particle velocity at the liquid surface to the velocity potential in an incident plane acoustic wave.

17

To this point the plane waves considered have been those which make up the focused acoustic image. The reference transducer also generates a plane wave which strikes the liquid surface. The necessity for this reference beam will become clear in section 5. Let $\phi_r = A_r e^{2\pi i \eta_r y}$ Rect $(\hat{t}/\Delta t)$ be the velocity potential in the reference beam; then

$$\bar{v}_{r,z}(\eta, 0, t) \propto 2ik_u \bar{g}_1(\eta_r) \bar{\phi}_r(\eta) \text{ Rect } (\hat{t}/\Delta t), \tag{60}$$

where $v_{r,z}$ is the z component of $\mathbf{v}_r$, the particle velocity due to the reference beam.

Thus the transfer function for the minitank is a simple multiplier in the spatial frequency domain, as shown in Fig. 6. The input is the velocity potential in either the acoustic image or the reference beam; for example, when the input is the acoustic image, the input $\bar{\phi}(\eta)$ is then $\bar{\psi}_1$ and the output $\bar{v}_z$ becomes $\bar{v}_{oz}$.
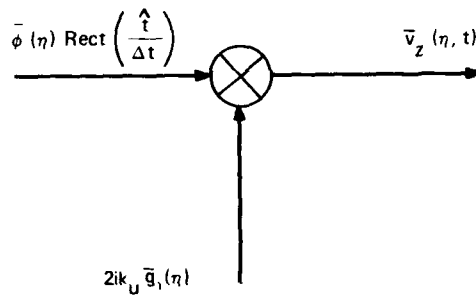

Fig. 6 — Transfer function for the minitank

In the preceeding, it was assumed that the minitank is infinite in lateral extent. In reality the minitank has a finite radius, typically of the order of $10^3 \lambda_u$; eventually some part of the internally reflected wave will reach the minitank wall. Consider a portion of $\bar{\phi}_o$ incident on the membrane at a distance Δy from the minitank wall. This will undergo N internal reflections before striking the wall, where $N \leqslant \Delta y/(2d \tan \theta_2)$. It will be shown that $|\bar{R}_{21}| \sim O(10^{-1})$ at low spatial frequencies for a typical plastic membrane separating water and Freon E-5 (imaging fluid). Hence the energy in the internally reflected waves will rapidly approach zero, since a sizable fraction of the energy leaves the minitank on each internal reflection. Thus, for a wave with significant energy to reach the minitank wall, N must be a small number, showing that $\Delta y \sim O(2d)$. Since typically $d \sim O(\lambda_u)$, only a small fraction of the incident acoustic wave is reflected from the minitank wall, and it can safely be ignored.

3.2. Effect of the Membrane on $\bar{T}_{12}$ and $\bar{R}_{21}$

It remains to calculate the transmission coefficient $\bar{T}_{12}(\eta)$ and the reflection coefficient $\bar{R}_{21}(\eta)$ for the membrane. To keep the problem simple, the following assumptions are made:

- A plane wave of infinite extent is incident on a thin membrane, also of infinite extent;

- The problem is two dimensional;

- The displacement w of the membrane is much less than λ_l and λ_u, the acoustic wavelengths in the lower and upper fluids respectively;

- The fluids above and below the membrane are inviscid.

Some comments need to be made about these assumptions. The thin-membrane assumption is valid if $2b \ll \lambda_l$ and λ_u, where $2b$ is the membrane thickness. It also requires that

$$T \frac{\partial^2 w}{\partial y^2} \gg \frac{E(2b)^3}{1 - \nu_p^2} \frac{\partial^4 w}{\partial y^4};$$

that is, the in-plane stretching forces in the membrane are much greater than flexural forces. Here T is the tension per unit length in the membrane, E is Young's modulus in the membrane, and ν_p is Poisson's ratio in the membrane. Furthermore the thickness $2b$ must be much less than the wavelengths of rotational and dilatational waves in the membrane itself [5].

It is assumed that w is much less than λ_l and λ_u because if $\lambda_u \neq \lambda_l$ and $w \sim O(\lambda_u)$, then an incident wave having a single spatial frequency η will be diffracted by the membrane and will propagate into the minitank with a multiplicity of spatial frequencies. This can have highly objectionable results on the acoustic imaging process. This subject will be considered in more detail later.

To calculate the transmission and reflection coefficients, it is necessary to derive the boundary conditions at the membrane. Continuity of vertical (z) velocity requires that

$$\dot{w} = \frac{\partial \phi_l}{\partial z} = \frac{\partial \phi_u}{\partial z} \tag{61}$$

at the membrane; now $z = 0$ at the membrane. Here ϕ_l and ϕ_u are velocity potentials for $z < 0$ and $z > 0$ respectively; that is, $\mathbf{v}_l = \nabla \phi_l$ and $\mathbf{v}_u = \nabla \phi_u$. Another condition is obtained by considering conservation of momentum. To this end a control volume of height Δz is erected straddling the membrane; see Fig. 7. Momentum conservation gives

$$\int \frac{\partial}{\partial t} (\rho \mathbf{v}) \, dV + \int \rho \mathbf{v} \mathbf{v} \cdot d\mathbf{A} = - \int p \, d\mathbf{A} + \int \mathbf{T} \, dx, \tag{62}$$

where

dV	=	volume element $(\Delta z) dx dy$,
$d\mathbf{A}$	=	area element,
$\mathbf{T}$	=	force per unit length in the membrane,
$\mathbf{v}$	=	velocity,
ρ	=	density,

and

p	=	pressure.

Letting $\Delta z \to 2b$, considering the force balance in the z direction, and using boundary condition (61) reduces (62) to

$$2\rho_M b \int \ddot{w} \, dA - \int (\rho_l - \rho_u) v_z^2 \, dA = \int (p_l - p_u) \, dA + \int T_z \, dx. \tag{63}$$
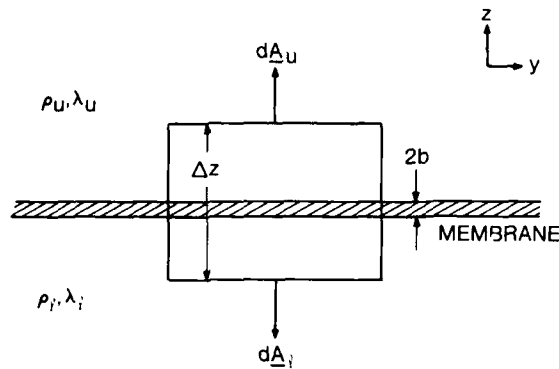
19

Fig. 7 — Control volume used to obtain the momentum
balance at the membrane

Constant membrane density ρ_M and thickness $2b$ are assumed. Here p_l is the pressure in the lower fluid, etc. Also, $v_z = v_{lz} = v_{uz}$ at the membrane $(z = 0)$; v_{lz} is the vertical particle velocity in the object tank and v_{uz} the vertical particle velocity in the minitank.

It is necessary to calculate T_z, the vertical force per unit length due to the tensioning of the membrane. The tension T in the membrane is assumed constant, so that the net T_z in Fig. 8 is

$$T_z = T[\sin (\theta + d\theta) - \sin \theta]. \tag{64}$$

For small displacements $\sin \theta \cong \tan \theta \cong \theta$ and $\tan \theta = \partial w/\partial y$; hence

$$\int T \, dx = T \int \frac{\partial^2 w}{\partial y^2} \, dy \, dx. \tag{65}$$

When the above is substituted into (63), there results

$$2\rho_M \, b\ddot{w} - T \frac{\partial^2 w}{\partial y^2} = (\rho_l - \rho_u)v_z^2 + (p_l - p_u). \tag{66}$$
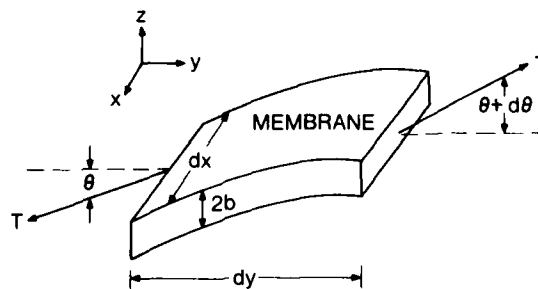

Fig. 8 — Membrane under uniform tension

20

The pair of equations (61) and (66) contain five unknowns: w, v_{lz}, v_{uz}, p_l, and p_u. Two more equations are obtained by considering the momentum equation

$$\rho(\dot{\mathbf{v}} + \mathbf{v} \cdot \nabla \mathbf{v}) = -\nabla p \tag{67}$$

as applied to the upper and lower fluids. Since the response of the membrane to an incident acoustic wave is being sought, one of the assumptions of linear acoustics, $|\mathbf{v}| \ll c$, is used; c is the sound speed in the fluid of interest. Then the momentum equation can be linearized and integrated to give $p = -\rho_0 \dot{\phi}$. Small density changes are assumed; that is, $\rho \cong \rho_0$, where ρ_0 is the equilibrium density.

The differential equation of the membrane can also be linearized for subsonic flow to give

$$2\rho_M \, b\ddot{w}_a - T \, \frac{\partial^2 w_a}{\partial y^2} = - (\rho_l \, \dot{\phi}_l - \rho_u \, \dot{\phi}_u) = \Delta p, \tag{68}$$

where Δp is the jump in the acoustic pressure at the membrane. The diplacement w_a, which is the response to the linear acoustic pressure, is measured from the position of static equilibrium of the membrane. (The response w_s of the membrane when nonlinear terms are retained will be calculated in section 5.6. The total membrane displacement w is the sum $w_a + w_s$.)

The reflection and transmission coefficients can now be calculated. By definition, $\bar{T}_{12} = \phi_{tr}/\phi_{inc}$, where the ratio is evaluated at the membrane. ϕ_{inc} is the velocity potential in an infinite acoustic plane wave incident on the membrane with spatial frequency η, and ϕ_{tr} is the velocity potential in the wave transmitted into the minitank. Let

$$\phi_{inc} = A \, e^{2\pi i \eta y} \, e^{2\pi i \zeta z} \, e^{-i\omega_a t}, \tag{69a}$$

$$\phi_{tr} = A \, \bar{T}_{12} \, (\eta) \, e^{2\pi i \eta y} \, e^{2\pi i \zeta_u z} \, e^{-i\omega_a t}, \tag{69b}$$

and

$$\phi_{refl} = A \, \bar{R}_{12} \, (\eta) \, e^{2\pi i \eta y} \, e^{-2\pi i \zeta z} \, e^{-i\omega_a t}, \tag{69c}$$

with ϕ_{refl} being the wave reflected back into the lower fluid.

The boundary condition $\dot{w}_a = \partial \phi_{tr}/\partial z$ on $z = 0$ gives

$$w_a(y, \, t) = - \frac{\bar{T}_{12} \, A}{\omega_a} \, 2\pi \, \zeta_u \, e^{2\pi i \eta y} \, e^{-i\omega_a t}. \tag{70}$$

Also, $\dot{w}_a = \partial(\phi_{inc} + \phi_{refl})/\partial z$ on $z = 0$, so

$$w_a = - \frac{A}{\omega_a} \, (1 - \bar{R}_{12}) \, 2\pi\zeta \, e^{2\pi i \eta y} \, e^{-i\omega_a t}, \tag{71}$$

which represents a ripple traveling along the membrane with spatial frequency η and phase velocity $\omega_a/(2\pi\eta)$. (Theoretically such a ripple would reach the minitank wall and be reflected. However, the results of Appendix B, which considers the effects of a finite wave impinging on a finite membrane, show this does not happen.)

With these results, the boundary condition (68) becomes

$$2\pi\zeta_u(-2\rho_M b\omega_a^2 + 4\pi^2\eta^2 T) \, \bar{T}_{12}(\eta) = -i\omega_a^2 \, [\rho_l(1 + \bar{R}_{12}) - \rho_u \bar{T}_{12}]. \tag{72}$$

Comparing terms on the left-hand side for the typical values

$$\omega_a = 2\pi(10^6) \text{ rad/s},$$
$$2b = 5(10^{-3}) \text{ cm},$$
$$\rho_M = 1.5 \text{ g/cm}^3,$$
$$T = 25 \text{ N/cm} = 2.5 (10^6) \text{ g/s}^2,$$

and

$$\lambda_l = 0.15 \text{ cm}$$

shows that $2\rho_M b\omega_a^2 >> 4\pi^2\eta^2 T$; that is, the inertial force of the membrane is much greater than the elastic restoring force. Using this inequality, and eliminating $\bar{R}_{12}$ via (70) and (71), allows (72) to be solved for $\bar{T}_{12}$:

$$\bar{T}_{12}(\eta) = \frac{2\rho_l \lambda_u \cos \theta_1}{\rho_l \lambda_l \cos \theta_2 + \rho_u \lambda_u \cos \theta_1 - 4\pi i \rho_M b \cos \theta_1 \cos \theta_2}. \qquad (73)$$

Recall that $\zeta = \cos \theta_1/\lambda_l$ and $\zeta_u = \cos \theta_2/\lambda_u$; see Fig. 5.

If $4\pi\rho_M b \cos \theta_1 \cos \theta_2 << (\rho_l\lambda_l \cos \theta_2 + \rho_u\lambda_u \cos \theta_1)$, the transmission coefficient reduces to the form appropriate to the interface between two acoustic fluids [1]. Let $\cos \theta_1 \sim O(1)$ and $\cos \theta_2 \sim O(1)$; the inequality is satisified for $\rho_M b << (\rho_u\lambda_u + \rho_l\lambda_l)$. The membrane is then said to be "light" and "thin". Satisfaction of the inequality $2\rho_M b\omega_a^2 >> 4\pi^2\eta^2 T$ shows that it is "flexible".

Suppose the lower fluid is water and the upper fluid is Freon E-5; then $\lambda_u = 0.47\lambda_l$ and $\rho_u = 1.8 \rho_l$. For $\omega_a = 2\pi(10^6)$ rad/s, $2b = 0.005$ cm, and $\rho_M = 1.5$ g/cm^3 there results

$$4\pi\rho_M b \cong 0.05 \text{ g/cm}^2,$$
$$\rho_l\lambda_l \cong 0.15 \text{ g/cm}^2,$$

and

$$\rho_u\lambda_u \cong 0.13 \text{ g/cm}^2.$$

It is seen that the effect of membrane inertia must be included in $\bar{T}_{12}$.

To calculate the reflection coefficient $\bar{R}_{21}$, it is necessary to solve the problem shown in Fig. 9. Here the plane wave incident on the membrane is traveling through the minitank (upper) fluid, and the transmitted wave emerges in the object tank. By definition, $\bar{R}_{21} = \phi_{refl}/\phi_{inc}$ at the membrane. An analysis similar to that performed in calculating $\bar{T}_{12}$ gives

$$\bar{R}_{21} = \frac{\rho_l\lambda_l \cos \theta_2 - \rho_u\lambda_u \cos \theta_1 - 4\pi i\rho_M b\cos \theta_1 \cos \theta_2}{\rho_l\lambda_l \cos \theta_2 + \rho_u\lambda_u \cos \theta_1 - 4\pi i\rho_M b\cos \theta_1 \cos \theta_2}. \qquad (74)$$

For a 0.005-cm-thick Tedlar membrane ($\rho_M \cong 2$ g/cm^3) separating Freon E-5 and water, $\bar{R}_{21} \cong 0.12 + 0.18i$ at 10 MHz, for $\cos \theta_1$ and $\cos \theta_2$ of the order of 1.

The expressions for $\bar{R}_{21}$ and $\bar{T}_{12}$ can now be substituted into (59) to determine $\bar{g}_1(\eta)$. The amplitude $|\bar{g}_1(\eta)|$ and phase angle $\angle\bar{g}_1(\eta)$ are plotted in Figs. 10 and 11 for various depth-to-wavelength ratios d/λ_u. The imaging fluid is assumed to be Freon E-5, and the object-tank fluid is water. The membrane density is taken to be 1.5 g/cm^3, and its thickness is assumed to be $\lambda_l/12$. As before, $\eta = (\sin \theta_1)/\lambda_l$.
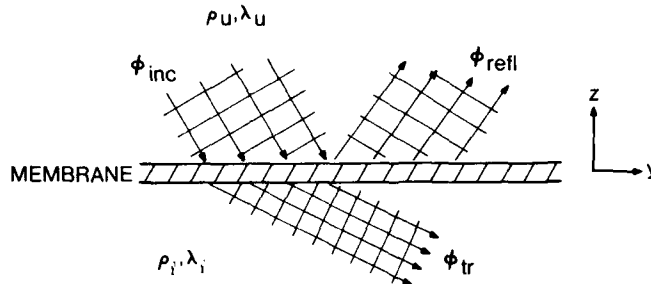
Fig. 9 — Quantities used in calculating the reflection coefficient $\bar{R}_{21}$
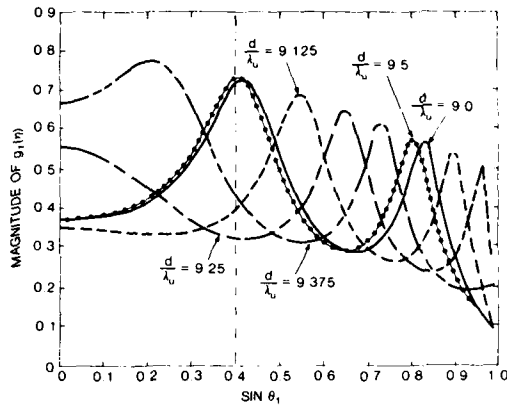
The cutoff imposed by a typical acoustic lens system is shown by the dashed vertical line in these figures. The cutoff corresponds to $D_1 = f_1$ and $D_2 = f_2$ in the focusing condition (18); that is, the object plane is the front focal plane of lens L_1, and the image plane is the back focal plane of L_2. It is assumed that $a/f_2 = 0.4$.

The plots in the right-hand columns in Figs. 10 and 11 correspond to the case $4\pi\rho_M b \ll \rho_u\lambda_u + \rho_l\lambda_l$ and were calculated by the authors of Refs. 1 and 2. Comparing the negligible membrane inertia curves with those which account for membrane inertia shows that for moderate depths $(d/\lambda_u \cong 2)$ and large depths $(d/\lambda_u \cong 10)$ the membrane shrinks the region where $\bar{g}_1(\eta) \cong$ constant. The acoustic image cannot be faithfully recorded unless $\bar{g}_1(\eta) \cong$ constant over the range of spatial frequencies passed by the acoustic lens system. Another effect of the membrane is to accentuate constructive and destructive interference effects at the liquid surface; these are indicated respectively by local maxima and minima on the $|\bar{g}_1(\eta)|$ plots.

The figures clearly indicate that better image fidelity is obtained at moderate depths $(d/\lambda_u \cong 2)$ and shallow depths $(d/\lambda_u \cong 0.1)$ than at large depths, even including effects of membrane inertia. Note the extreme sensitivity of $|\bar{g}_1(\eta)|$ to changes in d/λ_u for large depths. For example, Fig. 10b shows that a minitank depth of $9.5\lambda_u$ will accentuate high-frequency components of $\psi_1(\eta)$ (those near cutoff). This is useful for enhancing edge detection in the object. However, a depth of $9.375\lambda_u$ will have the opposite effect. Since a depth change of $0.125\lambda_u$ is typically about 10 μm, a method of controlling the minitank depth is desirable.

Of interest is the improvement in system performance which can result from using imaging and object-tank fluids which are dissimilar, when the membrane must be taken into account. Figure 12 shows that constructive interference effects become more pronounced when water is employed as both the imaging fluid and the object-tank fluid. Note the similiarity between the curves in Figs. 12a and 10a and between the curves in Figs. 12b and 11a. Note, however, that $d/\lambda_u \cong 2$ in Fig. 12, whereas $d/\lambda_u \cong 9$ in Figs. 10a and 11a. Hence, in the presence of the membrane, interference effects due to multiple internal reflections in the minitank become noticeable at lower d/λ_u ratios when both fluids are water.

Figure 12a also shows the behavior of $\bar{g}_1(\eta)$ for the case $4\pi\rho_M b \ll \rho_u\lambda_u$, with $\rho_u = \rho_l$. In this case $\bar{g}_1(\eta) = \sqrt{1 - \eta^2/k_u^2}$. Note that $\bar{g}_1(\eta)$ is fairly constant over the range of spatial frequencies passed by the acoustic lens system when $4\pi\rho_M b \ll \rho_u\lambda_u$. It is necessary to retain the membrane to isolate the liquid surface from environmental disturbances, so that $\rho_M b$ cannot vanish. It remains a matter of experiment to see if better imaging can be obtained by reducing $\rho_M b/\rho_u\lambda_u$ such that it is much less than 1 and using identical imaging and object-tank fluids.

23

(a) Large minitank depths assumed (d/λ_u = 9 to 9.5) and significant membrane inertia (ρ_M/ρ_l = 1.5 and $2b/\lambda_l$ = 0.0833)

(b) Large minitank depths assumed (d/λ_u = 9 to 9.5) and negligible membrane inertia

(c) Moderate minitank depths assumed (d/λ_u = 2 to 2.5) and significant membrane inertia (ρ_M/ρ_l = 1.5 and $2b/\lambda_l$ = 0.0833)

(d) Moderate minitank depths assumed (d/λ_u = 2 to 2.5) and negligible membrane inertia

(e) Small minitank depths assumed (d/λ_u = 0.125 to 0.5) and significant membrane inertia (ρ_M/ρ_l = 1.5 and $2b/\lambda_l$ = 0.0833)

(f) Small minitank depths assumed (d/λ_u = 0.125 to 0.5) and negligible membrane inertia

Fig. 10 — Magnitude of the minitank transfer function for a membrane separating Freon E-5 and water (ρ_u/ρ_l = 1.8 and λ_u/λ_l = 0.47)
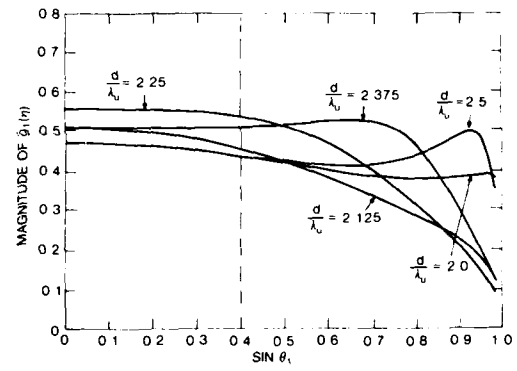
24

(a) Large minitank depths assumed $(d/\lambda_u = 9$ to 9.5) and significant membrane inertia $(\rho_M/\rho_l = 1.5$ and $2b/\lambda_l = 0.0833)$
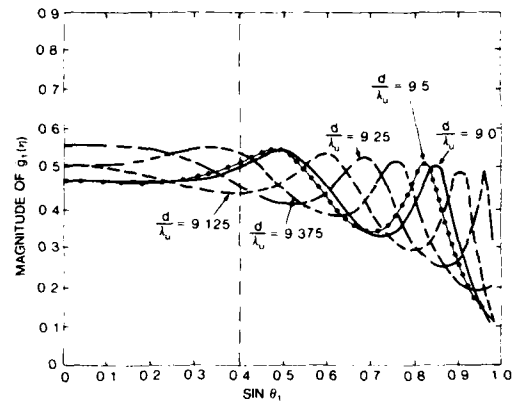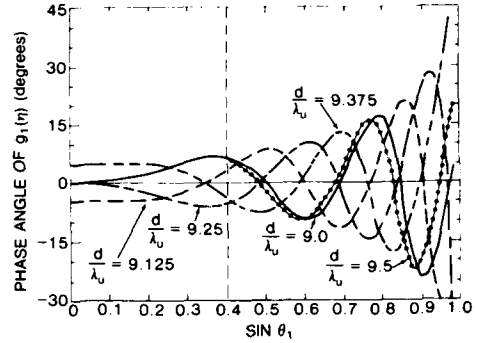
(b) Large minitank depths assumed $(d/\lambda_u = 9$ to 9.5) and negligible membrane inertia
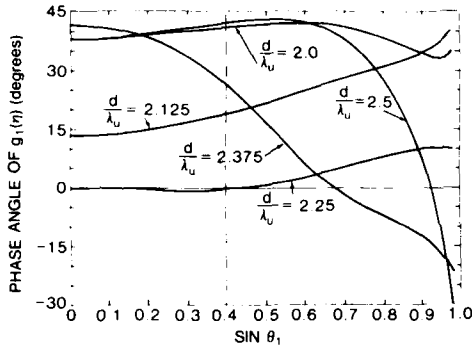
(c) Moderate minitank depths assumed $(d/\lambda_u = 2$ to 2.5) and significant membrane inertia $(\rho_M/\rho_l = 1.5$ and $2b/\lambda_l = 0.0833)$
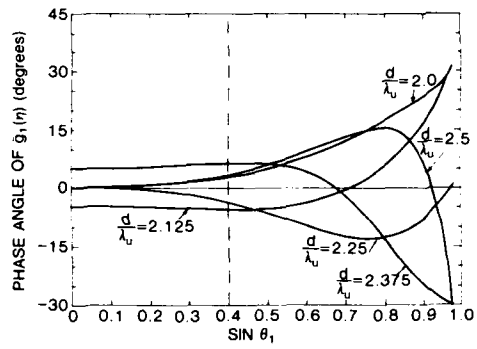
(d) Moderate minitank depths assumed $(d/\lambda_u = 2$ to 2.5) and negligible membrane inertia
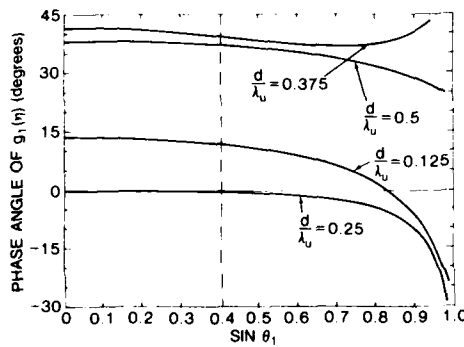
(e) Small minitank depths assumed $(d/\lambda_u = 0.125$ to 0.5) and significant membrane inertia $(\rho_M/\rho_l = 1.5$ and $2b/\lambda_l = 0.0833)$

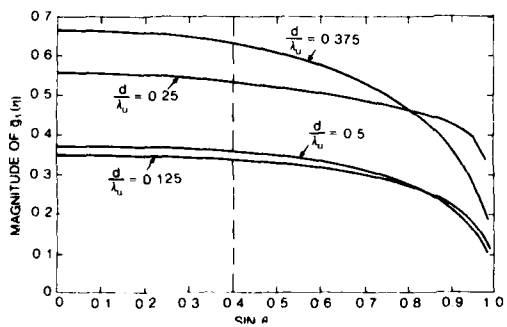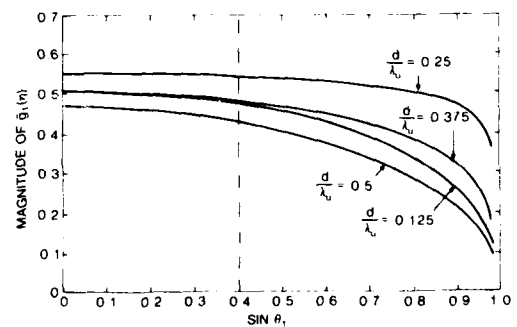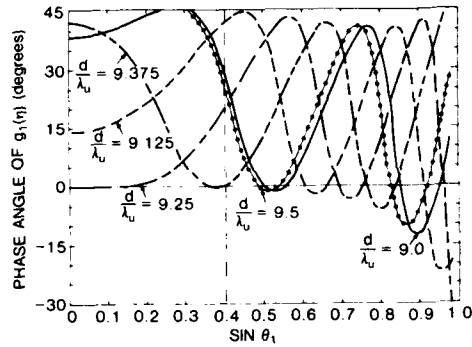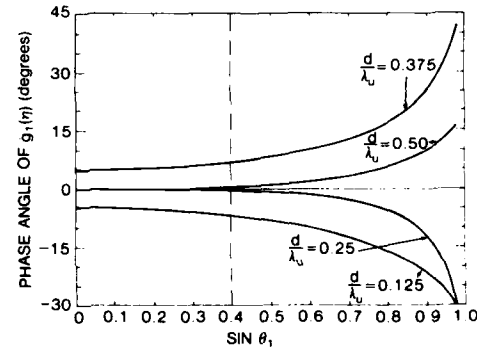(f) Small minitank depths assumed $(d/\lambda_u = 0.125$ to 0.5) and negligible membrane inertia

Fig. 11 — Phase angle of the minitank transfer function for membrane separating Freon E-5 and water $(\rho_u/\rho_l = 1.8$ and $\lambda_u/\lambda_l = 0.47)$

25
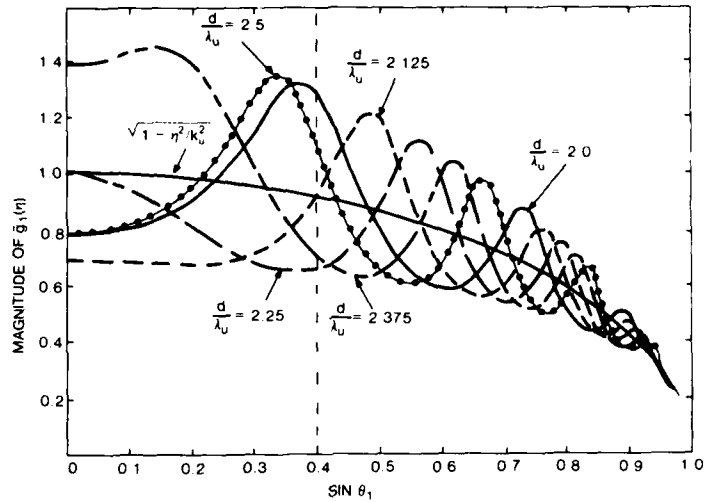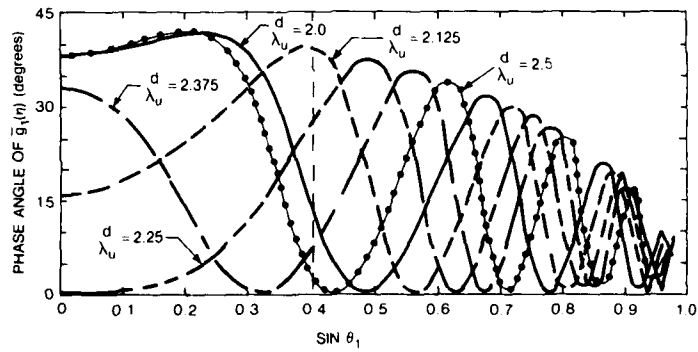
(a) Magnitude

(b) Phase angle

Fig. 12 — Magnitude and phase angle of the minitank transfer function for a membrane $(\rho_M/\rho_I = 1.5$ and $2b/\lambda_I = 0.0833)$ separating identical fluids $(\rho_u/\rho_I = 1$ and $\lambda_u/\lambda_I = 1)$

3.3 Effect of the Membrane Displacement on Acoustic Imaging

In calculating $\overline{T}_{12}$ and $\overline{R}_{21}$ it was assumed that the membrane displacement w is much less than λ_I and λ_u. The reason for this assumption and the consequences of its violation will now be examined. For simplicity it is assumed that the membrane is deformed into a sinusoidal standing-wave pattern such that $w = W \cos 2\pi\eta'y$; recall that $w = w_a + w_s$. The effect of this displacement on one spatial frequency component of the focused acoustic image will be considered.

This situation is depicted in Fig. 13, where the incident wave ϕ_{inc} is of the form

$$\phi_{inc} = A\ e^{2\pi i \eta y}\ e^{2\pi i \zeta z}\ e^{-i\omega_a t}. \tag{75}$$

26
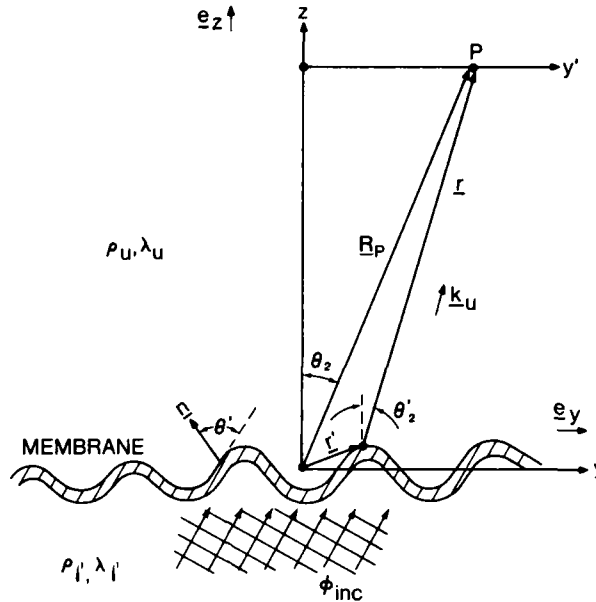
Fig. 13 — Quantities used in the far-field calculation of a
wave diffracted by a membrane

The field ϕ_{tr} transmitted into the minitank is calculated from the Helmholtz integral equation
(1), which can be put in the form

$$4\pi\phi_{tr} = \int \left[\phi_{tr} \frac{\partial}{\partial n} \left(\frac{e^{ik_u \cdot r}}{r} \right) - \frac{e^{ik_u \cdot r}}{r} \frac{\partial \phi_{tr}}{\partial n} \right] dy, \tag{76}$$

where the integration is over the membrane. Here

$$k_u = \frac{2\pi}{\lambda_u} (e_y \sin \theta_2' + e_z \cos \theta_2'), \tag{77}$$

with e_y and e_z being unit vectors and θ_2' being the angle between r and the z axis (Fig. 13). The
unit normal to the membrane is n, and $n = |n|$.

Consider a point P far removed from the membrane such that $\theta_2' \cong \theta_2$, with θ_2 being the
angle between the z axis and the vector R_P connecting the origin with the point P. Let r' be a
vector from the origin to a point on the membrane. Since $r = R_P - r'$ and $|R_P| \gg |r'|$ for
$\theta_2' \cong \theta_2$,

$$\frac{e^{ik_u \cdot r}}{r} \cong \frac{e^{ik_u R_P}}{R_P} e^{-ik_u(y\sin\theta_2 + z\cos\theta_2)}. \tag{78}$$

Here $k_u = 2\pi/\lambda_u$ and the relation $r' = ye_y + ze_z$ has been used. Now if $(\partial w/\partial y) \ll 1$, then
$\partial/\partial n \cong \partial/\partial z$ and

$$\frac{\partial}{\partial n} \left(\frac{e^{ik_u \cdot r}}{r} \right) \cong \frac{e^{ik_u R_P}}{R_P} (-ik_u \cos \theta_2) e^{-ik_u(y\sin\theta_2 + z\cos\theta_2)}. \tag{79}$$

27

Let $\phi_{tr} = \bar{T}_{12}(\theta')\phi_{inc}$ at the membrane, where $\bar{T}_{12}(\theta')$ is the local transmission coefficient and θ' is the local angle of incidence. This assumes that the membrane can be considered locally flat, which requires that the radius of curvature be much larger than the acoustic wavelength [6]. It is also required that $(\eta')^{-1} \gg \lambda_u$ and λ_l. As shown in Fig. 13, θ' is the angle between $\mathbf{n}$ and the direction of propagation of the incident wave ϕ_{inc}. With θ_1 indicating the angle between the z axis and the direction of propagation of ϕ_{inc},

$$\bar{T}_{12}(\theta') \cong \bar{T}_{12}(\theta_1) + \frac{\partial \bar{T}_{12}(\theta_1)}{\partial \theta} (\theta' - \theta_1). \tag{80}$$

Since $\bar{T}_{12}$ is as given by (73), it is easy to show that $\partial \bar{T}_{12}(\theta_1)/\partial\theta \sim O[\bar{T}_{12}(\theta_1)]$. Furthermore $\theta' - \theta_1 \cong \partial w/\partial y$ at the membrane for small slopes; hence, if $\partial w/\partial y \ll 1$, then $\bar{T}_{12}(\theta') \cong \bar{T}_{12}(\theta_1)$ and $\phi_{tr} \cong \bar{T}_{12}(\theta_1)\phi_{inc}$. In like fashion it is found that, for $\phi_{inc} = Ae^{ik_l(y\sin\theta_1 + z\cos\theta_1)}$,

$$\frac{\partial \phi_{tr}}{\partial n} \cong ik_l \cos\theta_1 \, \bar{T}_{12}(\theta_1) \, e^{ik_l(y\sin\theta_1 + w\cos\theta_1)} \tag{81}$$

at the membrane.

Combining all results gives

$$\phi_{tr} = \frac{-iA}{4\pi R_P} e^{ik_u R_P} \bar{T}_{12}(\theta_1) e^{-i\omega_a t} \left[\int (k_u \cos\theta_2 + k_l \cos\theta_1) \right.$$
$$\left. \times e^{i(k_l\sin\theta_1 - k_u\sin\theta_2)y} e^{i(k_l\cos\theta_1 - k_u\cos\theta_2)w} \, dy \right]. \tag{82}$$

Let the further restriction of a bounded incident beam be added; that is, at the membrane $\phi_{inc} = A e^{ik_l y\sin\theta_1} e^{ik_l z\cos\theta_1}$ Rect (y/y_b). If $R_P \gg y_b$, then $k_u \cos\theta_2 \cong$ constant in (82). The term $e^{i(k_l\cos\theta_1 - k_u\cos\theta_2)w}$ becomes [7]

$$e^{i(k_l\cos\theta_1 - k_u\cos\theta_2)w} = \sum_{m=-\infty}^{\infty} \{i^m J_m([k_l\cos\theta_1 - k_u\cos\theta_2] W) e^{-2\pi i m\eta' y}\}, \tag{83}$$

where J_m is the mth-order Bessel function of the first kind. Consequently

$$\phi_{tr} \propto A \, \bar{T}_{12}(\theta_1) \sum_m \left\{ i^m J_m([k_l\cos\theta_1 - k_u\cos\theta_2] W) \int_{-\infty}^{\infty} \text{Rect } (y/y_b) \, e^{2\pi i\eta_m y} \, dy \right\}. \tag{84}$$

where $\eta_m \equiv (1/\lambda_l)\sin\theta_1 - (1/\lambda_u)\sin\theta_2 - m\eta'$ has units of spatial frequency. Performing the integration gives

$$\phi_{tr} \propto A \, \bar{T}_{12}(\theta_1) \sum_m \left\{ i^m J_m([k_l\cos\theta_1 - k_u\cos\theta_2] W) \text{ sinc } (2\pi\eta_m y_b) \right\}. \tag{85}$$

For the point P in the y' plane as shown in Fig. 13, $\sin\theta_2 \cong y'/R_P$. Furthermore, from Snell's law, $(\sin\theta_1)/\lambda_l = (\sin\tilde{\theta}_2)/\lambda_u$, where $\tilde{\theta}_2$ is the angle between the z axis and the direction of propagation of ϕ_{tr} when the membrane is flat. The zero diffracted order is proportional to sinc $(2\pi\eta_0 y_b)$, a sinc function centered at $y' = R_P \tilde{\theta}_2$; the width of its main lobe is $R_P\lambda_u/y_b$. Similarly the Mth diffracted order is proportional to a sinc function centered at $y' = R_P\tilde{\theta}_2 - NR_P\lambda_u\eta'$ and also has a main-lobe width $R_P\lambda_u/y_b$.

Hence the field in the y' plane consists of various diffracted orders, whose magnitudes are given by $J_m(k'W)$, where $k' = k_l\cos\theta_1 - k_u\cos\theta_2$. Unless $J_m(k'W) \to 0$ for $m > 0$, (85)

predicts that when the membrane is insonified by an incident beam having one spatial frequency, the transmitted field will consist of beams having a multiplicity of spatial frequencies. Obviously this multiplicity will degrade the focused acoustic image.

This multiplicity is avoided if $k'W \ll 1$, since $J_m(k'W) \propto (k'W)^{|m|}$ for small values of the argument. The inequality requires either that $k_u \cong k_l$ or that the membrane displacement be much less than an acoustic wavelength. When $k'W \ll 1$, (84) shows that the far-field velocity potential is proportional to the Fourier transform of the incident velocity potential multiplied by the transmission factor $\overline{T}_{12}(\theta_1)$.

Several remarks are in order here. It should be recalled that, in order to use linear acoustic theory, $|\mathbf{v}|$ must be much less than c. For quasimonochromatic radiation this requires that fluid particle displacement be much less than an acoustic wavelength. Since w_a equals the normal component of the particle displacement at the membrane, the requirement $w_a \ll \lambda_a$ is automatically satisfied.

However, the displacement w_a as calculated in section 3.2 is the response to the first-order acoustic pressure. There will also be a displacement w_s due to nonlinear terms in the membrane equation of motion (66); w_s will be calculated in section 5.6. The total displacement is $w_a + w_s$. It is possible for w_s to exceed an acoustic wavelength if the nonlinear pressure is large enough. This subject will be taken up in more detail in section 5.7.

Another point to be made is that the calculations performed above are valid at large distances from the insonified portion of the membrane. However, the minitank depth is typically of the order of λ_u, so that strictly speaking the above analysis is not appropriate to the actual operational system; that is, the exact form of ϕ_{tr} near the membrane will not be given by (85). Nevertheless the requirement $k'W \ll 1$ for no distortion of the acoustic image still remains valid, even near the membrane.

This conclusion is based on the following line of reasoning. For small displacements such that $k'W \ll 1$ the transmitted velocity potential is approximated by

$$\phi_{tr} \propto A \, \overline{T}_{12}(\theta_1) \sum_{m=-\infty}^{\infty} i^m J_m(k'W) \, e^{ik_u(y\sin\theta_m + z\cos\theta_m)}, \tag{86}$$

with $\sin\theta_m = \sin\theta_1 + 2\pi m \eta'/k_u$. The transmitted field consists of various diffracted orders in the form of plane waves propagating with direction cosines given by $\cos\theta_m$. This result is true at points near the membrane when the finite size of the incident beam can be ignored. As the membrane displacement is increased, the amplitude of the diffracted orders $m \neq 0$ will increase, at the expense of the $m = 0$ order.

For a point S on the liquid surface, the total velocity potential is the sum of all velocity potentials in the orders incident upon it (Fig. 14). The sum is approximately over all orders having inclination angles θ_m such that $y(S) - y_b \leqslant d\tan\theta_{2m} \leqslant y(S) + y_b$. Here $y(S)$ is the y coordinate of the point S and y_b is the beamwidth. Since $y(S) + y_b \gg d$ for $d \sim O(\lambda_u)$, there will in general be many orders incident on point S. To faithfully record the acoustic image on the surface, all orders except $m = 0$ must be suppressed, which again leads to the requirement $k'W \ll 1$.
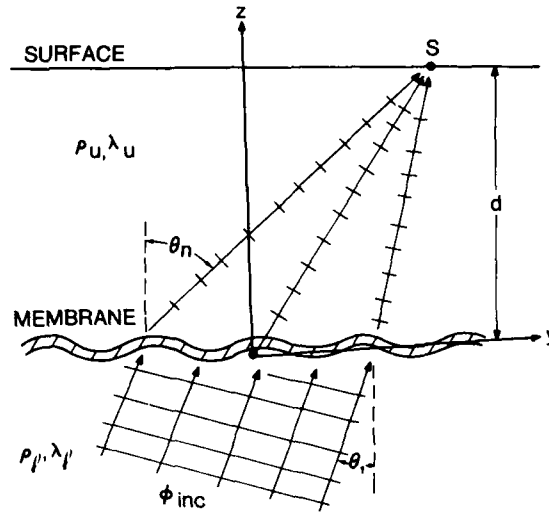
Fig. 14 — Diffracted orders of sound incident
on the liquid surface

4. EFFECT OF INTERFERENCE BETWEEN THE ACOUSTIC IMAGE AND THE REFERENCE BEAM

Consider the momentum balance for an inviscid fluid with negligible body forces:

$$\int \frac{\partial}{\partial t}(\rho v) \, dV = - \int (\rho vv \cdot n + pn) \, dA. \tag{87}$$

Here the volume integral represents the time rate of change of momentum of fluid within the control volume V. The surface integral is the flux of momentum out of the surface A bounding the control volume, and n is the unit vector normal to the surface. Hence the vector $\rho vv \cdot n + pn$ is the momentum flux per unit area.

Suppose the time-varying part of v is $ie^{-i\omega_a t}$ Rect $(\hat{t}/\Delta t)$. Then vv is to be interpreted as Re (v) Re (v), where Re (v) denotes the real part of v. The time-varying part of vv is $\sin^2\omega_a t$ Rect $(\hat{t}/\Delta t)$, which equals $(1/2)$ $(1 - \cos 2\omega_a t)$ Rect $(\hat{t}/\Delta t)$. Note that Re (v) Re (v) has a low-frequency term $(1/2)$ Rect $(\hat{t}/\Delta t)$ and a high-frequency term $(1/2)$ $\cos 2\omega_a t$ ×Rect $(\hat{t}/\Delta t)$, for $\omega_a \gg 1/\Delta t$. The low-frequency term is proportional to $<vv>$ Rect $(\hat{t}/\Delta t)$, where

$$<vv> = \frac{1}{2\Delta t} \int_0^{2\Delta t} \text{Re } (v) \text{ Re } (v) \, dt; \tag{88}$$

that is, $<vv>$ is the time average of Re (v) Re (v) over the pulse duration $2\Delta t$. The pressure p will be shown in section 5 to contain a component which also does not average to zero over the pulse duration. Consequently the momentum flux per unit area will have a low-frequency component and a high-frequency component. Consider the low-frequency component, and let

$$[<\rho vv \cdot n> + <pn>] \text{ Rect } (\hat{t}/\Delta t) \equiv P_r, \tag{89}$$

where P_r is called the radiation pressure vector [8].

30

Suppose the control volume of (87) is erected such that it straddles the interface between two fluids. Then the momentum flux/area out of the control volume is

$$-\mathbf{P}_r = [<(\rho_l \mathbf{v}_l \mathbf{v}_l - \rho_u \mathbf{v}_u \mathbf{v}_u) \cdot \mathbf{n}_u > + <(p_l - p_u)\mathbf{n}_u>] \text{ Rect } (\hat{t}/\Delta t), \tag{90}$$

where ρ_l is the density in lower fluid, the other subscripted quantities have related definitions, and the vector $\mathbf{n}_u$ points into the upper fluid. If (90) is evaluated at the liquid surface of the minitank, where $\rho_l \gg \rho_u$ and $p_l \gg p_u$, then

$$-\mathbf{P}_r = [<\rho_l \mathbf{v}_l \mathbf{v}_l \cdot \mathbf{n}_u> + <p_l \mathbf{n}_u>] \text{ Rect } (\hat{t}/\Delta t). \tag{91}$$

Anticipating a result to be derived in section 5, it is the vertical (z) component of $-\mathbf{P}_r$ which levitates the liquid surface; for simplicity the quantity $-\mathbf{P}_r \cdot \mathbf{n}_u$ is denoted as P_r, the radiation pressure. Hence the liquid surface responds to the vertical component of the low-frequency portion of the momentum flux per unit area incident on the liquid surface. The momentum flux is due to the presence of the focused acoustic image ψ_1 and the reference beam ϕ_r.

At the liquid surface P_r can be reduced to the simpler form

$$P_r = \frac{1}{2} \rho_u <v_z^2> \text{ Rect } (\hat{t}/\Delta t), \tag{92}$$

which is done in section 5. In (92) ρ_u is now the equilibrium density of the imaging fluid and v_z is the vertical velocity as predicted by linear acoustic theory at the liquid surface. Let

$$v_{oz} = |V_o(y)| e^{i\chi_o(y)} e^{-i\omega_a t} \text{ Rect } (\hat{t}/\Delta t) \tag{93a}$$

and

$$v_{rz} = |V_r(y)| e^{i\chi_r(y)} e^{-i\omega_a t} \text{ Rect } (\hat{t}/\Delta t), \tag{93b}$$

where it will be recalled that v_{oz} is the vertical component of the particle velocity in the object's acoustic image, and v_{rz} is the corresponding quantity in the reference beam. Then

$$<v_z^2> = <[\text{Re } (v_{oz}) + \text{Re } (v_{rz})]^2 > \tag{94a}$$

$$= \frac{1}{2} [|V_o|^2 + |V_r|^2 + 2|V_o||V_r| \cos (\chi_o - \chi_r)], \tag{94b}$$

where it is required that $\omega_a \Delta t \gg 1$. It is assumed that both transducers operate at the same frequency or, if the difference in frequency between the transducers is $\Delta\omega$, it is sufficient to require $\Delta\omega \Delta t \ll 1$. Using (94b) in (92) gives for the radiation pressure at the liquid surface

$$P_r = \frac{1}{4} \rho_u [|V_o|^2 + |V_r|^2 + 2|V_o||V_r| \cos (\chi_o - \chi_r)] \text{ Rect } (\hat{t}/\Delta t). \tag{95}$$

Each term can be given a physical interpretation. For example the term $\rho_u |V_o(y)|^2/4$ is the radiation pressure if only the focused acoustic image is present. Likewise, $\rho_u |V_r|^2/4$ is the radiation pressure due to the reference beam only.

The term $\frac{1}{2}\rho_u |V_o||V_r| \cos (\chi_o - \chi_r)$ can be rewritten in the form

$$\frac{1}{4}\rho_u [(|V_o|e^{i\chi_o}) (|V_r|e^{-i\chi_r}) + (|V_o| e^{-i\chi_o}) (|V_r| e^{i\chi_r})].$$

31

From (58) and (60),

$$v_z = 2ik_u g_1(y) \overset{s}{\oplus} [\psi_1(y) + \phi_r(y)] e^{-i\omega_a t} \text{Rect} (\hat{t}/\Delta t), \tag{96}$$

where $g_1(y)$ is the inverse transform of the minitank transfer function $\bar{g}_1(\eta)$. From (93) through (96),

$$\frac{1}{2}\rho_u |V_o||V_r| \cos(\chi_o - \chi_r) = \frac{1}{2}\rho_u \left[\left(g_1 \overset{s}{\oplus} \psi_1\right) \left(g_1 \overset{s}{\oplus} \phi_r\right)^* + \left(g_1 \overset{s}{\oplus} \psi_1\right)^* \left(g_1 \overset{s}{\oplus} \phi_r\right) \right], \tag{97}$$

where $g_1 \overset{s}{\oplus} \psi$, represents the action of the minitank on the focused acoustic image, an asterisk indicates a complex conjugate, and a factor $2ik_u$ has been absorbed into $g_1(y)$. Hence the term $(1/2) \rho_u |V_o||V_r| \cos (\chi_o - \chi_r)$, due to the interference between the reference beam and the the acoustic image, contains a term $P_{ri} \equiv (1/4)\rho_u(g_1 \overset{s}{\oplus} \psi_1) (g_1 \overset{s}{\oplus} \phi_r)^*$ carrying information about the image and a term $P_{rc} \equiv P_{ri}^*$ containing information about its complex conjugate.

It is also interesting to take the spatial Fourier transform of P_r and consider the meaning of each term in the spatial frequency domain. For instance,

$$\frac{1}{4} \rho_u |\bar{V}_o(\eta)|^2 = \frac{1}{4} \rho_u [\bar{g}_1(\eta)\bar{\psi}_1(\eta)] \overset{\eta}{\oplus} [\bar{g}_1(\eta) \bar{\psi}_1(\eta)]^* = \bar{P}_{ro}(\eta), \tag{98}$$

where $\overset{\eta}{\oplus}$ denotes the convolution operation in the spatial frequency domain. As was indicated by (22), the maximum bandwidth of spatial frequencies in $\bar{\psi}_1(\eta)$ passed by the acoustic lens system is $|\eta| \leqslant \eta_m$. Convolution causes the bandwidth of $\bar{P}_{ro}$ to extend from $-2\eta_m$ to $2\eta_m$ (Fig. 15).
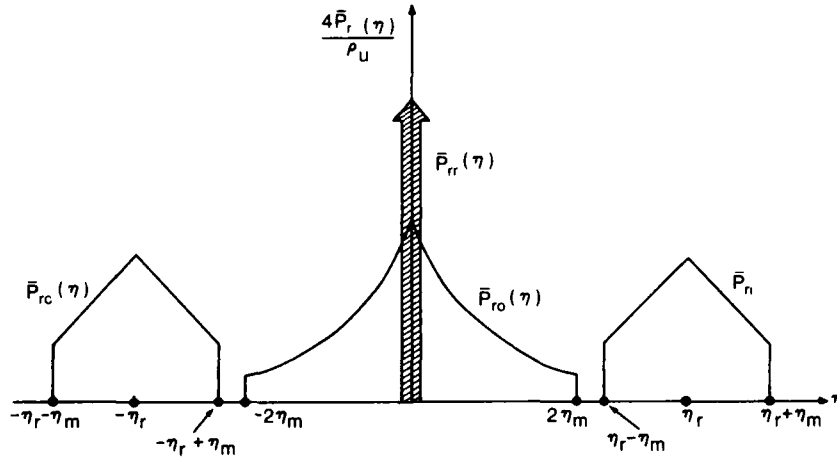
Fig. 15 — Spatial frequency components of $\bar{P}_r(\eta)$

Suppose that $\phi_r = A_r e^{-2\pi i \eta_r y}$ at the liquid surface; then $\bar{\phi}_r(\eta) = A_r \delta(\eta - \eta_r)$ and

$$\frac{1}{4} \rho_u |\bar{V}_r(\eta)|^2 = \frac{1}{4} A_r^2 \rho_u |\bar{g}_1(\eta_r)|^2 \delta(\eta) = \bar{P}_{rr}(\eta). \tag{99}$$

Hence the radiation pressure $\bar{P}_{rr}$ in the reference beam has only a "d.c." term in the spatial frequency domain, as shown in Fig. 15.

The radiation pressure $\bar{P}_{rb}(\eta)$ given by

$$\bar{P}_{rb}(\eta) \equiv \frac{1}{4} \rho_u \left\{ [\bar{g}_1(\eta)\bar{\psi}_1(\eta)] \overset{\eta}{\oplus} [\bar{g}_1^{\bullet}(\eta)\bar{\psi}_1^{\bullet}(\eta)] + A_r^2 |\bar{g}_1(\eta_r)|^2 \, \delta(\eta) \right\} \qquad (100)$$

will cause a low spatial frequency levitation $\bar{h}_b(\eta)$ of the liquid surface. This "bulge" is the "background" in the phase hologram caused by levitation of the liquid surface.

The "image" term $\bar{P}_{ri}(\eta)$ is given by

$$\bar{P}_{ri} = \frac{1}{4} \rho_u A_r \bar{g}_1^{\bullet}(\eta_r) [\bar{g}_1(\eta_1)\bar{\psi}_1(\eta_1)]_{\eta_1 = \eta - \eta_r}; \qquad (101)$$

that is, the action of the reference beam is to upshift the spatial frequency components of $\bar{g}_1(\eta)\bar{\psi}_1(\eta)$ by an amount η_r. This is depicted in Fig. 15. Likewise, the conjugate image term has its spectrum downshifted by an amount η_r:

$$\bar{P}_{rc}(\eta) = \frac{1}{4} \rho_u A_r \bar{g}_1(\eta_1) [\bar{g}_1^{\bullet}(\eta_1) \; \bar{\psi}_1^{\bullet}(\eta_1)]_{\eta_1 = \eta + \eta_r}. \qquad (102)$$

In Fig. 15 it is assumed that $\eta_r > 3\eta_m$, so that the spectrum of $\bar{P}_{rb}$ does not overlap those of $\bar{P}_{ri}$ and $\bar{P}_{rc}$. This allows information about the image to be extracted upon optical reconstruction of the phase hologram at the liquid surface. Otherwise light scattered from the bulge h_b will also be present as "noise" in the optical image. More will be said about this later.

In reality the reference beam is finite in lateral extent, so that at the liquid surface $\phi_r = A_r e^{-2\pi i \eta_r y}$ Rect (y/y_b), where y_b is the width of the reference beam. Then, with the assumption $\bar{g}_1(\eta) \cong$ constant over $\eta \sim O(\pi/y_b)$,

$$\bar{\phi}_r^{\bullet} \propto A_r \, \text{sinc} \, (2\pi(\eta - \eta_r)y_b) \qquad (103)$$

and

$$\bar{P}_{ri} \propto A_r \, [\bar{g}_1(\eta)\bar{\psi}_1(\eta)] \overset{\eta}{\oplus} \bar{g}_1^{\bullet}(\eta) \, \text{sinc} \, (2\pi(\eta - \eta_r)y_b). \qquad (104)$$

This represents an upshift of $\bar{g}_1(\eta)\bar{\psi}_1(\eta)$ by an amount η_r followed by a scanning by the sinc function. For large simple objects such that the dominant spatial frequencies of $\bar{\psi}_1$ are small compared to π/y_b, the convolution operation causes a distortion; that is, $\bar{P}_{ri}$ is no longer proportional to $\bar{\psi}_1(\eta - \eta_r)$. For complex objects which have most of their spatial frequencies in the range $|\eta| \gg \pi/y_b$,

$$[\bar{g}_1(\eta) \, \bar{\psi}_1(\eta)] \overset{\eta}{\oplus} \text{sinc} \, (2\pi(\eta - \eta_r)y_b) \cong [\bar{g}_1(\eta_1)\bar{\psi}_1(\eta_1)]_{|\eta_1 = \eta - \eta_r}; \qquad (105)$$

so the spatial frequency content of $\bar{g}_1(\eta)\bar{\psi}_1(\eta)$ is preserved.

Let the surface levitation caused by $\bar{P}_{ri}$ be denoted $\bar{h}_i$ and that caused by $\bar{P}_{rc}$ be $\bar{h}_c$. Either $\bar{h}_i$ or $\bar{h}_c$ represents a phase hologram, which, when illuminated with laser light, can be used to reconstruct the acoustic image. With the assumption that $\bar{P}_{ri}$ is to be used for imaging, the transfer function which relates this quantity with $\bar{v}_{oz}(\eta, t)$ is proportional to the convolution of sinc $(2\pi(\eta - \eta_r)y_b)$ with $\bar{v}_{oz}$, as shown in Fig. 16.

$$\overset{\eta}{\oplus} \left[\frac{1}{4} \ \rho_u \ A_r \ g_i{}^* \ (\eta_r) \ \text{sinc} \ (2\pi(\eta - \eta_r)y_b) \right]$$

$\bar{v}_{oz} (\eta, t)$ $\bar{P}_{r_i} (\eta) \ \text{Rect}\left(\dfrac{\hat{t}}{\Delta t}\right)$
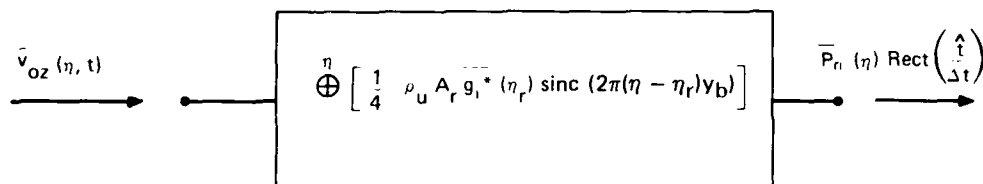
Fig. 16 — Transfer function for the interference between the acoustic image and the reference beam

5. RESPONSE OF THE LIQUID SURFACE

This section considers the response of the liquid surface to a pulse of radiation pressure. In the minitank, perturbations in velocity, pressure, and density are caused by the acoustic field. The radiation pressure in the acoustic field causes the liquid surface to levitate. The motion of the liquid surface in turn induces additional perturbations in velocity, pressure, and density in the minitank.

The nonlinearity of the equations of mass and momentum conservation which govern the behavior of the imaging fluid could conceivably cause a coupling between, for example, velocities in the acoustic field and in the field induced by surface motion. This could lead to serious problems in recording the acoustic image at the liquid surface. However, it will be shown that to the degree of approximation considered here the acoustic field is unaffected by motion of the surface.

The radiation pressure is caused by nonlinear effects in the acoustic field which result in a steady momentum flux per unit area. To show how this comes about, it is advantageous to review some results of nonlinear acoustic theory.

5.1 Nonlinear Acoustics

Consider the propagation of an acoustic wave through an inviscid homogenous fluid. Let the density ρ and acoustic particle velocity v be given by $\rho = \rho_0 + \rho_{1a} + \rho_{2a}$ and $v = v_{1a} + v_{2a}$, where ρ_0 is the density in the equilibrium state of the fluid and ρ_{1a} and ρ_{2a} are the first- and second-order perturbations in density respectively. Denote the acoustic Mach number by M_a. It is assumed [9] that $M_a \sim O(\rho_{1a}/\rho_0) = O(\rho_{2a}/\rho_{1a})$. Let V_{1a} be the amplitude of v_{1a} and V_{2a} be the amplitude of v_{2a}. Then it is assumed [9] that $O(V_{1a}/V_{2a}) = O(M_a)$, where M_a is assumed $\ll 1$.

The above forms of ρ and v are substituted into the mass conservation equation

$$\dot{\rho} + \nabla \cdot (\rho v) = 0, \tag{106}$$

which then becomes

$$[\dot{\rho}_{1a} + \nabla \cdot (\rho_0 v_{1a})] + [\dot{\rho}_{2a} + \nabla \cdot (\rho_0 v_{2a} + \rho_{1a} v_{1a})]$$
$$+ \nabla \cdot [\rho_{2a}(v_{1a} + v_{2a}) + \rho_{1a} v_{2a}] = 0. \tag{107}$$

Let the wave be quasimonochromatic, so that, neglecting phase factors which are functions of spatial variables,

34

$$\mathbf{v}_{1a} \propto \mathbf{V}_{1a} \sin \omega_a t \ \text{Rect} \ (\hat{t}/\Delta t),$$

$$\rho_{1a} \propto R_{1a} \sin \omega_a t \ \text{Rect} \ (\hat{t}/\Delta t),$$

and similarly for $\mathbf{v}_{2a}$ and ρ_{2a}. Then $\dot{\rho}_{1a} \sim O(\omega_a \rho_{1a})$ and $\nabla \cdot (\rho_0 \mathbf{v}_{1a}) \sim O(\rho_0 V_{1a}/\lambda_a)$. The terms in the first bracket on the left-hand side of (107) are of the order of $\omega_a \rho_0 M_a$, and those in the second bracket are of the order of $\omega_a \rho_0 M_a^2$. Groups of terms which are of the same order of magnitude in powers of M_a are set equal to zero; that is, to first order in M_a

$$\dot{\rho}_{1a} + \nabla \cdot (\rho_0 \mathbf{v}_{1a}) = 0 \tag{108}$$

and to second order

$$\dot{\rho}_{2a} + \nabla \cdot (\rho_0 \mathbf{v}_{2a} + \rho_{1a} \mathbf{v}_{1a}) = 0. \tag{109}$$

Consider next the relation between pressure and density. For isentropic flow (non-heat-conducting fluid) the pressure can be expanded in the Taylor series

$$p = P_0 + \left[\frac{\partial P}{\partial \rho}\right]_0 \rho' + \left[\frac{\partial^2 P}{\partial \rho^2}\right]_0 \frac{(\rho')^2}{2!} + \dots, \tag{110}$$

where

P_0 = equilibrium pressure,

$\rho' = \rho - \rho_0$,

$(\partial P/\partial \rho)_0 = c_0^2$,

and

c_0 = sound speed at equilibrium.

Now $c^2 = 1/\rho\beta$, with β being the bulk modulus of the fluid, so $(\partial^2 P/\partial \rho^2)_0 = -c_0^2/\rho_0$. Setting $P = p - P_0$ and retaining only those terms in (110) which are at least of the order of $c_0^2 \rho_0 M_a^2$ gives

$$P = c^2(\rho_{1a} + \rho_{2a} - \rho_{1a}^2/2\rho_0). \tag{111}$$

In this and subsequent expressions it is to be understood that P is now the pressure perturbation and c is the sonic velocity at equilibrium. Note that $P = P_{1a} + P_{2a}$, where

$$P_{1a} = c^2 \rho_{1a}, \tag{112}$$

$$P_{2a} = c^2 (\rho_{2a} - \rho_{1a}^2/2\rho_0), \tag{113}$$

and $P_{2a}/P_{1a} \sim O(M_a)$.

These results will be of use in considering the momentum equation

$$\rho[\dot{\mathbf{v}} + \mathbf{v} \cdot \nabla \mathbf{v}] = -\nabla P + \mu \nabla^2 \mathbf{v} + (\mu' + \mu/3) \nabla(\nabla \cdot \mathbf{v}) + \rho \mathbf{g}. \tag{114}$$

Here μ is the coefficient of shear viscosity, μ' is the coefficient of dilatational viscosity, and $\mathbf{g}$ is the gravitational acceleration. The term $\rho \mathbf{g}$ can be rewritten as $\rho g \nabla z$, where $g = |\mathbf{g}|$. This body force term is negligible compared to inertial terms, since $M_a c \omega_a \gg g$ for typical values of $c \sim O(10^5 \text{ cm/s})$ and $\omega_a \sim O(10^7 \text{ rad/s})$.

To first order the inertial force is $\rho_0 \dot{\mathbf{v}}_{1a}$, which is of the order of $\rho_0 \omega_a c M_a$. The lowest order viscous force term is $\mu \nabla^2 \mathbf{v}_{1a} + (\mu' + \mu/3) \nabla (\nabla \cdot \mathbf{v}_{1a})$, which is of the order of $\mu c M_a / \lambda_a$. The ratio of inertial to viscous forces is the Reynolds number R_e, which is $c\lambda_a/\nu$. Here ν is the coefficient of kinematic viscosity μ/ρ_0.

It is assumed that $R_e \gg 1$. Then there will be one set of terms in (114) which are of the order of $\rho_0 \omega_a c M_a$, another set of terms which are of the order of $\rho_0 \omega_a c M_a^2$, and a third set of terms which are of the order of $\rho_0 \omega_a c M_a^2 / M_a R_e$. Those terms which are of the order of $\rho_0 \omega_a c M_a$ are grouped together, giving

$$\rho_0 \dot{\mathbf{v}}_{1a} + \nabla P_{1a} = 0. \tag{115}$$

Likewise the set of terms of the order of $\rho_0 \omega_a c M_a^2$ or smaller gives

$$\rho_0 \dot{\mathbf{v}}_{2a} + \rho_{1a} \dot{\mathbf{v}}_{1a} + \rho_0 \mathbf{v}_{1a} \cdot \nabla \mathbf{v}_{1a} + \nabla P_{2a} = \mu \nabla^2 \mathbf{v}_{1a} + (\mu' + \mu/3) \nabla (\nabla \cdot \mathbf{v}_{1a}). \tag{116}$$

In this equation the right-hand side is negligible if $1/R_e \ll M_a$.

Assume irrotational flow so that $\mathbf{v}_{1a} = \nabla \phi_{1a}$, and $\mathbf{v}_{2a} = \nabla \phi_{2a}$. Equation (116) can be spatially integrated to give

$$\rho_0 (\dot{\phi}_{2a} + \mathbf{v}_{1a} \cdot \mathbf{v}_{1a}/2) - c^2 \rho_{1a}^2 / 2\rho_0 + P_{2a} = \left[\frac{4}{3} \mu + \mu' \right] \nabla^2 \phi_{1a}. \tag{117}$$

An arbitrary function of time has been absorbed into ϕ_{2a}, and the momentum equation (115) has been used in conjunction with (112). Recall that first-order quantities ρ_{1a} and $\mathbf{v}_{1a}$ are time harmonic, so that, for example, $\rho_{1a}^2 \propto (1/2)(1 - \cos 2\omega_a t) \, \text{Rect} \, (t/\Delta t)$. Here the trigonometric identity $\sin^2 \omega_a t \equiv (1/2)(1 - \cos 2\omega_a t)$ has been used. It is seen that terms such as ρ_{1a}^2 and $\mathbf{v}_{1a} \cdot \mathbf{v}_{1a}$ will have low temporal frequency components.

These low-frequency components give rise to a small but constant pressure during the pulse duration $0 \leqslant t \leqslant 2\Delta t$. To see how this comes about, the time average of (117) is taken over the pulse duration, giving

$$<P_{2a}> = \frac{c^2}{2\rho_0} <\rho_{1a}^2> - \frac{\rho_0}{2} <\mathbf{v}_{1a} \cdot \mathbf{v}_{1a}>, \tag{118}$$

where

$$<P_{2a}> \equiv \int_0^{2\Delta t} \frac{P_{2a}(t) \, dt}{2\Delta t}. \tag{119}$$

Note that the quantity $<\dot{\phi}_{2a}>$ does not appear in (118). In the absence of viscosity (whose effect has been neglected on this time scale), the presence of a constant pressure gradient $\nabla <P_{2a}>$ would give rise to an increasing velocity. However,

$$<\dot{\phi}_{2a}> = \frac{\phi_{2a}(2\Delta t) - \phi_{2a}(0)}{2\Delta t}. \tag{120}$$

which is of the order of $V_{2a} \lambda_a / \Delta t$. Recall that V_{2a} is by definition the maximum value assumed by $\mathbf{v}_{2a}$. The term $<\mathbf{v}_{1a} \cdot \mathbf{v}_{1a}>$ in (118) is of the order of V_{1a}^2; since $\omega_a \Delta t \gg 1$ and $V_{2a}/V_{1a} = M_a$, $<\dot{\phi}_{2a}>$ can be neglected compared to $<\mathbf{v}_{1a} \cdot \mathbf{v}_{1a}>$.

36

Just as there is a steady component of pressure in the acoustic wave, there is also a steady component of momentum flux per unit area, called the radiation pressure vector $\mathbf{P}_r$. For an inviscid, non-heat-conducting fluid, the time-averaged momentum flux per unit area through a given surface is given by (89), repeated here in the form

$$\mathbf{P}_r = <P> \mathbf{n} + \rho_0 <\mathbf{vv} \cdot \mathbf{n}>, \tag{121}$$

where $\mathbf{n}$ is a unit vector normal to the surface. Since $<P_{1a}> = 0$, this becomes

$$\mathbf{P}_r = <P_{2a}> \mathbf{n} + \rho_0 <\mathbf{v}_{1a}\mathbf{v}_{1a} \cdot \mathbf{n}>, \tag{122}$$

where quantities smaller than the second order have been neglected.

Suppose the fluid is bounded. In particular let the acoustic wave travel through the mini-tank and strike the liquid surface. A boundary condition can be derived from (66) by letting $b \rightarrow 0$, $w \rightarrow h$, and $T \rightarrow \gamma$, where h is the height of the liquid surface and γ is the surface tension coefficient. Furthermore ρ_u becomes the density of air and ρ_l becomes the density of the imaging fluid.

Since $\rho_u \ll \rho_l$, conservation of momentum in the vertical direction at the liquid surface requires

$$P + \rho(\mathbf{v} \cdot \mathbf{e}_z)^2 + \gamma \frac{\partial^2 h}{\partial y^2} = 0, \tag{123}$$

where P and ρ refer to the pressure and density of the imaging fluid and $\mathbf{e}_z$ is a unit vector in the vertical (z) direction. Due to the second-order acoustic quantities the low-frequency term $[<P_{2a}> + \rho_0<(\mathbf{v}_{1a} \cdot \mathbf{e}_z)^2>]$ Rect $(\hat{t}/\Delta t)$, which equals $-\mathbf{P}_r \cdot \mathbf{n}$, will appear in (123). This will induce low-frequency motions of the liquid surface, and this motion in turn causes additional pressure, density, and velocity perturbations in the minitank. It is natural to assume therefore that in the minitank

$$P = P_{1a} + P_{2a} + P_s, \tag{124a}$$

$$\rho' = \rho_{1a} + \rho_{2a} + \rho_s, \tag{124b}$$

and

$$\mathbf{v} = \mathbf{v}_{1a} + \mathbf{v}_{2a} + \mathbf{v}_s. \tag{124c}$$

The subscript s refers to perturbations associated with motion of the liquid surface. Substituting ρ' into (110) gives $P_s = c^2 \rho_s$.

To use the liquid surface to record the focused acoustic image, it is necessary that the acoustic field quantities, such as $\mathbf{v}_{1a}$ and $\mathbf{v}_{2a}$ be unaffected by $\mathbf{v}_s$. It will be shown later that this occurs if $C_s \ll c$ and $\omega_\eta \ll \omega_a$, where C_s is the velocity of propagation of a free wave on the liquid surface, and ω_η is the corresponding frequency of free vibration. The possibility of coupling between the acoustic field and the surface-wave field exists because of terms such as $\nabla \cdot (\rho \mathbf{v})$ in the mass conservation equation (106) and $\mathbf{v} \cdot \nabla \mathbf{v}$ in the momentum conservation equation (114).

5.2 Propagation of Free Waves on the Liquid Surface

At this point it is necessary to consider free-wave propagation on the liquid surface in the absence of the acoustic field; i.e., $P = P_s$, $\rho' = \rho_s$, and $\mathbf{v} = \mathbf{v}_s$. For negligible viscosity the momentum equation (114) becomes

$$\rho(\dot{\mathbf{v}}_s + \mathbf{v}_s \cdot \nabla \mathbf{v}_s) = -\nabla P_s - \rho g \nabla z_s. \tag{125}$$

For irrotational flow $\mathbf{v}_s = \nabla \phi_s$ and (125) integrates to Bernoulli's equation

$$P_s = -\rho_0 \dot{\phi}_s - \frac{\rho_0 \mathbf{v}_s \cdot \mathbf{v}_s}{2} - \rho_0 g z_s. \tag{126}$$

Here ρ_s has been neglected compared to ρ_0 and an arbitrary function of time has been absorbed into ϕ_s.

Evaluating the above at the liquid surface (where $z_s = h_s$) and substituting the result into the boundary condition (123) gives

$$-\rho_0 \dot{\phi}_s - \rho_0 g h_s + \gamma \nabla_1^2 h_s = 0, \tag{127}$$

where $\nabla_1^2 \equiv \partial^2/\partial y^2$. The nonlinear term $\rho_0 \mathbf{v}_s \cdot \mathbf{v}_s$ has been neglected compared to, for example, $\rho_0 \dot{\phi}_s$. This linearization is valid if $|\mathbf{v}_s| \ll C_s$.

At the liquid surface $\dot{h}_s = \partial \phi_s/\partial z$, so (127) can be solved for h_s once ϕ_s is known. An equation for ϕ_s can be obtained from the mass conservation equation

$$\dot{\rho}_s + \nabla \cdot (\rho \mathbf{v}_s) = 0. \tag{128}$$

Now $\dot{\rho}_s \sim O(\omega_s \rho_s)$ for ω_s a characteristic frequency of oscillation of the liquid surface. This term will be negligible compared to $\nabla \cdot (\rho \mathbf{v}_s)$ if $\rho_s/\rho_0 \ll \hat{h}_s/\lambda_s$ for λ_s a characteristic wavelength and $\hat{h}_s$ a characteristic displacement caused by motion of the surface. Since $\rho_s = P_s/c^2$ and from Bernoulli's equation (126) $P_s \sim O(\rho_o \dot{\phi}_s)$, it can be shown that $\rho_s/\rho_o \ll \hat{h}_s/\lambda_s$ if $C_s^2 \ll c^2$. The latter inequality will be proven later. Using $\mathbf{v}_s = \nabla \phi_s$ the mass conservation equation becomes

$$\nabla^2 \phi_s = 0. \tag{129}$$

At the bottom of the minitank ($z = -d$), $\partial \phi_s/\partial z$ equals the membrane velocity $\dot{w}_s$. Assume that $w_s \ll h_s$; it will be shown later in this section that when $w_s \ll h_s$, the boundary condition at the membrane is effectively $\partial \phi_s/\partial z = 0$. Then a solution to (129) is

$$\phi_s = A \left[\cosh \hat{\eta}(z + d)\right] e^{i\hat{\eta}y} e^{-i\omega t}. \tag{130}$$

To satisfy the kinematic boundary condition $\dot{h}_s = \partial \phi_s/\partial z$ at the liquid surface, let

$$h_s = -\left[\frac{A}{i\omega}\right] \hat{\eta} \, e^{i\hat{\eta}y} e^{-i\omega t} \sinh \hat{\eta} d. \tag{131}$$

Substituting these results into (127) leads to

$$A \left[-\omega^2 + (\rho_0 g + \gamma \hat{\eta}^2)(\hat{\eta}/\rho_0) \tanh \hat{\eta} d\right] = 0. \tag{132}$$

For nontrivial solutions

$$\omega_\eta^2 = (\rho_0 g + \gamma \hat{\eta}^2)(\hat{\eta}/\rho_0) \tanh \hat{\eta} d, \tag{133}$$

where ω_η is the frequency of oscillation associated with the traveling wave $h_s \propto e^{i\hat{\eta}y} e^{-i\omega_\eta t}$.

It is of interest to compare the magnitude of ω_η with ω_a, the operating frequency of the transducers. The wavelength λ_s of a traveling wave on the liquid surface is given by $2\pi/\hat{\eta}$.

Typically $\lambda_s \gtrsim \lambda_a$, so that $\hat{\eta} \lesssim O(2\pi/\lambda_a)$. The notation $\hat{\eta} \lesssim O(2\pi/\lambda_a)$ means that the order of $\hat{\eta}$ is less than or equal to $2\pi/\lambda_a$. For transducers operating at 5 MHz in water, $\lambda_a = 0.03$ cm. Let $\gamma \sim O(100\,\mu\text{N/cm})$, $\rho_0 \sim O(1\ \text{g/cm}^3)$, and $d \sim O(0.1\ \text{cm})$. For this example, (133) gives $\omega_\eta^2 \lesssim O(10^7\ \text{rad}^2/\text{s}^2)$, which is much less than ω_a^2.

Another quantity of interest is C_s, the speed of propagation of a free wave on the liquid surface. Since $C_s = \omega_\eta/\hat{\eta}$, its general form is

$$C_s = \left[\frac{(\rho_0 g + \gamma\hat{\eta}^2)\hat{\eta}\ \tanh\hat{\eta}d}{\rho_0} \right]^{1/2} /\hat{\eta}. \tag{134}$$

In the limit of long wavelengths $\hat{\eta} \to 0$; then $C_s \to \sqrt{gd}$, which is the speed of propagation of a gravity wave on the liquid surface [10]. For short wavelengths, $\hat{\eta} \to 2\pi/\lambda_a$, so that $C_s \to \sqrt{(1/\rho_0)\gamma\hat{\eta}\ \tanh\hat{\eta}d}$, the speed of propagation of a capillary wave [10]. For the values of ρ_0, γ, and d used previously, $C_s \sim O(10\ \text{cm/s})$ for both small and large $\hat{\eta}$. Hence the speed of propagation is many orders of magnitude less than the sonic velocity. The inequalities $\omega_\eta \ll \omega_a$ and $C_s \ll c$ will be useful when considering the response of the liquid surface to a pulse of radiation pressure.

5.3 Levitation of the Liquid Surface By Radiation Pressure

Consider forced motion of the liquid surface due to radiation pressure in the acoustic field. It is assumed that the pressure, density and velocity are given by (124a), (124b), and (124c), where the acoustic quantities are calculated from the acoustic mass and momentum conservation equations (108), (109), (115), and (116). The quantities ρ_s, P_s, and v_s associated with motion of the liquid surface are assumed calculable from (125) and (128) plus the relation $P_s = c^2 \rho_s$.

It is necessary to show that the general mass conservation equation (106) and momentum conservation equation (114) are satisfied by the choice of ρ, P, and v, given by (124a) through (124c). Before this can be done, orders of magnitude must be assigned to P_s, ρ_s, and v_s. These are assigned by considering the balance of forces per unit area acting vertically at the liquid surface, which is given by (123). With the preceding assumptions as to the form of pressure, velocity, and density, (123) becomes

$$P_{1a} + P_{2a} + P_s + (\rho_0 + \rho')[(v_{1a} + v_{2a} + v_s)\cdot e_z]^2 + \gamma\nabla_t^2(h_{1a} + h_{2a} + h_s) = 0. \tag{135}$$

Assume that $P_{1a} \gg P_s$ and $P_{1a} \gg \gamma\nabla_t^2 h_{1a}$ in the boundary condition (135). Then (135) reduces to the pressure-release condition $P_{1a} = 0$ which was used in the calculation of the mini-tank transfer function. It will be shown later that the inequality $P_{1a} \gg P_s$ satisfies the general forms of the mass and momentum conservation equations. The inequality $P_{1a} \gg \gamma\nabla_t^2 h_{1a}$ in conjunction with the relation $h_{1a} \sim O(V_{1a}/\omega_a)$ requires that $\gamma/\rho_0 c^2 \lambda_a \ll 1$. This is easily satisfied for imaging fluids of interest, such as Freon and water.

For $P_{1a} = 0$ the boundary condition (135) becomes

$$P_s + \gamma\nabla_t^2 h_s = -\{P_{2a} + (\rho_0 + \rho')[(v_{1a} + v_{2a} + v_s)\cdot e_z]^2 + \gamma\nabla_t^2(h_{1a} + h_{2a})\}. \tag{136}$$

If the momentum equation (125) is assumed true, then P_s is given by its integral, the Bernouilli equation (126). Substituting (126) into the boundary condition (136) gives

39

$$-\rho_0\dot{\phi}_s - \rho_0 g h_s + \gamma \nabla_1^2 h_s = -\{P_{2a} + \rho_0[(\mathbf{v}_{1a} \cdot \mathbf{e}_z)^2 + (\mathbf{v}_{1a} \cdot \mathbf{e}_z)(\mathbf{v}_s \cdot \mathbf{e}_z)]$$

$$+ \gamma \nabla_1^2(h_{1a} + h_{2a})\}. \tag{137}$$

Here the nonlinear term $\rho_0(\mathbf{v}_s \cdot \mathbf{e}_z)^2$ has been neglected compared to $\rho_0\dot{\phi}_s$ on the assumption that $|\mathbf{v}_s| \ll C_s$. The terms which are of order $\rho_0(\mathbf{v}_{2a} \cdot \mathbf{e}_z)(\mathbf{v}_s \cdot \mathbf{e}_z)$ have been neglected also. In the absence of the acoustic field (137) reduces to (127), the equation for propagation of free surface waves. When the acoustic field is present, terms on the right-hand side have the character of driving forces per unit area.

Consider, for example, the term P_{2a}. Now $P_{2a} \propto \cos^2 \omega_a t$ Rect $(\hat{t}/\Delta t)$, which has high- and low-frequency components in the temporal frequency domain. The high frequencies are of the order of ω_a; ω_a has been shown to be much greater than ω_η, the characteristic frequency associated with the free surface wave $h_s \propto e^{i\hat{\eta}s} e^{-i\omega_\eta t}$. Hence it is to be expected that the liquid surface responds to $<P_{2a}>$ Rect $(\hat{t}/\Delta t)$, which contains the low temporal frequencies of P_{2a}. In like fashion the surface will respond to $\rho_0<(\mathbf{v}_{1a} \cdot \mathbf{e}_z)^2>$ Rect $(\hat{t}/\Delta t)$, the low-frequency component of $\rho_0(\mathbf{v}_{1a} \cdot \mathbf{e}_z)^2$. However, the term $\rho_0(\mathbf{v}_{1a} \cdot \mathbf{e}_z)(\mathbf{v}_s \cdot \mathbf{e}_z)$ has dominant temporal frequencies of the order of ω_a and can be neglected as a driving pressure.

Since the liquid surface has frequencies of free vibration ω_η, it will respond to temporal frequency components which are of the order of ω_η. The frequency components of Rect$(t/\Delta t)$ are proportional to sinc $(\omega \Delta t)$, which is of the order of $1/\omega_\eta \Delta t$ for $\omega \sim O(\omega_\eta)$. The frequency components of h_{1a} are proportional to sinc $((\omega - \omega_a)\Delta t)$, which is of the order of $1/\omega_a \Delta t$ for $\omega \sim O(\omega_\eta)$. Consequently the term $\gamma \nabla_1^2 h_{1a}$ can be disregarded compared to, for example, $<\rho_0(\mathbf{v}_{1a} \cdot \mathbf{e}_z)^2>$ Rect $(\hat{t}/\Delta t)$, provided that $\gamma/\rho_0 c^2 \lambda_a \ll M_a(\omega_a/\omega_\eta)$, which is met for most imaging fluids of interest.

Finally it is necessary to consider the term $\gamma \nabla_1^2 h_{2a}$. Now $<\mathbf{v}_{2a}> = 0$ at the liquid surface, since otherwise $h_{2a} \to \infty$ for $\Delta t \to \infty$. Hence

$$h_{2a} \propto V_{2a} \int_0^t (\cos 2\omega_a t) \text{ Rect } (\hat{t}/\Delta t) \, dt, \tag{138}$$

which leads to

$$<h_{2a}> \propto (V_{2a}/2\omega_a)/(\omega_a \Delta t). \tag{139}$$

Consequently, $\gamma \nabla_1^2 <h_{2a}>$ is much less than $\rho_0<(\mathbf{v}_{1a} \cdot \mathbf{e}_z)^2>$, since the requirement $\gamma/\rho_0 c^2 \lambda_a \ll \omega_a \Delta t$ is easily satisfied.

Using all of the preceding simplifies the boundary condition (137) to

$$-\rho_0\dot{\phi}_s - \rho_0 g h_s + \gamma \nabla_1^2 h_s = -[<P_{2a}> + \rho_0<(\mathbf{v}_{1a} \cdot \mathbf{e}_z)^2>] \text{ Rect } (\hat{t}/\Delta t). \tag{140}$$

Now $\dot{\phi}_s \sim O(\omega_\eta \lambda_s V_s)$, and the above equation shows that $V_s \sim O(V_{1a}^2/C_s)$. Furthermore, since $\rho_0\dot{\phi}_s \sim O(P_s)$ from (126), it follows that $P_s \sim O(P_{2a})$. Recalling that $P_s = c^2\rho_s$ and $P_{2a} \sim O(c^2\rho_{2a})$ gives $\rho_s \sim O(\rho_{2a})$.

In summary, the boundary condition (135) leads to the following estimate of the orders of magnitude of pressure, density, and velocity:

$$P_s \sim O(P_{2a}), \tag{141a}$$

$$\rho_s \sim O(\rho_{2a}), \tag{141b}$$

and

$$V_s \sim O(V_{1a}^2/C_s).$$ (141c)

These results will now be used to show that the acoustic field is, to the approximation considered here, unaffected by motions of the liquid surface. The momentum equation for inviscid, irrotational flow when the acoustic field and surface-wave field are both present is

$$(\rho_0\dot{v}_{1a} + \nabla P_{1a}) + (\rho_0\dot{v}_{2a} + \rho_{1a}\dot{v}_{1a} + \rho_0 v_{1a} \cdot \nabla v_{1a} + \nabla P_{2a}) + \rho_0 v_s \cdot \nabla v_{1a}$$

$$+ \rho_0 v_{1a} \cdot \nabla v_s + (\rho_0\dot{v}_s + \rho_0 g\nabla z_s + \nabla P_s) = 0.$$ (142)

It is assumed that $|v_s| \ll C_s$, and terms of order $\rho_{1a}\omega_a V_{2a}$ have been neglected. All terms in the above are greater than this, provided that $\lambda_a/\lambda_s \gg M_a$.

If this inequality is not satisfied, then $\rho_0\dot{v}_s \sim O(\rho_{1a}\dot{v}_{2a})$. However, the dominant temporal frequencies of $\rho_0\dot{v}_s$ are of the order ω_η, and those of $\rho_{1a}\dot{v}_{2a}$ are of the order of ω_a. Since $\omega_\eta \ll \omega_a$, terms such as $\rho_{1a}\dot{v}_{2a}$ do not couple with, for example, $\rho_0\dot{v}_s$ and hence will be disregarded. For the same reason, the terms $\rho_0 v_s \cdot \nabla v_{1a}$ and $\rho_0 v_{1a} \cdot \nabla v_s$ may couple with, for example, $\rho_0\dot{v}_{2a}$ if $|v_s| \sim O(V_{1a})$ and $\lambda_s \sim O(\lambda_a)$. However, they will not couple with $\rho_0\dot{v}_s$.

The group of terms in (142) having the largest order of magnitude is $\rho_0\dot{v}_{1a} + \nabla P_{1a}$, which is of the order of $\rho_0\omega_a cM_a$. The terms in the second and third parentheses in (142) are of the order of $\rho_0\omega_a cM_a^2$ and $\rho_0\omega_a cM_a^2\lambda_a/\lambda_s$ respectively. The entire equation can be made dimensionless by dividing through by $\rho_0\omega_a c$. Then terms which are of the order of M_a and M_a^2 are set to zero separately. This gives, for the order of M_a

$$\rho_0\dot{v}_{1a} + \nabla P_{1a} = 0$$ (143)

and for the order of M_a^2

$$\rho_0\dot{v}_{2a} + \rho_{1a}\dot{v}_{1a} + \rho_0 v_{1a} \cdot \nabla v_{1a} + \nabla P_{2a} = \rho_0(v_s \cdot \nabla v_{1a} + v_{1a} \cdot \nabla v_s).$$ (144)

If irrotational flow is assumed, the above can be integrated over space and time-averaged to give

$$<P_{2a}> = \frac{c^2}{2\rho_0} <\rho_{1a}^2> - \frac{\rho_0}{2} <v_{1a} \cdot v_{1a}>.$$ (145)

Here (143) and the relation $P_{1a} = c^2\rho_{1a}$ have been used. The term in (142) which is of the order of $M_a^2\lambda_a/\lambda_s$ is also set to zero, giving

$$\rho_0\dot{v}_s + \rho_0 g\nabla z_s + \nabla P_s = 0.$$ (146)

The dimensional forms have been used in (143) through (146).

When $\lambda_a \sim O(\lambda_s)$, terms in (144) and (146) are the same order of magnitude. However, they are still separated as above, since otherwise there will be more unknowns (such as P_{1a} and P_{2a}) than equations to solve for them, and since the momentum equation (142) is satisfied to the order of M_a^2.

The first-order acoustic momentum equation is recovered, since (143) is identical to (115). The second-order equation (144) contains coupling terms on the right-hand side which are negligible if $|v_s| \ll V_{1a}$. If $|v_s| \sim O(V_{1a})$, then the high-frequency (of the order of ω_a) components of the second-order quantities v_{2a} and P_{2a} may be affected by the surface-wave

41

field, as seen by comparing (144) with (116). However, the low-frequency components of v_{2a} and P_{2a} are unaffected by surface motion, as seen by comparing (145) with its counterpart, (118). This is fortunate, since it is the low-frequency components of the second-order acoustic quantities which give rise to radiation pressure, which levitates the surface. Note also that the momentum equation involving v_s and P_s is independent of the acoustic field.

The momentum balance involving first-order acoustic quantities and the low-frequency, second-order acoustic quantities can be calculated separately from that involving surface-wave quantities. If the same can be shown to be true with regard to mass conservation, then acoustic field quantities and surface-wave quantities can be calculated separately in the minitank.

Hence it is necessary to consider the mass-conservation equation

$$[\dot{\rho}_{1a} + \nabla \cdot (\rho_0 v_{1a})] + [\dot{\rho}_{2a} + \nabla \cdot (\rho_{1a} v_{1a} + \rho_0 v_{2a}) + \nabla \cdot (\rho_{1a} v_s)]$$
$$+ \nabla \cdot (\rho_0 v_s) = 0. \tag{147}$$

The equation can be made dimensionless by dividing by $\rho_0 \omega_a$. The left-hand side consists of three groups of terms, having orders of magnitude of M_a, M_a^2, and $M_a^2(c/C_s)(\lambda_a/\lambda_s)$. Equating each group to zero and returning to dimensional form gives

$$\dot{\rho}_{1a} + \nabla \cdot (\rho_0 v_{1a}) = 0, \tag{148}$$

$$\dot{\rho}_{2a} + \nabla \cdot (\rho_{1a} v_{1a} + \rho_0 v_{2a}) = - \nabla \cdot (\rho_{1a} v_s), \tag{149}$$

and

$$\nabla \cdot v_s = 0. \tag{150}$$

Note that $(c/C_s)(\lambda_a/\lambda_s)$ can be of the order of 1, for long wavelengths, so that (149) and (150) can be the same order of magnitude. If they are retained as separate equations, there will be enough equations to solve for the unknown quantities P, ρ, and v. That is, the set (143), (144), (146), (148), (149), and (150) gives 12 equations to solve for 15 unknowns. Three other relations are

$$P_{1a} = c^2 \rho_{1a}, \tag{151}$$

$$P_{2a} = c^2 [\rho_{2a} - \rho_{1a}^2/(2\rho_0)], \tag{152}$$

and

$$P_s = c^2 \rho_s. \tag{153}$$

Furthermore mass conservation is now satisfied to the order of $\rho_0 \omega_a M_a^3 c/c_s$.

The first-order acoustic mass conservation equation (148) has the same form as (108), which is the equation in the absence of the surface-wave field. The second-order acoustic equation (149) contains the coupling term $\nabla \cdot (\rho_{1a} v_s)$, which is negligible if $|v_s| \ll V_{1a}$. Even if $|v_s| \sim O(V_{1a})$, the time average of (149) is the same as the time average of (109). Hence the low-frequency second-order acoustic quantities can be calculated independently of the surface-wave quantities. Furthermore the mass conservation equation in the surface-wave field is independent of the acoustic field, as comparison of (150) and (129) shows.

If viscosity is considered, then terms such as $\mu \nabla^2 v_{1a}$ will appear on the right-hand side of (144). However, these terms, as stated previously, are negligible if $M_a R_e \ll 1$. Furthermore, the time average of these terms is zero, so that (145) remains unchanged. There will also be

terms such as $\mu < \nabla^2 \mathbf{v}_{2a} >$ Rect $(\hat{t}/\Delta t)$ on the right-hand side of (146). These will be negligible if $R_e \gg (\lambda_s/\lambda_a)$. For typical fluids of interest (such as water and Freon) $\nu \sim O(10^{-2} \text{ cm}^2/\text{s})$ and $c \sim O(10^5 \text{ cm}/\text{s})$. For typical frequencies in the megahertz range, $\lambda_a \sim O(10^{-2} \text{ cm})$; consequently, $R_e \sim O(10^5)$. In any practical system of interest, λ_s is limited by the finite size of the system; typically $\lambda_s \lesssim O(10 \text{ cm})$. Hence the inequality $R_e \gg \lambda_a/\lambda_s$ is easily satisfied.

Finally, terms such as $\mu \nabla^2 \mathbf{v}_s$, which would appear in (146), can be ignored if $C_s \lambda_s/\nu \gg 1$. This dimensionless quantity is the Reynolds number appropriate to the surface-wave field. For long wavelengths (of the order of 10 cm), this Reynolds number is much greater than 1, for fluids of interest. At short wavelengths (of the order of λ_a), it is of the order of 10.

Thus viscosity will affect neither the first-order acoustic quantities nor the low-frequency second-order acoustic quantities. Its only practical effect is to induce small viscous forces in the surface-wave field.

5.4 Transfer Function For Levitation of the Liquid Surface

It is now possible to calculate the form of the transfer function for the liquid surface. To do so, (140) is used, which is repeated here in the form

$$\rho_u \dot{\phi}_s + \rho_u g h_s - \gamma \nabla_t^2 h_s = (<P_{2a}> + \rho_u <(\mathbf{v}_{1a} \cdot \mathbf{e}_z)^2>) \text{ Rect } (\hat{t}/\Delta t), \qquad (154)$$

with ρ_u being the equilibrium density of the imaging fluid. It was shown earlier that the radiation pressure vector $\mathbf{P}_r$ at an arbitrary surface with outward unit normal $\mathbf{n}$ is given by $\mathbf{P}_r = (<P_{2a}>\mathbf{n} + \rho_0 <\mathbf{v}_{1a} \mathbf{v}_{1a} \cdot \mathbf{n}>) \text{ Rect } (\hat{t}/\Delta t)$. At the liquid surface $\mathbf{n} = \mathbf{e}_z$, so that the right-hand side of (154) is $\mathbf{P}_r \cdot \mathbf{n} = P_r$, the radiation pressure. This shows that levitation of the liquid surface is caused by the radiation pressure, as was anticipated in the paragraph following (91) in section 4.

From the acoustic boundary condition $P_{1a} = 0$ it follows that $\rho_{1a} = 0$ at the liquid surface, and from (118) $<P_{2a}> = -\rho_u <\mathbf{v}_{1a} \cdot \mathbf{v}_{1a}>/2$ there. Also, the fact that $P_{1a} = 0$ implies that every incident compression wave in the acoustic field is reflected as a rarefaction wave and vice versa. This causes the y component of $\mathbf{v}_{1a}$ to vanish at the liquid surface, which makes $(\mathbf{v}_{1a} \cdot \mathbf{e}_z)^2 = \mathbf{v}_{1a} \cdot \mathbf{v}_{1a}$ there. Consequently the radiation pressure at the liquid surface is just $(1/2)\rho_u <v_z^2>$ Rect $(\hat{t}/\Delta t)$, or $(1/2)\rho_u <(v_{oz} + v_{rz})(v_{oz}^* + v_{rz}^*)>$ Rect $(\hat{t}/\Delta t)$.

The transfer function will give the levitation of the liquid surface due to a temporal pulse of radiation pressure of duration $2\Delta t$ having spatial frequency $\hat{\eta} = 2\pi\eta$. Recall that the liquid surface is the top of a thin layer of imaging fluid of thickness d; the bottom of this layer is in contact with a thin membrane whose properties were analyzed in section 3.

As long as the levitation of the liquid surface h_s is much larger than the displacement of the membrane, it is possible to assume that $\mathbf{v}_s \cdot \mathbf{e}_z = 0$ at the membrane $(z = -d)$. It will be shown in section 5.6 that

$$\dot{h}_s \gg (\mathbf{v}_s \cdot \mathbf{e}_z) |_{z=-d} \qquad (155)$$

for $\lambda_s \lesssim O(1 \text{ cm})$. At these short wavelengths the exact solution for h_s, accounting for membrane elasticity, is essentially the same as the value of h_s calculated using the rigid-membrane boundary condition $\mathbf{v}_s \cdot \mathbf{e}_z = 0$ at $z = -d$.

43

To calculate the response of the liquid surface to a pulse of radiation pressure, it is necessary to solve the equations

$$\nabla^2 \phi_s = 0 \tag{156}$$

and

$$P_s + \rho_u \dot{\phi}_s + \rho_u g z_s = 0. \tag{157}$$

The Laplace equation (156) is the form assumed by the mass conservation equation (150) for irrotational flow, or $v_s = \nabla \phi_s$. Equation (157) is the linearized Bernoulli equation, the first integral of the linearized momentum equation (146) for inviscid flow. The boundary conditions (for liquid surface of infinite lateral extent) are

$$-\rho_u \dot{\phi}_s - \rho_u g h_s + \gamma \nabla_1^2 h_s = -P_r, \quad z = 0, \tag{158}$$

$$\frac{\partial \phi_s}{\partial z} = \dot{h}_s, \quad z = 0, \tag{159}$$

and

$$\frac{\partial \phi_s}{\partial z} = 0, \quad z = -d. \tag{160}$$

As a solution of the Laplace equation (156) let

$$\phi_s(y, z, t) = \int\!\!\int_{-\infty}^{\infty} \bar{\bar{A}}(\hat{\eta}, \omega) \, e^{i\hat{\eta}y} \{\cosh [\hat{\eta}(z + d)]\} \, e^{-i\omega t} \, d\hat{\eta} d\omega, \tag{161}$$

which automatically satisfies $\partial \phi_s / \partial z = 0$ at $z = -d$. To satisfy $\partial \phi_s / \partial z = \dot{h}_s$ at $z = 0$, set

$$h_s(y, t) = -\int\!\!\int_{-\infty}^{\infty} (\hat{\eta}/i\omega) \, \bar{\bar{A}}(\hat{\eta}, \omega) \, (\sinh \hat{\eta}d) \, e^{i\hat{\eta}y} \, e^{-i\omega t} \, d\hat{\eta} d\omega. \tag{162}$$

Taking the Fourier transform of the boundary condition (158) with respect to time and space variables gives

$$\left[-\omega^2 \cosh \hat{\eta}d + (\rho_u g + \gamma \hat{\eta}^2) \frac{\hat{\eta}}{\rho_u} \sinh \hat{\eta}d \right] \bar{\bar{h}}_s(\hat{\eta}, \omega)$$

$$= \frac{2\hat{\eta}}{\rho_u} (\Delta t) \, \bar{p}_r(\hat{\eta}) \, (\text{sinc } \omega \Delta t) \, e^{i\omega \Delta t} \sinh \hat{\eta}d. \tag{163}$$

Here the radiation pressure has the Fourier integral representation

$$P_r(y, t) = 2\Delta t \int\!\!\int_{-\infty}^{\infty} \bar{p}_r(\hat{\eta}) \, (\text{sinc } \omega \Delta t) \, e^{i\omega \Delta t} e^{i\hat{\eta}y} \, e^{-i\omega t} \, d\hat{\eta} d\omega. \tag{164}$$

Using $\bar{\bar{h}}_s = -(\hat{\eta}/i\omega) \bar{\bar{A}}$ and $\omega_\eta^2 = (\rho_u g + \gamma \hat{\eta}^2) (\hat{\eta}/\rho_u) \tanh \hat{\eta}d$ leads to

$$\bar{\bar{h}}_s(\hat{\eta}, \omega) = \frac{2\bar{p}_r(\hat{\eta}) \, \omega_\eta^2 \Delta t \, (\text{sinc } \omega \Delta t) \, e^{i\omega \Delta t}}{(\rho_u g + \gamma \hat{\eta}^2) \, (-\omega^2 + \omega_\eta^2)} \tag{165}$$

with inverse transform

$$\bar{h}_s(\hat{\eta}, t) = \frac{\bar{p}_r(\hat{\eta})}{\rho_u g + \gamma \hat{\eta}^2} \, \omega_\eta \sin \omega_\eta t \overset{t}{\oplus} \text{Rect} (\hat{t}/\Delta t), \tag{166}$$

where $\oplus$ denotes temporal convolution. This can be put in the form $\bar{h}_s(\hat{\eta},\ t) = \bar{H}(\eta,\ t)\ \bar{p}_r(\eta)$, where the transfer function $\bar{H}(\hat{\eta},\ t)$ is

$$\bar{H}(\hat{\eta},\ t) = \frac{\omega_\eta \sin \omega_\eta t \overset{t}{\oplus} \text{Rect } (\hat{t}/\Delta t)}{\rho_u g + \gamma \hat{\eta}^2}. \tag{167}$$

For the general case where the radiation pressure has many spatial frequency components,

$$h_s(y,\ t) = \int_{-\infty}^{\infty} \bar{H}(\hat{\eta},\ t)\ \bar{p}_r(\hat{\eta})\ e^{i\hat{\eta}y} d\hat{\eta} \tag{168}$$

or, using the convolution theorem of Fourier analysis,

$$h_s(y,\ t) = H(y,\ t) \overset{s}{\oplus} p_r(y). \tag{169}$$

It was shown earlier that

$$P_r = \frac{1}{4} \rho_u \left[|V_o|^2 + |V_r|^2 + 2|V_o|\ |V_r| \cos(\chi_o - \chi_r) \right] \text{Rect}(\hat{t}/\Delta t). \tag{95}$$

Recall that v_{oz} is the particle velocity at the liquid surface, due to the object's focused acoustic image, and v_{rz} is the particle velocity at liquid surface, due to the reference beam. Note that v_{oz} and v_{rz} are first-order (in M_a) quantities and are given by (93a) and (93b), repeated here for convenience:

$$v_{oz} = |V_o| e^{i\chi_o}\ e^{-i\omega_a t} \text{Rect}(\hat{t}/\Delta t) \tag{93a}$$

and

$$v_{rz} = |V_r| e^{i\chi_r}\ e^{-i\omega_a t} \text{Rect}(\hat{t}/\Delta t). \tag{93b}$$

It is convenient to let

$$p_r = \frac{1}{4}\rho_u \left[|V_o|^2 + |V_r|^2 + 2|V_o|\ |V_r| \cos (\chi_o - \chi_r) \right]. \tag{170}$$

The first term on the right-hand side is the radiation pressure at the liquid surface if only the focused acoustic image is present. The second term is the radiation pressure if only the reference beam strikes the surface. The third term represents the interference of the focused acoustic image with the reference beam. This term can be decomposed into two components, P_{ri} and P_{rc}; P_{ri} contains information about ψ_1, the focused acoustic image, and P_{rc} contains information about ψ_1^*, the complex conjugate of ψ_1. The surface levitation h_i, due to P_{ri}, can be calculated from

$$h_i(y,\ t) = H(y,\ t) \overset{s}{\oplus} P_{ri}(y). \tag{171}$$

In the spatial frequency domain (171) becomes $\bar{h}_i(\hat{\eta},\ t) = \bar{H}(\hat{\eta},\ t)P_{ri}(\hat{\eta})$, which has the black-box representation shown in Fig. 17. $\bar{H}(\eta,\ t)$ is represented by the convolution $\omega_\eta \sin \omega_\eta t \overset{t}{\oplus} \text{Rect } (\hat{t}/\Delta t)$, followed by multiplication by $1/(\rho_u g + \gamma \hat{\eta}^2)$.

5.5 Transfer Function as Modified for a Slightly Viscous Imaging Fluid

The transfer function (167) predicts that the liquid surface will oscillate forever when struck by a pulse of radiation pressure. A more realistic transfer function must account for the
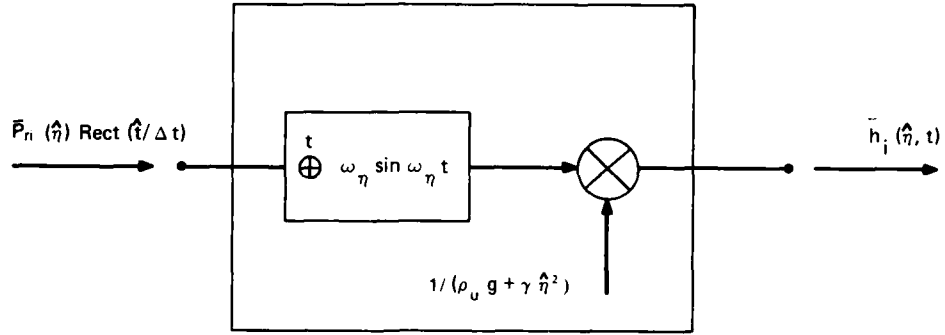
Fig. 17 — Transfer function for the liquid surface when viscosity is negligible

action of viscosity, which has been neglected to this point. It was shown previously that for $\mu/(\rho_0 c \lambda_a) \ll M_a$ viscous effects are negligible in the first- and second-order acoustic mass and momentum conservation equations. Recall that $\rho_0 c \lambda_a/\mu$ is the acoustic Reynolds number. However, the Reynolds number $\rho_0 C_s \lambda_s/\mu$ associated with the surface-wave field can be much smaller than the acoustic Reynolds number. Hence viscous effects will first become significant in the surface-wave field.

The stress-strain rate relations for a viscous fluid are [11]

$$\sigma_{zz} = -P + 2\mu \, \frac{\partial v_z}{\partial z} \tag{172a}$$

and

$$\sigma_{yz} = \mu \left(\frac{\partial v_y}{\partial z} + \frac{\partial v_z}{\partial y} \right); \tag{172b}$$

here $v_z = v_s \cdot e_z$, etc. Since there is no shear stress at the liquid surface, there will be an additional boundary condition

$$\frac{\partial v_y}{\partial z} + \frac{\partial v_z}{\partial y} = 0 \tag{173}$$

to satisfy at $z = 0$. In addition the vertical momentum balance becomes

$$P_s = - P_r - \gamma \frac{\partial^2 h_s}{\partial y^2} + 2\mu \, \frac{\partial v_z}{\partial z}. \tag{174}$$

Finally the no-slip boundary condition at the bottom of the minitank is

$$v_s = 0, \qquad z = -d. \tag{175}$$

An analytic solution for the motion of the imaging fluid can be obtained for slight viscosity when $d \to \infty$, following Lamb [11]. The motion will be approximately irrotational, so that $v_s = \nabla \phi_s + \text{curl } \Psi$, where it is expected that $|\Psi_s| \ll \phi_s$. If two-dimensional motion is assumed, $\Psi_s = \Psi_s e_x$. Since $\nabla \cdot (\text{curl } \Psi) \equiv 0$, the mass conservation equation remains $\nabla^2 \phi_s = 0$. The momentum equation becomes

$$\nabla (\rho_u \dot\phi_s + P_s + \rho_u g z_s) = -\text{curl } (\rho_u \dot\Psi - \mu \nabla^2 \Psi). \tag{176}$$

For approximately irrotational motion, let the relation between ϕ_s and P_s be $\rho_u \dot{\phi}_s + \rho_u g z_s + P_s = 0$, as in the case of inviscid flow. Then the momentum equation gives

$$\dot{\Psi}_s = \nu \nabla^2 \Psi_s, \tag{177}$$

for $\nu = \mu/\rho_u$, the kinematic viscosity.

Assume solutions in the form

$$\phi_s = \int\!\!\int_{-\infty}^{\infty} \bar{\bar{A}}(\hat{\eta}, \omega) \; e^{\hat{\eta}z} \, e^{i\hat{\eta}s} \, e^{-i\omega t} \, d\hat{\eta} d\omega \tag{178}$$

and

$$\Psi_s = \int\!\!\int_{-\infty}^{\infty} \bar{\bar{B}}(\hat{\eta}, \omega) \; e^{mz} \, e^{i\hat{\eta}s} \, e^{-i\omega t} \, d\hat{\eta} d\omega, \tag{179}$$

where to satisfy (177), $m^2 = \hat{\eta}^2 - i\omega/\nu$. The boundary condition of zero shear stress gives

$$\frac{\bar{\bar{B}}(\hat{\eta}, \omega)}{\bar{\bar{A}}(\hat{\eta}, \omega)} = \frac{-2\hat{\eta}^2 \nu i}{-i\omega + 2\hat{\eta}^2 \nu}. \tag{180}$$

For slight viscosity, ω is $O(\omega_\eta)$, and $\omega_\eta \gg 2\hat{\eta}^2 \nu$. Hence $\bar{\bar{B}} \ll \bar{\bar{A}}$, allowing boundary condition (174) to be written as

$$-\rho_u \dot{\phi}_s - \rho_u g h_s - 2\mu \phi_{s,zz} + \gamma h_{s,yy} = -P_r. \tag{181}$$

The relation $\phi_{s,z} = \dot{h}_s$ at $z = 0$ gives

$$h_s \cong -\int\!\!\int_{-\infty}^{\infty} \frac{\hat{\eta} \bar{\bar{A}}(\hat{\eta}, \omega)}{i\omega} \; e^{i\hat{\eta}s} \, e^{-i\omega t} \, d\hat{\eta} d\omega. \tag{182}$$

The Fourier transform of the boundary condition (181) gives

$$\bar{\bar{h}}_s = \frac{\bar{\bar{P}}_r(\hat{\eta}, \omega)}{\rho_u g + \gamma \hat{\eta}^2} \left[\frac{\omega_\eta^2}{-\omega^2 - 2i\omega\hat{\eta}^2 \nu + \omega_\eta^2} \right]. \tag{183}$$

Taking the inverse transform with respect to ω gives

$$\bar{h}(\hat{\eta}, t) = \frac{\bar{p}_r(\hat{\eta})}{\rho_u g + \gamma \hat{\eta}^2} \left[\frac{\omega_\eta^2}{\omega_\eta'} \right] \left[e^{-2\hat{\eta}^2 \nu t} \sin \omega_\eta' t \; \oplus \text{Rect} \; (t/\Delta t) \right], \tag{184}$$

where $(\omega_\eta')^2 = \omega_\eta^2 - (2\hat{\eta}^2 \nu)^2$. For slight viscosity, $\omega_\eta' \cong \omega_\eta$, and the transfer function becomes

$$\bar{H}(\hat{\eta}, t) = \frac{\omega_\eta \, e^{-2\hat{\eta}^2 \nu t} \sin \omega_\eta t \; \oplus \text{Rect} \; (t/\Delta t)}{\rho_u g + \gamma \hat{\eta}^2}. \tag{185}$$

The case of finite depth is more complicated, and it becomes necessary to numerically integrate the governing equations. This was done by Pille and Hildebrand [2] for a minitank with a rigid bottom. The resulting transfer function is the same as (185), except for shallow depths, defined by $d\hat{\eta} < \pi/2$. In this case they found by numerical analysis that

$$\bar{H}(\hat{\eta}, t) = \frac{\omega_\eta \, e^{-q\omega_\eta t} \sin \beta\omega_\eta t \; \oplus \text{Rect} \; (t/\Delta t)}{(\rho_u g + \gamma \hat{\eta}^2)\beta}. \tag{186}$$

47

where

$$\beta = \sqrt{1 - q^2},$$

$$q = 2\mu\hat{\eta}\sqrt{\frac{\hat{\eta}}{\rho_u(\rho_u g + \gamma\hat{\eta}^2)}} \; (\tanh \hat{\eta}d)^E,$$

and

$$E = 0, \qquad d\hat{\eta} > \pi/2,$$
$$= -2.3, \quad d\hat{\eta} < \pi/2.$$

Pille and Hildebrand [2] observed that, based on their numerical results, the criterion $\omega_\eta \gg \hat{\eta}^2\nu$ which has been used to define the fluid as being slightly viscous may be too restrictive. That is, the transfer function for a viscous fluid may be adequately described by (186) even if $\omega_\eta \sim O(2\hat{\eta}^2\nu)$. They also observed that the addition of the factor $(\tanh \hat{\eta}d)^{-2.3}$ in (186) gave a good fit to their numerical results for depths as small as $0.02\lambda_s$, where $\lambda_s = 2\pi/\hat{\eta}$. They did not perform any numerical analysis for $d < 0.02\lambda_s$. Furthermore they state that (186) may be invalid for small $\hat{\eta}$.

A typical plot of $\overline{H}(\hat{\eta}, t)$ for a given value of $\hat{\eta}$ is shown in Fig. 18, taken from Pille and Hildebrand [2], where $H_N = 1/\rho_u g$. It is seen that good agreement exists between their numerical results and (186). Note that the surface levitation decays with time due to the effect of viscosity.
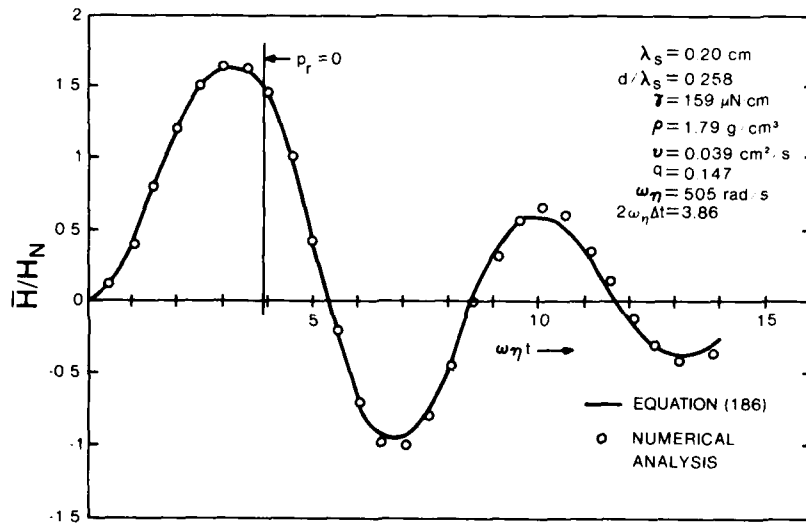
Fig. 18 — Response of the liquid surface to a pulse of radiation pressure having spatial frequency $2\pi/\lambda_s$. This figure is taken from Refs. 1 and 2, by permission.

A plot of $\bar{H}(\hat{\eta}, t)$ with time t as the parameter and $\hat{\eta}$ varying is shown in Fig. 19, also from Pille and Hildebrand [2]. Here the minitank depth d is greater than $\lambda_s/4$ for the spatial frequencies considered and, by definition, $dB \equiv 10 \log_{10}(\bar{H}/H_N)$. The curves were terminated at the point at which $\bar{H}(\hat{\eta}, t)$ becomes negative. Note that for any given time t_s there exists a band of spatial frequencies for which $\bar{H}(\hat{\eta}, t_s)$ is approximately constant. At this time the liquid surface faithfully records the corresponding spatial frequency components of the focused acoustic image.
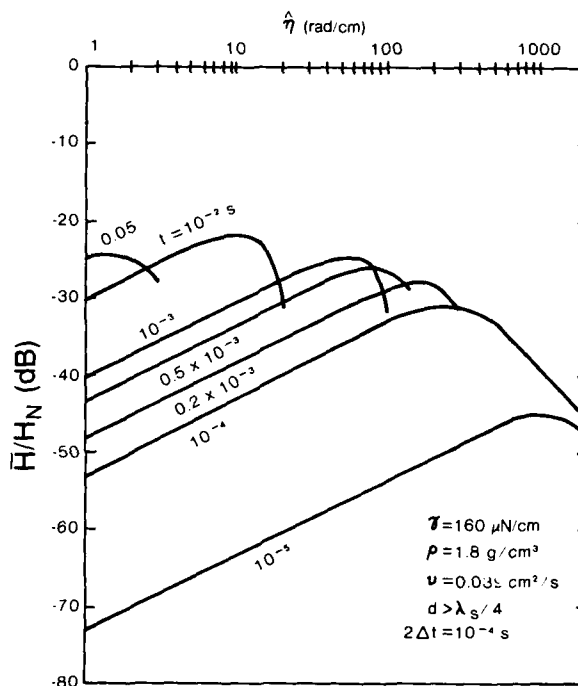
Fig. 19 — Transfer function for the liquid surface as a function of spatial frequency, with time as a parameter. The surface is subjected to a pulse of radiation pressure; the minitank depth is effectively infinite. This figure is taken from Refs. 1 and 2, by permission.

Figure 20 shows the behavior of the transfer function for a finite depth ($d = 0.015$ cm). It is seen that the effect of finite depth is to reduce the magnitude of $\bar{H}(\hat{\eta}, t)$ at low spatial frequencies.

In the preceeding two figures the pulse duration $2\Delta t$ has been finite. Figure 21 shows $\bar{H}(\hat{\eta}, t)$ for $\Delta t \rightarrow \infty$, that is, for continuous excitation of the liquid surface by radiation pressure for $t > 0$. The figure clearly shows that the liquid surface experiences an increase in response to the lower spatial frequencies when excited by a step function of radiation pressure, as opposed to a pulse. However, it was shown by (105) that the spatial frequency components in the acoustic image have been upshifted by $\hat{\eta}_r$ due to the interference of the acoustic image
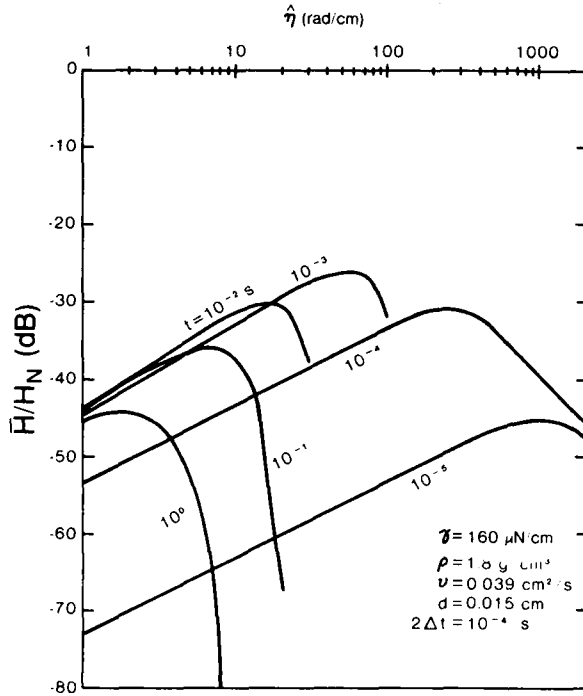
Fig. 20 — Transfer function for the liquid surface as a function of spatial frequency, with time as a parameter. The surface is subjected to a pulse of radiation pressure; the minitank depth is finite. This figure is taken from Refs. 1 and 2, by permission.
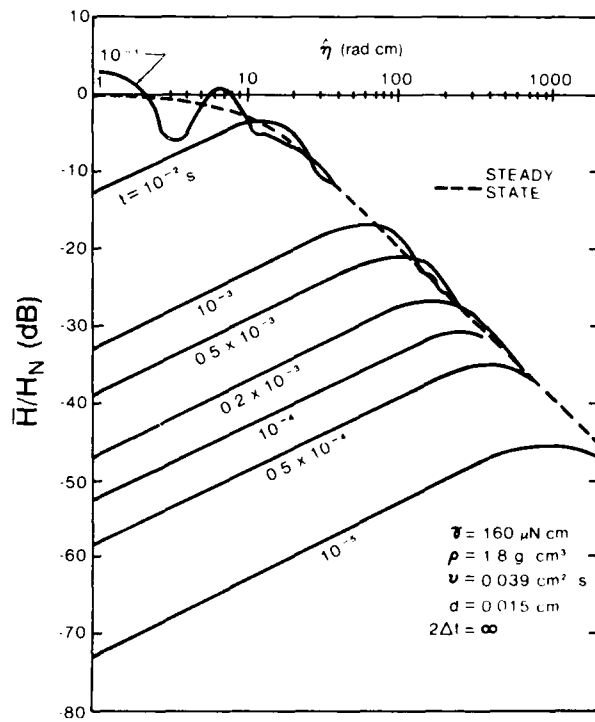
Fig. 21 — Transfer function for the liquid surface subjected to a step function of radiation pressure ($\Delta t = \infty$); the minitank depth is finite. This figure is taken from Refs. 1 and 2, by permission.

with the reference beam $\phi_r \propto A_r \exp(i\hat{\eta}_r y)$. For $\hat{\eta}_r$ greater than approximately 10 rad/cm the steady-state value of $\tilde{H}(\hat{\eta}, t)$ in Fig. 21 is not constant, which will cause distortion of the image.

Hence better image fidelity is obtained by subjecting the liquid surface to a train of pulses. Recall that only those spatial frequencies in the bandpass $|\hat{\eta}| \leqslant \hat{\eta}_m$ are passed by the acoustic lens system. Since the reference wave upshifts these frequencies, the surface must record frequencies in the band $-\hat{\eta}_m + \hat{\eta}_r \leqslant \hat{\eta} \leqslant \hat{\eta}_r + \hat{\eta}_m$. The previous figures show that there exists a time t_s after the initiation of the pulse when $\tilde{H}(\hat{\eta}, t_s)$ is approximately constant in this band of spatial frequencies. It is at this time that the liquid surface is sampled with a short pulse of laser light. Since the levitation damps out due to viscosity, the surface will eventually return to its quiescent state. Then it can be subjected to another pulse of radiation pressure and, after the same time delay t_s, again sampled with laser light. This process is repeated with a repetition rate such that a flicker-free optical reconstruction of the acoustic image can be formed.

A typical sampling rate is 60 Hz. It is of interest to determine whether the liquid surface has returned to its undisturbed state $1/60$ second after being subjected to a pulse of radiation pressure. Let the response to $\bar{P}_{r_1}(\hat{\eta})$ be $\bar{h}_1$, and assume $\hat{\eta} \cong 20$ rad/cm, or $\lambda_s \sim O(0.1 \text{ cm})$. The transfer function for levitation of the surface is given by (186). Let the minitank depth d be of the order of 0.1 cm; then the damping factor $e^{-q\omega_\eta t}$ in (186) becomes $e^{-2\hat{\eta}^2 \nu t}$, since $\hat{\eta}d > \pi/2$. Assume Freon E-5 to be the imaging fluid, so that $\gamma = 160 \ \mu\text{N/cm}$, $\nu = 0.04$ cm^2/s, and $\rho_u = 1.8$ g/cm^3. For $2\Delta t = 10^{-4}$ s it is found that $\omega_\eta \Delta t \ll 1$; hence for $t > 2\Delta t$

$$\omega_\eta \ e^{-2\hat{\eta}^2 \nu t} \sin \beta\omega_\eta t \ \oplus \text{Rect} \ (\hat{t}/\Delta t) = 2\omega_\eta \Delta t \ e^{-2\hat{\eta}^2 \nu t} \sin \omega_\eta t. \tag{187}$$

Let t_1 be the time at which a new pulse of radiation pressure is applied. Then from (186) the levitation of the surface just prior to the application of the pulse is

$$\bar{h}_1(\hat{\eta}, t_1) = \frac{2\bar{P}_{r_1}(\hat{\eta})}{\rho_u g + \gamma\hat{\eta}^2} \ \omega_\eta \Delta t \ e^{-2\hat{\eta}^2 \nu t_1} \sin \omega_\eta t_1. \tag{188}$$

In order for $\bar{h}_1(\hat{\eta}, t_1) \to 0$, it is necessary that $e^{-2\hat{\eta}^2 \nu t_1} \to 0$ or $2\hat{\eta}^2 \nu t_1 \gg 1$. For $t = 1/60$ s, $2\hat{\eta}^2 \nu t_1 \cong 0.5$ for $\hat{\eta} = 20$ rad/cm; hence $\bar{h}_1(\hat{\eta}, t_1)$ has not decayed sufficiently when the next pulse of radiation pressure arrives at the surface.

Two options are available to make $\bar{h}_1(\hat{\eta}, t_1) \to 0$; either the spatial frequency can be increased (by increasing the acoustic frequency for example) or the minitank depth can be decreased. Suppose that $\hat{\eta} \cong 100$ rad/cm; then $e^{-2\hat{\eta}^2 \nu t_1} \to 0$ and $\bar{h}_1(\hat{\eta}, t_1) \to 0$. If $\hat{\eta}$ is still 20 rad/cm but d is decreased to the order of 0.01 cm, then $d\hat{\eta} < \pi/2$ and the damping factor $e^{-q\omega_\eta t}$ in (186) becomes $\exp[-2\hat{\eta}^2 \nu t_1 (\hat{\eta}d)^{-2.3}]$. The argument of this exponential is of the order of 10, so that $\bar{h}_1(\hat{\eta}, t_1) \to 0$.

5.6 Levitation of the Liquid Surface Accounting for Membrane Elasticity

It is necessary to justify the use of the rigid membrane boundary condition (160) which was used in calculating $\tilde{H}(\hat{\eta}, t)$. To do this, consider the response of the system composed of the imaging fluid, membrane, and object-tank fluid to a pulse of radiation pressure. The object-tank fluid is assumed to be semi-infinite (to extend to $z = -\infty$). For simplicity, viscosity is assumed negligible.

51

The boundary condition at the membrane is given by (66) with the subscript l referring to the lower (object-tank) fluid and the subscript u referring to the upper (imaging) fluid. The boundary condition can be rewritten as

$$2\rho_M b(\ddot{w}_a + \ddot{w}_s) - T \frac{\partial^2}{\partial y^2}(w_a + w_s) = -[\Delta P_{1a} + \Delta P_{2a} + \Delta P_s + \Delta\rho_0(\mathbf{v}_{1a} \cdot \mathbf{e}_z)^2]. \quad (189)$$

Here ΔP_{1a} is the jump in first-order acoustic pressure across the membrane, ΔP_{2a} is the jump in second-order acoustic pressure, $\Delta\rho_0$ is the jump in equilibrium-state fluid density, and $\Delta P_s = P_{su} - P_{sl}$, where P_{sl} is the pressure induced in the object tank by low-frequency membrane motion and P_{su} is the corresponding pressure in the minitank. Since the displacement w_a caused by ΔP_{1a} is calculated from (68), the boundary condition (189) reduces to

$$2\rho_M b\ddot{w}_s - T \frac{\partial^2 w_s}{\partial y^2} = -(\Delta P_r + \Delta P_s)_{z=-d}. \quad (190)$$

The membrane deflection w_s is measured from its static equilibrium position. In accordance with (90) the radiation pressure at the membrane ΔP_r is given by

$$\Delta P_r = [<\Delta P_{2a}> + (\Delta\rho_0) <(\mathbf{v}_{1a} \cdot \mathbf{e}_z)^2>] \text{ Rect } (\hat{t}/\Delta t). \quad (191)$$

The linearized Bernouli equation gives

$$P_{sl} = -\rho_l\dot{\Phi}_l - \rho_l g z_l \quad (192a)$$

and

$$P_{su} = -\rho_u\dot{\Phi}_u - \rho_u g z_u. \quad (192b)$$

The velocity potentials Φ_u and Φ_l for the imaging and object-tank fluids are governed by the Laplace equations

$$\nabla^2\Phi_u = 0, \qquad 0 > z > -d, \quad (193a)$$

and

$$\nabla^2\Phi_l = 0, \qquad z < -d. \quad (193b)$$

In addition the boundary condition at the membrane is now

$$\frac{\partial\Phi_u}{\partial z} = \frac{\partial\Phi_l}{\partial z} = \dot{w}_s, \qquad z = -d. \quad (194)$$

Finally it is necessary to satisfy the following boundary conditions at $z = 0$:

$$-\rho_u\dot{\Phi}_u - \rho_u g h_s + \gamma \frac{\partial^2 h_s}{\partial y^2} = -P_r \quad (195)$$

and

$$\frac{\partial\Phi_u}{\partial z} = \dot{h}_s. \quad (196)$$

To satisfy the Laplace equations, let

$$\Phi_u = \int\int_{-\infty}^{\infty} [\bar{\bar{A}}(\hat{\eta}, \omega) \sinh \hat{\eta} z' + \bar{\bar{B}}(\hat{\eta}, \omega) \cosh \hat{\eta} z'] \, e^{i\hat{\eta} y} e^{-i\omega t} \, d\hat{\eta} d\omega \quad (197a)$$

and

$$\Phi_l = \iint\limits_{-\infty}^{\infty} \bar{\bar{C}}(\hat{\eta}, \omega) \, e^{\hat{\eta} z'} \, e^{i\hat{\eta} y} \, e^{-i\omega t} \, d\hat{\eta} d\omega. \tag{197b}$$

Note that $z' = z + d$. Furthermore set

$$w_s = \iint\limits_{-\infty}^{\infty} \bar{\bar{w}}(\hat{\eta}, \omega) \, e^{i\hat{\eta} y} \, e^{-i\omega t} \, d\hat{\eta} d\omega \tag{198}$$

and

$$h_s = \iint\limits_{-\infty}^{\infty} \bar{\bar{h}}(\hat{\eta}, \omega) \, e^{i\hat{\eta} y} \, e^{-i\omega t} \, d\hat{\eta} d\omega. \tag{199}$$

From the boundary condition $\partial \Phi_u / \partial z = \dot{w}_s$ at $z' = 0$, it follows that $\bar{\bar{A}} = -i\omega \bar{\bar{w}}_s / \hat{\eta}$. To match membrane and fluid particle velocities on the plane $z' = 0$, rather than on the moving surface of the membrane, requires that $w_s \ll 1/\hat{\eta}$. The boundary condition $\partial \Phi_u / \partial z = \partial \Phi_l / \partial z$ at $z' = 0$ gives $\bar{\bar{A}} = \bar{\bar{C}}$. The last kinematic boundary condition $h_s = \partial \Phi_u / \partial z$ at $z' = d$ is used in conjunction with the above results to give

$$\bar{\bar{h}}_s(\hat{\eta}, \omega) = - \frac{\hat{\eta}}{i\omega} (\bar{\bar{A}} \cosh \hat{\eta} d + \bar{\bar{B}} \sinh \hat{\eta} d). \tag{200}$$

Since $\bar{\bar{\Phi}}_u = \bar{\bar{A}} \sinh \hat{\eta} d + \bar{\bar{B}} \cosh \hat{\eta} d$ at the liquid surface, the Fourier transform of boundary condition (195) becomes

$$\left[-\omega^2 \tanh \hat{\eta} d + \frac{\omega_\eta^2}{\tanh \hat{\eta} d} \right] \bar{\bar{A}}(\hat{\eta}, \omega) + (\omega_\eta^2 - \omega^2) \, \bar{\bar{B}}(\hat{\eta}, \omega) = \frac{-i\omega}{\rho_u} \left[\frac{\bar{\bar{P}}_r(\hat{\eta}, \omega)}{\cosh \hat{\eta} d} \right]. \tag{201}$$

In like fashion the boundary condition (190) governing motion of the membrane can be Fourier-transformed to give

$$\{-2\rho_M b\omega^2 + [T\hat{\eta}^2 + (\rho_l - \rho_u)g]\} \, \bar{\bar{w}}_s = -i\omega(\rho_u \bar{\bar{\Phi}}_u - \rho_l \bar{\bar{\Phi}}_l) - \Delta \bar{\bar{P}}_r. \tag{202}$$

Here the boundary condition $\partial \Phi_u / \partial z = \partial \Phi_l / \partial z = \dot{w}_s$ has been used as well as the Bernoulli equations (192a) and (192b). After some manipulation (202) can be rewritten as

$$\left\{ -\omega^2 \left[1 + \frac{2\rho_M b\hat{\eta}}{\rho_l} \right] + [T\hat{\eta}^2 + (\rho_l - \rho_u)g] \, \hat{\eta}/\rho_l \right\} \bar{\bar{A}}(\hat{\eta}, \omega)$$

$$+ (\omega^2 \rho_u / \rho_l) \, \bar{\bar{B}}(\hat{\eta}, \omega) = \frac{i\omega}{\rho_l} \, \Delta \bar{\bar{P}}_r(\hat{\eta}, \omega). \tag{203}$$

Let

$$\omega_m^2 = [(\rho_l - \rho_u)g\hat{\eta} + T\hat{\eta}^3]/\rho_l', \tag{204}$$

in which

$$\rho_l' = \rho_l + 2\rho_M b\hat{\eta}, \tag{205}$$

and let

$$\rho_R = \rho_u / \rho_l'. \tag{206}$$

Then the boundary conditions governing the motion of the liquid surface and of the membrane can be combined into the matrix equation

$$\left[\begin{array}{cc}\left(-\omega^2\tanh\hat\eta d+\dfrac{\omega_\eta^2}{\tanh\hat\eta d}\right) & (-\omega^2+\omega_\eta^2) \\ (-\omega^2+\omega_m^2) & \omega^2\rho_R\end{array}\right]\left\{\begin{array}{c}\bar{\bar A}\\ \bar{\bar B}\end{array}\right\}=i\omega\left\{\begin{array}{c}\left(\dfrac{-\bar{\bar P}_r}{\rho_u\cosh\hat\eta d}\right)\\ \left(\dfrac{\Delta\bar{\bar P}_r}{\rho_l'}\right)\end{array}\right\}$$

(207)

Consider the magnitudes of the frequencies ω_η and ω_m for typical values $T\sim$ O(10 N/cm), $\gamma\sim$ O(100 μN/cm), $d\leqslant$ O(0.10 cm), and ρ_M, ρ_u, and ρ_l all of the order of 1 g/cm^3. Assume $\hat\eta^2>$ O$[(\rho_l-\rho_u)g/T]$ for stability of the system; otherwise, if $\rho_l-\rho_u$ is negative, the membrane (and upper fluid) will sink. For the values quoted above, this requires $\hat\eta^2\geq$ O(10^{-3} rad^2/cm^2). Then $\omega_m^2\gg\omega_\eta^2$ for $\hat\eta\gg10^{-2}$ rad/cm. Physically this means that the membrane is much stiffer than the liquid surface. The determinant of the matrix equation can then be approximated by $\alpha[-\omega^4+\omega^2(\omega_m')^2-\omega_\eta^2(\omega_m')^2]$, where $(\omega_m')^2=\omega_m^2/\alpha$ and $\alpha=\rho_R\tanh\hat\eta d+1$. Cramer's rule can be used to solve for $\bar{\bar A}$ and $\bar{\bar B}$, which are then substituted into the appropriate expressions for $\bar h_s$ and $\bar w_s$. Taking the inverse transform with respect to ω gives

$$\bar h_s(\hat\eta,\ t)=\frac{\bar P_r(\hat\eta,\ t)\overset{'}{\oplus}\omega_\eta\sin\omega_\eta t}{\rho_u g+\gamma\hat\eta^2}+\frac{\hat\eta}{\alpha\rho_l'\omega_m'}\left[\bar P_r(\hat\eta,\ t)\overset{'}{\oplus}\left(\frac{\sin\omega_m' t}{\cosh^2\hat\eta d}-\frac{\omega_\eta}{\omega_m'}\sin\omega_\eta t\right)\right.$$
$$\left.-\frac{\Delta\bar P_r(\hat\eta,\ t)}{\cosh\hat\eta d}\overset{'}{\oplus}\left(\sin\omega_m' t-\frac{\omega_\eta}{\omega_m'}\sin\omega_\eta t\right)\right]$$

(208)

and

$$\bar w_s(\hat\eta,\ t)=-\frac{\hat\eta\Delta\bar P_r(\hat\eta,\ t)\overset{'}{\oplus}\sin\omega_m' t}{\alpha\rho_l'\omega_m'}+\left(\frac{\hat\eta}{\alpha\rho_l'\omega_m'\cosh\hat\eta d}\right)$$
$$\times\left\{\bar P_r(\hat\eta,\ t)\overset{'}{\oplus}\left[\sin\omega_m' t-\frac{\omega_\eta}{\omega_m'}\sin\omega_\eta t\right]\right\}.$$

(209)

In the preceding, the inequality $(\omega_m'/\omega_\eta)^2\tanh\hat\eta d\gg1$ has been used, which is valid for $\hat\eta^2\gg10^{-3}$ rad^2/cm^2.

The first term on the right-hand side of (208) gives the surface levitation for the case of the rigid membrane, as comparison with (166) shows. The remaining terms arise because of the coupling between motion of the membrane and motion of the liquid surface.

The coupling term

$$\frac{-\hat\eta}{\alpha\rho_l'\omega_m'}\left[\bar P_r(\hat\eta,\ t)\overset{'}{\oplus}\frac{\omega_\eta}{\omega_m'}\sin\omega_\eta t\right]$$

will become negligible compared to the rigid-membrane surface levitation term if

$$\left(\frac{\omega_m'}{\omega_\eta}\right)^2\frac{\tanh\hat\eta d}{\rho_R}\gg1.$$

(210)

The inequality is easily satisfied at large depths and/or high spatial frequencies. For low spatial frequencies and small depths it may not be satisfied. For fidelity in recording the acoustic

54

image at the surface, it is desirable that the spatial frequencies in $\bar{P}_{r_i}(\hat{\eta})$ be large enough so that coupling terms are negligible. This will place a lower limit on $\hat{\eta}_r$. Hence it is of interest to determine the smallest spatial frequency range for which the above inequality is satisfied. For the values of T, ρ_u, ρ_M, d, etc. that were quoted, the inequality is satisfied if the order of $\hat{\eta}^2$ is much greater than the order of 10^{-3} rad^2/cm^2.

Similarly the coupling term

$$\left(\frac{\hat{\eta}}{\alpha \rho_l \omega_m'}\right) \left| \frac{\bar{P}_r(\hat{\eta}, t) \oplus \sin \omega_m' t}{\cosh^2 \hat{\eta} d} \right|$$

will be negligible if

$$\left(\frac{\omega_m'}{\omega_\eta}\right)^2 \frac{\tanh \hat{\eta} d}{\rho_R} \left(\frac{\cos \omega_m'(t - 2\Delta t) - \cos \omega_m' t}{\cos \omega_\eta(t - 2\Delta t) - \cos \omega_\eta t} \right) \gg 1. \tag{211}$$

For $\hat{\eta} \sim O(10 \text{ rad/cm})$ and $d \geq O(10^{-2} \text{ cm})$ the system parameters give free-vibration frequencies ω_η of the order of 100 rad/s. Typically the pulse duration $2\Delta t$ will be of the order of 10^{-4} s, so that $\cos \omega_\eta(t - 2\Delta t) - \cos \omega_\eta t \sim O(\omega_\eta \Delta t)$. Likewise, $\omega_m' \sim O(10^4 \text{ rad/s})$, so $\cos \omega_m'(t - 2\Delta t) - \cos \omega_m' t \sim O(1)$. The left-hand side of the inequality then is at least of the order of 100, so that the inequality is satisfied. If $\hat{\eta}$ is decreased to the order of 1 rad/cm, then the left hand side is of the order of 1, and the coupling term is no longer negligible.

The coupling term

$$\frac{\omega_\eta}{\omega_m'} \left| \frac{\Delta \bar{P}_r(\hat{\eta}, t) \oplus \sin \omega_\eta t}{\cosh \hat{\eta} d} \right|$$

is negligible if

$$\frac{\bar{P}_r}{\Delta \bar{P}_r} \left(\frac{\omega_m'}{\omega_\eta}\right)^2 \frac{\sinh \hat{\eta} d}{\rho_R} \gg 1. \tag{212}$$

It is shown in Appendix C that $\Delta \bar{P}_r \leq O(\bar{P}_r)$ when $|\rho_u - \rho_l| \sim O(\rho_l)$. Even if $|\rho_u - \rho_l|$ is much less than ρ_l, $\Delta \bar{P}_r$ still may not be negligible, due to the discontinuity in $<P_{1a}^2>$ caused by the presence of the membrane; however, $\Delta \bar{P}_r$ will still be of the order of $\bar{P}_r$ at most. Hence, as in the case of (210), the inequality above is satisfied for $\hat{\eta}^2$ much greater than the order of 10^{-3} rad^2/cm^2.

The remaining coupling term

$$\frac{-\Delta \bar{P}_r(\hat{\eta}, t) \oplus \sin \omega_m' t}{\cosh \hat{\eta} d}$$

is negligible if

$$\frac{\bar{P}_r(\hat{\eta}, t)}{\Delta \bar{P}_r(\hat{\eta}, t)} \left(\frac{\omega_m'}{\omega_\eta}\right)^2 \frac{\sinh \hat{\eta} d}{\rho_R} \left(\frac{\cos \omega_m'(t - 2\Delta t) - \cos \omega_m' t}{\cos \omega_\eta(t - 2\Delta t) - \cos \omega_\eta t} \right) \gg 1. \tag{213}$$

Since $\Delta \bar{P}_r \leq O(\bar{P}_r)$, this is satisfied if inequality (211) is satisfied; hence, for the values of T, γ, ρ_u, ρ_M, d, etc. cited previously, $\hat{\eta}$ must be at least of the order of 10 rad/cm.

At first glance it would seem that, since $\omega_m^2 >> \omega_\eta^2$, the coupling terms should always be negligible. However, the rigid membrane levitation term is analogous to the response of a mass-spring oscillator driven by the motion of the base to which it is connected. The base-motion input is an impulse of duration $2\Delta t$. Since $\omega_\eta \Delta t << 1$, the response of this low-frequency oscillator becomes smaller as $\hat{\eta}$ decreases.

Conversely the coupling terms become larger. For instance the coupling term

$$\frac{\hat{\eta}}{\alpha \rho_I \omega_m'} \left[\frac{\bar{P}_r(\hat{\eta}, t) \overset{t}{\oplus} \sin \omega_m' t}{\cosh^2 \hat{\eta} d} \right]$$

is analogous to the response of a high-frequency oscillator ($\omega_m >> \omega_\eta$) driven by a pulse whose duration is of the order of the oscillator period: $\Delta t \sim O(1/\omega_m')$. When $\hat{\eta} \sim O(1 \text{ rad/cm})$, the responses of the low-frequency and high-frequency oscillators are of the same order of magnitude.

In like fashion, it can be shown that $\bar{h}_s(\hat{\eta}, t) >> \bar{w}_s(\hat{\eta}, t)$ for $\hat{\eta} \geq O(10 \text{ rad/cm})$; that is, the membrane appears rigid at these spatial frequencies, as compared to the liquid surface. This justifies the use of the rigid membrane boundary conditions (160) and (175) used in calculating the transfer function for inviscid and slightly viscous fluids respectively. Since $\lambda_s = 2\pi/\hat{\eta}$, the transfer functions (167) and (186) are valid for wavelengths of the order of 1 cm or less.

Recall that, from section 4, $\bar{P}_r(\hat{\eta}, t)$ consists of four terms:

$$\bar{P}_r(\hat{\eta}, t) \propto \left[\bar{\psi}_1(\eta) \overset{\eta}{\oplus} \bar{\psi}_1^{\bullet}(\eta) + \bar{\phi}_r(\eta) \overset{\eta}{\oplus} \bar{\phi}_r^{\bullet}(\eta) \right.$$
$$\left. + \bar{\psi}_1(\eta - \eta_r) + \bar{\psi}_1^{\bullet}(\eta + \eta_r) \right] \text{Rect} (\hat{t}/\Delta t), \tag{214}$$

where $\bar{g}_1(\eta)$, the minitank transfer function calculated in section 3.1, is assumed constant over the bandwidth of interest. ψ_1 is the velocity potential in the focused acoustic image, ϕ_r is the velocity potential in the reference beam, and η_r is its spatial frequency in lines/cm.

The term $\bar{\psi}_1(\eta - \eta_r)$, or its downshifted complex conjugate $\bar{\psi}_1^{\bullet}(\eta + \eta_r)$, will be used when the acoustic image is optically reconstructed. All spatial frequencies in these functions should be at least of the order of 10 rad/cm; recall that $\hat{\eta} = 2\pi\eta$. Because of the cutoff due to the acoustic lens system, $\bar{\psi}_1(\eta - \eta_r)$ will occupy the bandwidth $-\eta_m + \eta_r \leq \eta \leq \eta_m + \eta_r$, where η_m is the maximum spatial frequency passed by the lens system. In section 2.1 it was pointed out that if a is the lens radius, λ_I is the acoustic wavelength in the object tank, and D_2 is the distance from lens L_2 to the liquid surface, then $\eta_m = a/\lambda_I D_2$. This assumes L_2 is the limiting aperture. Also, $\eta_r = (\sin \theta_r)/\lambda_I$, for θ_r, the angle between the acoustic axis and the direction of the propagation of the reference wave. Since it is desired that $-\eta_m + \eta_r$ be at least of the order of $10/2\pi$ lines/cm, the reference beam must be inclined at an angle such that

$$\sin \theta_r \geq \frac{10\lambda_I}{2\pi} + \frac{a}{D_2}. \tag{215}$$

For an operating frequency of 5 MHz in water, and assuming $a/D_2 = 0.3$, the above requires $\theta_r \geq 20°$.

Terms such as $\bar{\psi}_1(\eta) \overset{\eta}{\oplus} \bar{\psi}_1^{\cdot}(\eta)$ in (214) will contain spatial frequencies lower than 10 rad/cm, as shown by Fig. 15. In calculating the liquid-surface response to these components of $\bar{P}_r$, the transfer function (186) cannot rigorously be used, since $\bar{h}_s(\hat{\eta}, t)$ is given by (208).

Some simplification in (208) is possible at low spatial frequencies (of the order of 1 rad/cm), if $\Delta \bar{P}_r \ll \bar{P}_r$. Now

$$\Delta \bar{P}_r = <\Delta P_{2a}> + <(\Delta \rho_0) \, (v_{1a} \cdot e_z)^2> \tag{216}$$

and

$$<\Delta P_{2a}> = <\Delta \left| \frac{P_{1a}^2}{\rho_0 c^2} \right|> - \frac{1}{2} <\Delta(\rho_0 v_{1a} \cdot v_{1a})>, \tag{217}$$

where $<\Delta P_{1a}^2>$ is the jump in the time average of P_{1a}^2 at the membrane, etc. Suppose that the imaging and object-tank fluids are the same; then $<(\Delta \rho_0) \, (v_{1a} \cdot e_z)^2>$ and $<\Delta(\rho_0 v_{1a} \cdot v_{1a})>$ vanish. Equation (68) shows that $\Delta P_{1a}^2 \sim O[(2\rho_M b \omega_a^2 w_a)^2]$; furthermore, $w_a \sim O(h_{1a})$, where again h_{1a} is the liquid-surface displacement predicted by linear acoustics. Consequently, for system parameters quoted previously,

$$\frac{\Delta P_{1a}^2}{\rho_0 c^2} \ll P_r \tag{218}$$

if $(\rho_u/\rho_M)^2 \gg (4\pi b/\lambda_u)^2$. For $\rho_u/\rho_M \sim O(1)$, the inequality is satisfied if the membrane is "thin"; that is, if $b \ll \lambda_u$. Then, for $t > 2\Delta t$ and $\hat{\eta} \sim O(1 \text{ rad/cm})$,

$$\bar{h}_s(\hat{\eta}, t) \cong \bar{p}_r(\hat{\eta}) \left[\frac{\omega_\eta \Delta t \, \sin \omega_\eta t}{\rho_u g} + \frac{\hat{\eta} \Delta t \, \sin \omega_m' t}{\omega_m' \rho_l} \right], \tag{219}$$

where the first term in parentheses is the form assumed by (166) for small ω_η. If $d \sim O(0.1 \text{ cm})$ then the first term is 10 times larger than the second; if $d \sim O(0.01 \text{ cm})$, they are the same order of magnitude. Note that, even if $\Delta P_r = 0$, $\bar{h}_s \sim O(10 \, \bar{w}_s)$ for $d \sim O(0.1 \text{ cm})$, and $\bar{h}_s \sim O(\bar{w}_s)$ for $d \sim O(0.01 \text{ cm})$.

Another factor to be considered is the finite lateral dimension of the minitank. In reality spatial frequencies lower than π/R_l cannot exist, for R_l the minitank radius. (This assumes a reflecting minitank wall. For a perfectly absorbent wall $\hat{\eta}$ can approach, but not equal, zero.) In fact the analysis of this section must be restricted to spatial frequencies much greater than π/R_l. The analysis of the oscillations of the imaging fluid contained in a finite minitank with a flexible membrane is rather complicated and will not be attempted here. The case of the finite minitank with a rigid bottom is considered in Appendix D.

5.7 Upper Bounds On Radiation Pressure and Mach Numbers

It was pointed out earlier that $|k_u - k_l|w$ must be much less than 1, so that displacement of the membrane causes negligible degradation of the acoustic image. Now $w = w_a + w_s$, where w_a is the displacement due to first-order acoustic pressure acting on the membrane. For subsonic flow the particle displacement in the acoustic field is much less than λ_a. Since there is continuity of displacement at the membrane, w_a must also be much less than λ_a. Hence, it is necessary only to determine whether $|k_u - k_l|w_s \ll 1$. Obviously, if the imaging fluid is the same as the object-tank fluid, the inequality is satisfied. The more interesting case occurs when, for example, $|k_u - k_l| \sim O(k_l)$.

57

From (209) the order of magnitude of $\bar{w}_s(\hat{\eta}, t)$ for $\hat{\eta} \geq O(10 \text{ rad/cm})$ is given by

$$\bar{w}_s(\hat{\eta}, t) \sim O\left[\frac{\hat{\eta}\bar{p}_r(\hat{\eta})}{\rho_l'(\omega_m')^2}\right].\tag{220}$$

Here previously cited values of T, γ, ρ_M, ρ_u, d, etc. have been used. Suppose that P_r has one dominant spatial frequency $\hat{\eta}$. Then, if w_s is to be much less than $1/|k_u - k_l|$, it is necessary that

$$P_r \ll \frac{\rho_l'(\omega_m')^2}{\hat{\eta}|k_u - k_l|}.\tag{221}$$

Assume that P_r is due to the interference between beams emitted by the object and reference transducers and that the average intensity in each beam is of the order of 10 mW/cm². Furthermore assume that each transducer has a pulse repetition rate of 60 Hz and a pulse duration of 10^{-4} s. The peak intensity in each beam is then of the order of 1 W/cm. For a plane acoustic wave $P_r = 2I/c$, where I is the acoustic intensity [7]; consequently $P_r \sim O(1 \text{ mN/cm}^2)$ for this example.

Let $\hat{\eta} \sim O(100 \text{ rad/cm})$, which corresponds to an acoustic frequency of 5 MHz in water and $\theta_r \cong 30°$. If the imaging fluid is Freon E-5 and the object-tank fluid is water, then $\lambda_u = 0.47\,\lambda_l$ and $1/|k_u - k_l| \cong 0.005$ cm. The inequality (221) is easily satisfied, since the right-hand side is of the order of 100 N/cm² and P_r is of the order of 1 mN/cm².

Suppose P_r has a dominant spatial frequency component which is of the order of 0.1 rad/cm; this would correspond, for example, to radiation pressure in the reference beam and in the acoustic image as given by the first two terms in (95). Then $\omega_m'\Delta t \ll 1$, so that in (209),

$$\bar{P}_r(\hat{\eta}, t) \overset{t}{\oplus} \sin \omega_m' t = \bar{p}_r(\hat{\eta})\Delta t \sin \omega_m' t$$

for $t > 2\Delta t$; consequently

$$\bar{w}_s \sim O\left[\frac{\hat{\eta}\Delta t P_r}{\rho_l \omega_m'}\right].\tag{222}$$

In order that $|k_u - k_l|w_s \ll 1$, it is required that

$$P_r \ll \frac{\rho_l' \omega_m'}{\hat{\eta}\Delta t |k_u - k_l|}.\tag{223}$$

Using previous system parameters, the right-hand side is found to be of the order of 0.1 N/cm², so that a radiation pressure of the order of 1 mN/cm² is again found to be permissible.

Comparison of inequalities (221) and (223) shows that the latter is more restrictive. It is interesting to rewrite (223) in terms of Mach numbers in the object and reference beams. Let $V_o \sim O(cM_o)$ and $V_r \sim O(cM_r)$, with V_o and V_r being the magnitude of the vertical particle velocity in the acoustic image and reference beam respectively and M_o and M_r being the corresponding Mach numbers. Use of (98) and (99) allows the inequality (223) to be rewritten as

$$M_o^2 + M_r^2 \ll \frac{4\omega_m'}{\rho_R c_u^2 \hat{\eta}\Delta t |k_u - k_l|}\tag{224a}$$

58

or

$$M_a^2 + M_r^2 \ll 10^{-5} \qquad (224b)$$

for system parameters cited previously.

If the object tank and minitank are filled with the same fluid, then every plane wave incident on the membrane with a given spatial frequency will be transmitted with the same spatial frequency, regardless of the magnitude of w_s. At first glance it would therefore appear advantageous to use identical minitank and object-tank fluids.

Suppose that both tanks are filled with water. Then Figs. 12a and 12b show that multiple internal reflections in the minitank can distort the acoustic image. Also, Figs. 22 and 23, taken from Ref. 2, indicate that $\bar{H}(\hat{\eta}, t)$ is constant over a smaller bandwidth for water than for Freon E-5. Consequently it is difficult to determine whether any advantage can be gained by using water as an imaging fluid as well as the object-tank fluid.
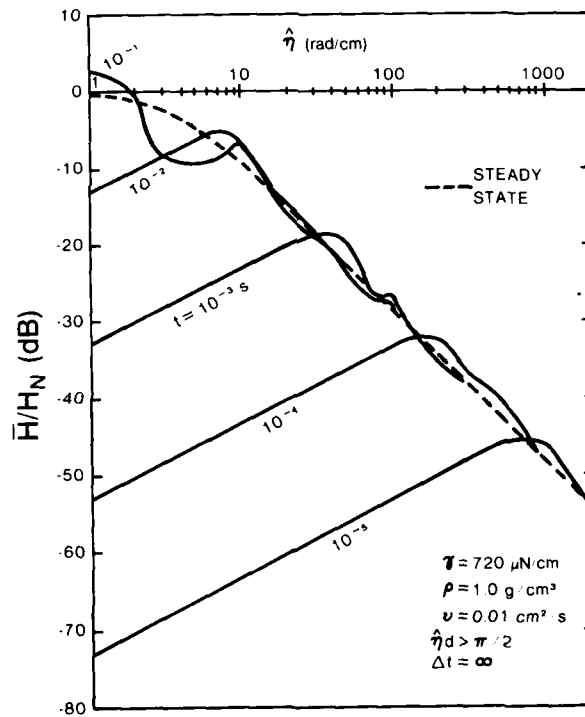
Fig. 22 — Transfer function for the liquid surface (water) subjected to a step function of radiation pressure ($\Delta t = \infty$); the minitank depth is effectively infinite. This figure is taken from Refs. 1 and 2, by permission.
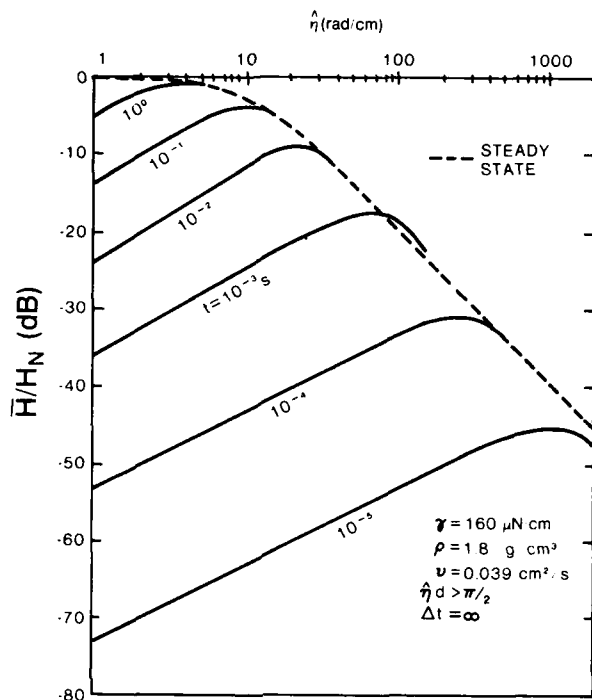
Fig. 23 — Transfer function for the liquid surface (Freon E-5) subjected to a step function of radiation pressure ($\Delta t = \infty$); the minitank depth is effectively infinite. This figure is taken from Refs. 1 and 2, by permission.

It is also interesting to estimate the bounds on the permissible Mach number such that the liquid surface responds linearly to a pulse of radiation pressure. Recall that for linearity the term $\rho_0(\mathbf{v}, \cdot \mathbf{e}_z)^2$ in boundary condition (136) was neglected on the assumption that $V_s \ll C$, or, equivalently, $h_s \ll \lambda_s$. From (168)

$$h_s \cong \sum_{j=-\infty}^{\infty} \overline{H}(\hat{\eta}_j, t) \ \bar{p}_r(\hat{\eta}_j) \ e^{i\hat{\eta}_j y} \ \Delta\hat{\eta} = \sum_{j=-\infty}^{\infty} h_j(y, t; \hat{\eta}_j), \qquad (225)$$

where $\Delta\hat{\eta}$ is small enough so that $\overline{H}(\hat{\eta}_j, t) \ \bar{p}_r(\hat{\eta}_j) \cong$ constant in the interval $(\hat{\eta}_j - \Delta\hat{\eta}, \hat{\eta}_j + \Delta\hat{\eta})$. Since λ_s varies with spatial frequency and $h_j(y, t; \hat{\eta}_j)$ is the displacement of the surface due to $\bar{p}_r(\hat{\eta}_j)$, it is necessary that $h_j \ll 2\pi/\hat{\eta}_j$.

Consider the case $\hat{\eta}_j \sim O(\hat{\eta}_r)$; then $\bar{p}_r \to \overline{P}_{ri}$, the radiation pressure due to interference between the focused image and the reference beam. From section 4,

$$\overline{P}_{ri} = \frac{1}{4}\rho_u y_b V \ \overline{V}_o(\hat{\eta}_1) \overset{\hat{\eta}_1}{\oplus} \text{sinc} \ (\hat{\eta}_1 y_b) \qquad (226)$$

for $V_r(y) = V \ \text{Rect}(y/y_b)$ and $\hat{\eta}_1 = \hat{\eta} - \hat{\eta}_r$. This shows that $\bar{p}_r$ will be constant over an increment $\Delta\hat{\eta} \sim O(1/y_b)$ due to scanning by the sinc function. Let M_r be the Mach number in the reference beam and M_o be the Mach number in the acoustic image. Then $|V_r| \sim O(c_u M_r)$ and $\overline{V}_o(\hat{\eta}_1) \leq O(c_u M_o y_b)$.

60

The latter follows from the definition

$$2\pi \bar{V}_o(\hat{\eta}) = \int_{-\infty}^{\infty} V_o(y)\, e^{-i\hat{\eta}y}\, dy; \tag{227}$$

assuming $V_o(y) = c_u M_o f(y)\, \text{Rect}(y/y_b)$ and applying the mean-value theorem of integral calculus gives

$$\bar{V}_o(\hat{\eta}) = 2c_u M_o f(y')\, y_b e^{-i\hat{\eta}y'}. \tag{228}$$

Here $-y_b \leqslant y' \leqslant y_b$ and it is assumed that $f(y)$ is continuous in $(-y_b, y_b)$. Since $f(y) \sim O(1)$, $f(y') \sim O(1)$ at most, so $\bar{V}_o(\hat{\eta}) \leq 0(c_u M_o y_b)$.

Assume that $\hat{\eta}_m \gg 1/y_b$; then in (226)

$$y_b \operatorname{sinc}(\hat{\eta}_1 y_b) \overset{\hat{\eta}_1}{\oplus} \bar{V}_o(\hat{\eta}_1) \cong \bar{V}_o(\hat{\eta}_1), \tag{229}$$

so that $\bar{P}_{ri} \sim O(\rho_u c_u^2 y_b M_o M_r/4)$. From (225), $h_j(y,\ t;\ \hat{\eta}_j)$ is given by $\bar{H}(\hat{\eta}_j,\ t)\, \bar{P}_{ri}(\hat{\eta}_j)\, e^{i\hat{\eta}_j y}\Delta\hat{\eta}$. $\bar{H}(\hat{\eta}_j,\ t)$ is obtained from (186) by replacing $\hat{\eta}$ by $\hat{\eta}_j$, etc., so that

$$\bar{H}(\hat{\eta}_j,\ t) \sim O\left[\frac{\hat{\eta}_j \Delta t\, \tanh \hat{\eta}_j d}{\rho_u \omega_j}\right]. \tag{230}$$

It is assumed that $\omega_j \Delta t \leqslant O(1)$. Recalling that $\Delta\hat{\eta} \sim O(1/y_b)$ and using all the preceding results allows the inequality $h_i \ll 2\pi/\hat{\eta}_i$ to be rewritten in the form

$$M_o M_r \ll \frac{4 C_s}{c_u^2 \hat{\eta}_i \Delta t\, \tanh \hat{\eta}_i d}. \tag{231a}$$

Let the imaging fluid be Freon E-5, so that $\rho_u = 1.8$ g/cm^3 and $c_u = 0.7$ km/s. It can be demonstrated that $C_s \cong 30$ cm/s when, for example, $\hat{\eta} \cong 100$ rad/cm and $d \sim O(0.1$ cm$)$. For a typical $\Delta t \sim O(10^{-4}$ s$)$ the inequality (231a) becomes

$$M_o M_r \ll 10^{-6}. \tag{231b}$$

Let $\hat{\eta}_i \sim O(0.1$ rad/cm$)$. Then $\bar{p}_r \to \bar{P}_{rb}$, the radiation pressure which gives rise to the bulge of the liquid surface; see Equation (100). An analysis similar to that performed gives

$$\bar{P}_{rb}(\hat{\eta}_i) \sim O[\rho_u c_u^2 y_b (M_o^2 + M_r^2)/4]. \tag{232}$$

The inequality $h_i \ll 2\pi/\hat{\eta}_i$ is satisfied if

$$M_o^2 + M_r^2 \ll \frac{4 C_s}{c_u^2 \hat{\eta}_i \Delta t\, \tanh \hat{\eta}_i d}. \tag{233a}$$

With use of the values of Δt, d, etc. that were quoted it is found that $C_s \sim O(10$ cm/s$)$ and

$$M_o^2 + M_r^2 \ll 10^{-2}. \tag{233b}$$

6. OPTICAL RECONSTRUCTION

6.1 Transfer Function for the Optical System

It has been shown that h_i, the surface levitation due to P_{ri}, contains information about the focused acoustic image. This information is extracted and displayed optically by illuminating

the liquid surface with a laser at the sampling times $t = nt_s$. Recall that $\overline{h_i}(\hat{\eta}, t) = \overline{H}(\hat{\eta}, t)\overline{P}_{ri}(\hat{\eta})$ and that $\overline{H}(\hat{\eta}, t_s) \cong$ constant over the bandwidth $\hat{\eta}_r - \hat{\eta}_m \leqslant \hat{\eta} \leqslant \hat{\eta}_r + \hat{\eta}_m$. The surface levitation modulates the phase of the reflected laser light and hence acts as a phase hologram.

In addition to h_i the surface levitation is also made up of h_c, the complex conjugate of h_i, as well as h_b, the liquid surface response to P_{rb}. Recall that P_{rb} is the sum of the radiation pressures in the reference beam and in the focused acoustic field. Since $h_s = h_i + h_c + h_b$, it is desired to eliminate the phase modulation of the laser light caused by $h_c + h_b$. Otherwise, upon optical reconstruction, there will be interference between the image, its conjugate, and background noise.

Let the liquid surface be illuminated with collimated quasimonochromatic light at normal incidence at $t = nt_s$. The reflected light passes through an optical train (Fig. 24) consisting of lens L_3 one focal length above the liquid surface, a spatial filter (pinhole) placed in the back focal plane of L_3, lens L_4 placed so that the spatial filter is in its front focal plane, and a ground glass viewing screen in the back focal plane of L_4.
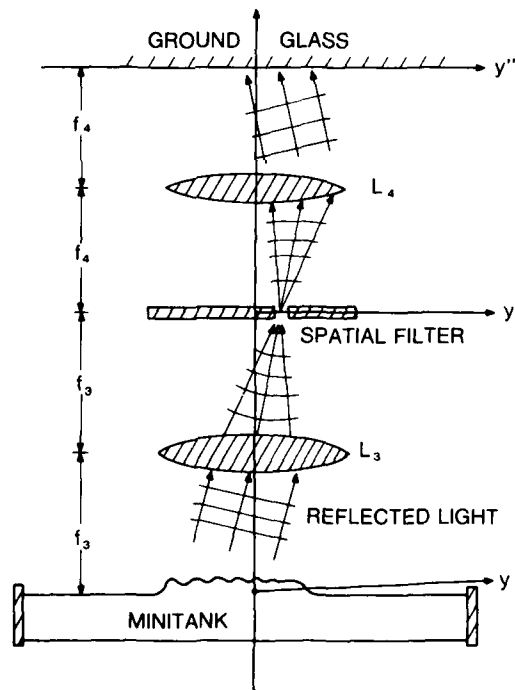
Fig. 24 — Passage of reflected light through the optical system. The drawing is not to scale.

The optical disturbance Ψ reflected from the liquid surface is the solution to the scalar wave equation

$$\nabla^2 \Psi + k_L^2 \Psi = 0 \tag{234}$$

62

for $k_L = 2\pi/\lambda_L$, where λ_L is the wavelength of coherent light. The acoustic velocity potential ϕ_{tr} also satisfies the scalar wave equation, for wavenumber $k_u = 2\pi/\lambda_u$; ϕ_{tr} is the field transmitted through the membrane into the minitank and is given by (76). Since both Ψ and ϕ_{tr} satisfy the wave equation, (76) can be used to calculate Ψ by replacing ϕ_{tr} by Ψ, and k_u by k_L, which gives

$$4\pi \ \Psi = \int \left[\Psi \ \frac{\partial}{\partial n} \left(\frac{e^{ik_L \cdot r}}{r} \right) - \frac{e^{ik_L \cdot r}}{r} \left(\frac{\partial \Psi}{\partial n} \right) \right] dy. \tag{235}$$

Here $k_L = (2\pi/\lambda_L) \ (\sin \theta_2' \, e_y + \cos \theta_2' \, e_z)$; compare Fig. 13 and Fig. 25. The optical disturbance in the far field can then be related to the disturbance in the back focal plane of L_3.
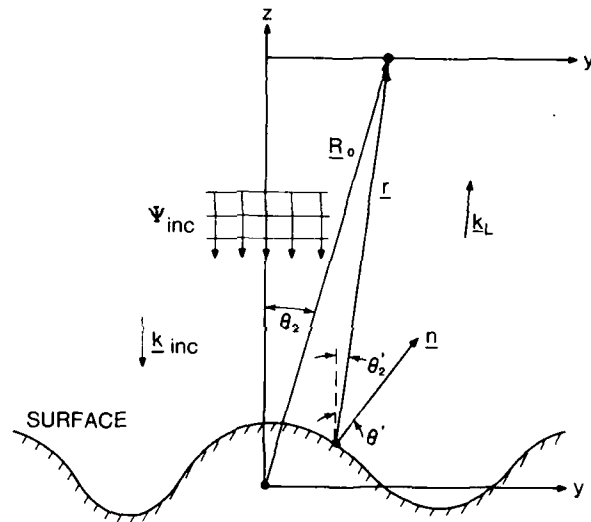
Fig. 25 — Quantities used in the far-field calculation of light
reflected from the liquid surface

It is necessary to calculate the values of Ψ and $\partial\Psi/\partial n$ on the liquid surface. The optical disturbance in the incident laser light is represented by $\Psi_{inc} = Ae^{-ik_L z}$ Rect (y/y_B), where y_B is the width of the laser beam. In the vicinity of the surface the reflected light is of the form

$$\Psi \propto Ae^{-ik_L h_s} R(\theta') e^{ik_L (z-h_s)\cos 2\theta'} \text{ Rect } (y/y_B), \tag{236}$$

where $\theta' \equiv \cos^{-1} (e_z \cdot n)$ is the local angle of incidence and $R(\theta')$ is the local reflection coefficient. For small angles $\theta' = \partial h_s/\partial y$, with $\partial h_s/\partial y << 1$ since it is required that $h_s << \lambda_s$. Then $R(\theta') \cong R$, the reflection coefficient for normal incidence, and

$$\Psi|_{z=h_s} = (1 + R) \ \Psi_{inc}|_{z=h_s}. \tag{237}$$

Likewise, since $\partial/\partial n \cong \partial/\partial z$ for small slopes,

$$\frac{\partial \Psi}{\partial n}\bigg|_{z=h_s} = -ik_L \ (1 - R) \ \Psi_{inc}|_{z=h_s}. \tag{238}$$

The quantities $e^{ik_L \cdot r}/r$ and $(\partial/\partial n)$ $(e^{ik_L \cdot r}/r)$ in (235) are calculated from (78) and (79) by replacing $\mathbf{k}_u$ with $\mathbf{k}_L$. Combining all results gives the optical disturbance in the far field, where $\theta_2' \cong \theta_2$,

$$\Psi = \frac{i\,A\,e^{ik_L R_0}}{2\,R_0 \lambda_L}[1 - \cos\theta_2 - R(1 + \cos\theta_2)]$$

$$\times \int_{-\infty}^{\infty} \text{Rect}\ (y/y_B)\ e^{-ik_L h_s(1+\cos\theta_2)} e^{-ik_L y \sin\theta_2}\ dy. \tag{239}$$

Recall that $h_s = h_i + h_c + h_b$, where $h_i + h_c$ is the response of the liquid surface to $P_{ri} + P_{rc}$, and h_b is the response to P_{rb}. Since the liquid surface is sampled at nt_s, and $P_{ri} + P_{rc}$ is given by (97),

$$h_i + h_c = \frac{1}{2}\,\rho_u\,\overline{H}(\hat{\eta}_r,\ t_s)\ |V_o(y)|V_r \cos[\hat{\eta}_r y + \chi_o(y)]$$

$$= |h_i| \cos[\hat{\eta}_r y + \chi_o(y)]. \tag{240}$$

Then the optical disturbance in the far field, where $\cos\theta_2 \cong 1$, is

$$\Psi \propto -\,RA\int_{-\infty}^{\infty} \text{Rect}\ (y/y_B)\ e^{-2ik_L h_b}\ e^{-2ik_L|h_i|\cos(\hat{\eta}_r y + \chi_o)}\ e^{-ik_L y \sin\theta_2}\ dy. \tag{241}$$

It is assumed for the moment that h_b is constant over the illuminated portion of the surface. There is an identity [7]

$$e^{-2ik_L|h_i|\cos(\hat{\eta}_r y + \chi_o)} \equiv \sum_{-\infty}^{+\infty} (-i)^m\, J_m(2k_L|h_i|)\, e^{im\chi_o}\, e^{im\hat{\eta}_r y}, \tag{242}$$

where J_m is the mth-order Bessel function of the first kind. Let $J_m(2k_L\,|h_i|)\, e^{im\chi_o}$ be denoted as ξ_m. For $2k_L|h_i| \ll 1$ the Bessel functions have the property $J_m(2k_L\,|h_i|) \propto (2k_L|h_i|)^{|m|}$, so that $\xi_m \propto (|h_i|e^{i\chi_o})^{|m|}$. From (240) $|h_i| \propto |V_o|$; hence $(|h_i|\,e^{i\chi_o})^{|m|} \propto (|V_o|\,e^{i\chi_o})^{|m|}$. The quantity $|V_o|\,e^{i\chi_o}$ is V_o; then $\xi_m \propto V_o^m$ for $m > 0$ and $\xi_m \propto (V_o^*)^{|m|}$ for $m < 0$. Since $V_o \propto g_1 \underset{s}{\oplus} \psi_1$, ξ_1 contains information about the focused acoustic image, and ξ_{-1} contains information about the complex conjugate of the acoustic image. If $\overline{g}_1(\eta) \cong$ constant over the bandwidth $|\eta| \leq \eta_m$, then $\xi_n \propto (\Lambda\psi_1)^n$ for $n > 0$ and $\xi_n \propto (\Lambda^*\psi_1^*)^{|n|}$ for $n < 0$, where $\Lambda = k_L\,\rho_u\,|\overline{g}_1(\eta_r)|^2\, A_r\, \overline{H}(\hat{\eta}_r,\ t_s)$, with A_r being the magnitude of the velocity potential in the reference beam. When $k_L\,|h_i|$ is of the order of 1 or larger, ξ_{+1} will be an amplitude-distorted image of ψ_1; the amplitude is distorted by the nonlinearity of $J_1(2k_L|h_i|)$.

Returning to (241) and performing the integration gives

$$\Psi \propto -\,Ry_B\,e^{-2ik_L h_b}\left[\sum_{n=-\infty}^{\infty} -\,i^n\, \text{sinc}\ (\hat{\eta}_n y_B) \overset{\hat{\eta}_n}{\oplus} \overline{\xi}_n\ (\hat{\eta}_n)\right], \tag{243}$$

where $\hat{\eta} = k_L \sin\theta_2$ and $\hat{\eta}_n = \hat{\eta} - n\,\hat{\eta}_r$. Since $\sin\theta_2 \cong y'/R_0$ in Fig. 25 and $\hat{\eta}_r = (2\pi/\lambda_l)\sin\theta_r$, the far-field optical disturbance consists of diffracted orders of light $\overline{\xi}_n$ centered at $y_n' = (n\,\lambda_L/\lambda_l)R_0 \sin\theta_r$. Each of these orders is scanned by the sinc $(\hat{\eta}_n y_B)$ function; if $\pi/y_B \ll \hat{\eta}_m$, then y_B sinc $(\hat{\eta}_n y_B) \overset{\hat{\eta}_n}{\oplus} \overline{\xi}_n\ (\hat{\eta}_n) \cong \overline{\xi}_n\ (\hat{\eta}_n)$. Recall that $\hat{\eta}_m$ is the maximum spatial frequency passed by the acoustic lens system and y_B is the width of the laser beam.

It remains to relate the far-field optical disturbance (243) to the field in the back focal plane of the optical lens L_3 shown in Fig. 24. Now (14) shows that the field in the back focal plane of a lens is the Fourier transform of the transmission function of an object placed in the front focal plane of the lens and illuminated at normal incidence. Obviously the same is true if the object reflects, rather than transmits, the disturbance.

The far field of a reflecting (or transmitting) object, illuminated at normal incidence, is also proportional to the Fourier transform of the reflection (or transmission) function of the object. In the case of the liquid surface (239) shows that the reflection function is R Rect (y/y_B) $e^{-2ik_L h_i}$. Consequently, the field in the back focal plane of L_3 is proportional to the far-field disturbance Ψ, which is given by (243). The back focal plane is the y' plane in Fig. 24, and now $\hat{\eta} = 2\pi y'/\lambda_L f_3$, where f_3 is the focal length of L_3.

A pinhole is placed at $y' = (\lambda_L/\lambda_i)f_3 \sin \theta_r$, or $-(\lambda_L/\lambda_i)f_3 \sin \theta_r$, to block out all orders except $\bar{\xi}_1$, or $\bar{\xi}_{-1}$. Since the maximum bandwidth of spatial frequencies in the acoustic image is $|\eta| \leqslant \eta_m$, the pinhole should have a radius of at least $\eta_m \lambda_L f_3$.

It should be noted that the spectrum of $\bar{\xi}_2(\hat{\eta}_2)$ will have a bandwidth of $4\hat{\eta}_m$ centered at $\hat{\eta} = +2\hat{\eta}_r$. In order that this spectrum not spill over into the region occupied by $\bar{\xi}_1$ ($\hat{\eta}_1$), it is required that $\hat{\eta}_r > 3\hat{\eta}_m$. The light field passed by the spatial filter then has the form

$$\Psi(y') \propto \left[\bar{\xi}_{+1}(\hat{\eta}_1) \overset{\hat{\eta}_1}{\oplus} \text{sinc}(\hat{\eta}_1 y_B) \right] \text{Rect}(\hat{\eta}_1/\hat{\eta}_m). \tag{244}$$

The light passes through lens L_4 and reaches the ground glass in its back focal plane. The field there is given by the Fourier transform of (244), with appropriate magnification:

$$\Psi(y'') \propto \left\{ \left[\xi_1 \left(\frac{-y'' f_3}{f_4} \right) \text{Rect} \left(\frac{f_3 y''}{f_4 y_B} \right) \right] \overset{s}{\oplus} \text{sinc} \left[\frac{f_3 y'' \hat{\eta}_m}{f_4} \right] \right\} e^{-i\hat{\eta}_r f_3 y''/f_4}, \tag{245a}$$

where f_4 is the focal length of L_4. Recalling that $\xi_1(y) = J_1(2k_0 |h_i|) e^{i\chi_0(y)}$ and setting $y_1 = -y'' f_3/f_4$ allows (245a) to be rewritten as

$$\Psi(y_1) \propto \left\{ \left[J_1(2k_L |h_i|) e^{i\chi_0(y_1)} \text{Rect}(y_1/y_B) \right] \overset{s}{\oplus} \text{sinc}(\hat{\eta}_m y_1) \right\} e^{i\hat{\eta}_r y_1}. \tag{245b}$$

This is the output of the optical system due to an input h_i. With the requirement $k_L h_i \ll 1$ the quantity $J_1(2k_L |h_i|) e^{i\chi_0(y_1)}$ can be rewritten as $2k_L h_i$. The spatial frequency components of the output optical field are then given by

$$\overline{\Psi}(\hat{\eta}) \propto \left[\bar{h}_i \left(\frac{-f_4 \hat{\eta}}{f_3} \right) \overset{\hat{\eta}_1}{\oplus} \text{sinc} \left[\frac{f_4 \hat{\eta}_1 y_B}{f_3} \right] \right] \text{Rect} \left(\frac{f_4 \hat{\eta}_1}{f_3 \hat{\eta}_m} \right), \tag{246}$$

where the shifting property of the Fourier transform has been used. Recall that the spectrum of $\bar{h}_i$ is centered at $\hat{\eta}_r$. Hence the transfer function for the optics can be represented as in Fig. 26.

65
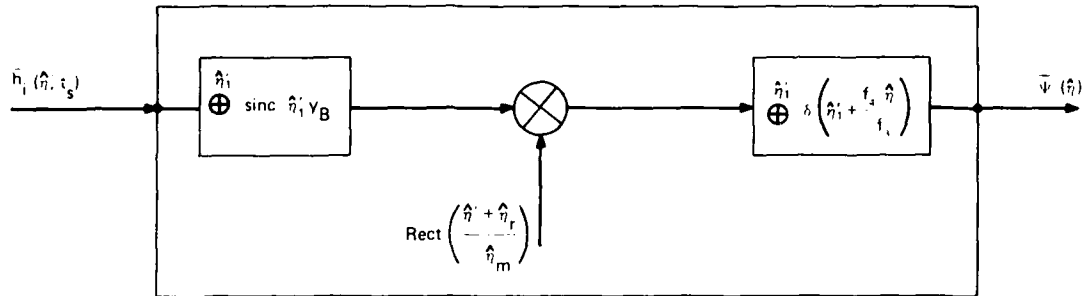
Fig. 26 — Transfer function of the optical lens system

With the assumption $y_B \gg 1/\eta_m$ the output of the lens system as given by (245b) simplifies to

$$\Psi(y_1) \propto \xi_1(y_1) \, e^{i\hat{\eta}_r y_1} \, \text{Rect} \, (y_1/y_B). \tag{247}$$

The optical intensity, proportional to $\xi_1 \, \xi_1^*$, is viewed by the observer. If $k_L \, h_i \ll 1$, then the intensity is proportional to $|g_1(y) \oplus \psi_1(y)|^2$; if $\bar{g}_1(\eta) \cong$ constant over $|\eta| \leqslant \eta_m$, then the intensity is proportional to $|\psi_1|^2$. If the inequality $k_L h_i \ll 1$ is not satisfied, then the image viewed by the observer is proportional to $J_1^2(\Lambda |\psi_1|)$.

If the pinhole is placed at $y' = -\eta_r \, \lambda_L \, f_3$, the observer views an optical intensity proportional to $\xi_{-1} \, \xi_{-1}^*$, which is proportional to $|\psi_1|^2$ if $k_L \, |h_i| \ll 1$. Hence, the -1 order light reflected from the liquid surface can also be used for imagery. This is true even if $k_L h_i$ is of the order of 1, since $\xi_{-1} \, \xi_{-1}^* \propto J_1^2(\Lambda |\psi_1|)$.

6.2. Nonlinear Optical Reconstruction

In many cases it is unimportant that the optical intensity be linearly related to $|\psi_1|^2$. For instance, suppose the acoustic object is a composite panel with an internal flaw, caused by a delamination. Then the acoustic transmission function S_o will be small at the delamination. Recall that for negligible defocusing

$$\bar{\psi}_1(\eta) \propto \bar{S}_o \left| \frac{-f_2 \eta}{f_1} \right| \text{Rect} \, (\eta/\eta_m),$$

where Rect (η/η_m) is the transfer function for the acoustic lens system, f_1 is the focal length of acoustic lens L_1, and f_2 is the focal length of acoustic lens L_2. Suppose the delamination is surrounded by a region in which S_o is much larger. Then the optical image will consist of a bright background with a darkened area corresponding to the delamination, provided that $\Lambda |\psi_1| \leqslant 1.8$. It is only necessary that the contrast between these two areas be detectable by eye. For visual detection of the flaw it is immaterial whether the observer views an intensity proportional to $|\psi_1|^2$ or to $J_1^2(\Lambda |\psi_1|)$.

Suppose there are regions of the liquid surface where $\Lambda \psi_1 \geqslant 1.8$. The corresponding regions in the optical reconstruction will then display a contrast reversal; as the acoustic intensity is increased in these regions (with corresponding increase in ψ_1), the optical intensity will

decrease. This is due to the behavior of $J_1^2(\Lambda|\psi_1|)$, which reaches a maximum at approximately $\Lambda|\psi_1| = 1.8$ and then decreases. When $\Lambda|\psi_1| \cong 3.8$, $J_1^2(\Lambda|\psi_1|)$ reaches its first zero. For $\Lambda|\psi_1| > 3.8$, $J_1^2(\Lambda|\psi_1|)$ increases again; now an increase in acoustic intensity gives an increase in brightness in the optical image. This will continue until the second maximum of $J_1^2(\Lambda|\psi_1|)$ is passed, when contrast reversal again occurs.

Return to the case of the delaminated composite panel, and let the acoustic image be idealized by $\psi_1 = A - B$ Rect $(y/\hat{y})$ with $B < A$. Suppose ΛA is < 1.8; then the optical image again consists of a bright background with a dark region $|y| \leqslant \hat{y}$. If the acoustic intensity is increased so that $1.8 < \Lambda A < 3.8$ and ΛB is still less than 1.8, then the region $|y| > \hat{y}$ becomes darker as the region $|y| < \hat{y}$ lightens. If A and B are such that $J_1(\Lambda A) = J_1(\Lambda B)$, then the object becomes invisible. If both ΛA and ΛB are greater than 1.8 but ΛA is still less than 3.8, then $J_1^2(\Lambda B)$ is greater than $J_1^2(\Lambda A)$. The bad (delaminated) area of the panel now appears brighter, and the good area is darker. This simple example suffices to illustrate the perils of nonlinear imaging.

However, in some situations such imagery is either advantageous or impossible to avoid. Consider, for example, a flaw in or near the corner of a highly attenuative panel. To obtain sufficient power to penetrate the panel, it may be necessary to increase the acoustic intensity to a level such that $\Lambda|\psi_1| > 1.8$ in that part of the acoustic image outside the panel. Another situation arises when the panel is made up of alternating areas of high and low transmission.

It is interesting to estimate the acoustic intensity and Mach number which would cause nonlinear imaging effects such as contrast reversal. One such estimate was made by Pille [1], who found that the intensity I in the reference beam should be less than 0.2 W/cm^2 and that the object beam intensity I_o should be less than 0.02 W/cm^2. This is based on the following set of assumptions:

- $2\Delta t = 10^{-4}$ s,

- The imaging fluid is Freon E-5, so that $\rho_u = 1.8$ g/cm^3 and $c_u = 0.7$ km/s;

- $\bar{g}_1(\eta) \cong 0.5$ for spatial frequencies of interest;

- P_{r_i} has one spatial frequency component, which has spatial frequency 200 rad/cm;

- The reference beam amplitude $|\phi_r|$ is 10 times greater than the object beam amplitude $|\psi_1|$;

- The wavelength of the laser light is 0.6 μm;

- The surface is sampled by the laser light at $t_s = 0.2$ ms, so that from Fig. 19, $\bar{H}(\hat{\eta}_r, t_s) = 0.275(10^{-2})/\rho_u g$.

- Attenuation is negligible.

The acoustic intensities can be easily rewritten in terms of Mach numbers for the case of plane waves. The radiation pressure at the liquid surface in a plane wave is $P_r = 2I/c$, with I being the intensity. Since $P_r = \rho_u|V_o|^2/4$ in the object beam and $P_r = \rho_u|V_r|^2/4$ in the reference beam, the requirement $I_r < 0.2$ W/cm^2 is equivalent to

$$M_r^2 < 10^{-8}, \tag{248}$$

and $I_o < 0.02$ W/cm^2 gives

$$M_o^2 < 10^{-9}. \tag{249}$$

Another set of bounds on Mach numbers was generated earlier by the requirements $|k_u - k_l| \, w_s \ll 1$ and $h_s \ll \lambda_s$, with the bounds for typical system parameters being given by

$$M_o^2 + M_r^2 \ll 10^{-5} \tag{224b}$$

at the membrane, and by

$$M_o \, M_r \ll 10^{-6} \tag{231b}$$

at the liquid surface. In the latter inequality h_s is taken to be the maximum value of h_i and $\lambda_s \sim O(\lambda_a)$.

The inequalities (248) and (249) lead to

$$M_o \, M_r \lesssim O(10^{-9}). \tag{250}$$

Hence the requirement $\Lambda\psi_1 < 1$, or equivalently $h_i(t_s) < \lambda_L/4\pi$, is more restrictive than either $|k_u - k_l| \, w_s \ll 1$ or $h_s \ll \lambda_a$. This is to be expected, since $\lambda_L \sim O(10^{-3} \lambda_a)$.

6.3 Effect of the Liquid Surface Bulge Caused by Intermodulation of the Focused Acoustic Image

As pointed out by Pille [1] and Pille and Hildebrand [2], there will in general be a low spatial frequency distortion, or bulge, of the liquid surface. This is caused by P_{rb}, the sum of radiation pressure in the reference beam and in the acoustic image. The latter is due to the intermodulation of sound in the focused image and is given by the first term on the right-hand side of (100). The effect of the bulge h_b has been ignored by assuming it to be constant over the illuminated portion of the liquid surface.

The restriction of constant h_b will now be relaxed somewhat. For simplicity it is assumed that the levitation of the liquid surface due to the radiation pressure in the reference beam is still constant, but the levitation due to the intermodulation in the focused acoustic image is not. The effect of this intermodulation on the optical reconstruction will now be studied.

The spatial frequency components of P_r are given by (100) through (102) and depicted in Fig. 15. In the figure it is assumed that $3\eta_m < \eta_r$, so that the spectra of $\bar{P}_{rb}(\eta)$ and $\bar{P}_{ri}(\eta)$ do not overlap. Now $\eta_r = (1/\lambda_l) \sin\theta_r$; if $D_1 < f_1$ in Fig. 3, then $\eta_m = a/\lambda_l D_2$. Typically $\sin\theta_r \cong 0.5$ and $a/D_2 \cong 0.3$, so η_r is not greater than $3\eta_m$. It was stated in section 4 that this could have an adverse effect on the optical reconstruction; the reason for this will now be made clear.

For simplicity it is assumed that $2k_L h_b \ll 1$, so that $e^{-2ik_L h_b} \cong 1 - 2ik_L h_b$. Here h_b will refer only to the levitation caused by the radiation pressure in the focused acoustic image. The optical field in the back focal plane (y' plane) of lens L_3 is given by (241). For the moment assume $2k_L h_i \ll 1$, so that (241) gives

$$\Psi \propto - 2R \ (\text{sinc} \ 2\pi\eta y_B) \overset{\eta}{\oplus} \{\delta(\eta) - 2ik_L \ [\bar{h}_i(\eta) + \bar{h}_b(\eta)]\}, \tag{251}$$

where terms of order $k_L^2 h_i h_b$ have been neglected and $\eta = y'/\lambda_l \ f_3$. The δ-function represents the focusing of the specularly reflected light by the lens. Since the laser samples the liquid surface at $t = nt_s$, $\bar{h}_i$ is proportional to $\bar{P}_{ri}$. Consider that part of the y' plane for which $\eta_r - \eta_m \leqslant \eta \leqslant \eta_r + \eta_m$. In this region, $\bar{h}_b(\eta) \propto \bar{H}(\eta_r, t_i) \ [\bar{\psi}_1(\eta) \overset{\eta}{\oplus} \bar{\psi}_1^*(\eta)]$, as indicated by (100), assuming that $\bar{g}_1(\eta) \cong$ constant over $|\eta| \leqslant \eta_m$. Likewise $\bar{h}_i(\eta) \propto \bar{H}(\eta_r, t_i) \times A_r \bar{\psi}_1(\eta - \eta_r)$ for $\phi_r = A_r e^{-2\pi i \eta_r y'}$.

That portion of $\bar{h}_b$ in this region will be passed by the spatial filter (pinhole) centered at $\eta = \eta_r$; $\bar{h}_i(\eta)$ will also be passed. Consequently in the back focal plane of L_4 the high spatial frequency components of light reflected from the bulge will interfere with the light which reconstructs the image. This may degrade the optical image.

The degradation may be negligible if $\bar{h}_b \ll \bar{h}_i$ in the bandpass Rect $[(\eta - \eta_r)/\eta_m]$ or if $\psi_1 \ll A_r$, where A_r is the magnitude of the velocity potential in the reference wave. If both object and reference transducers generate waves of equal acoustic intensity, then $\psi_1 \ll A_r$ for a large variety of imaging applications. This is due to the fact that the insertion loss, represented by the object transmission function S_o, may be quite high; recall that (neglecting degradations due to the acoustic lens system) $\psi_1 = S_o \ \phi_{inc}$, where ϕ_{inc} is the velocity potential due to the object transducer. Also, the attenuation will in general be greater in the focused acoustic image, since the acoustic path length L_o from the object transducer to the liquid surface is typically greater than L_r, the path length from the reference transducer to the surface.

The attenuation may be accounted for by multiplying the amplitude of the propagating acoustic waves by the factor $e^{-\Gamma L}$, where Γ is the absorption coefficient [1]. Hence, if $\phi_{inc} = \phi_r$, then for $\bar{h}_b$ to be much less than $\bar{h}_i$, it is necessary that $S_o \ e^{-\Gamma \Delta L}$ be much less than 1; here $\Delta L = L_o - L_r$. If a typical operating frequency of 10 MHz is assumed, then $\Gamma = 0.04$ cm^{-1} in water [12], and if, for example, $\Delta L = 75$ cm, then $e^{-\Gamma \Delta L} = e^{-3}$. Since $S_o \leqslant 1$, the inequality $S_o e^{-\Gamma \Delta L} \ll 1$ is easily satisfied.

It will be shown later in this section that maximum efficiency of the recording process at the liquid surface is achieved when $\psi_1 = A_r$. That is, the signal-to-noise ratio at the liquid surface, given by h_i/h_b, is maximized when $\psi_1 = A_r$; now h_b is the total bulge height, due to both terms in (100). This requires that the intensity of the acoustic field generated by the object transducer be much larger than that of the reference transducer.

If the object transducer is made more powerful, so that $\psi_1 \sim O(A_r)$, then the distortion due to that part of $\bar{h}_b$ in the bandpass Rect$[(\eta - \eta_r)/\eta_m]$ may become objectionable. One way to avoid this is to require $\eta_r < 3\eta_m$. If it is inconvenient to increase $\sin \theta_r$, then η_m may be decreased by stopping down the acoustic lens system. This will have the effect of decreasing the bandwidth Rect $[(\eta - \eta_r)/\eta_m]$, since η_m is proportional to the acoustic lens width (Fig. 3). Using smaller apertures in the acoustic lens system will degrade the quality of the acoustic image, unless f_1/f_2 is decreased in the ratio a/D_2, in accordance with (21). In this fashion the size of the acoustic image $\psi_1(-f_1 y/f_2)$ increases just as much as the line source response sinc $(2\pi ya/\lambda_l D_2)$. Recall that the magnification of the acoustic lens system is f_2/f_1, with f_1 being the focal length of acoustic lens L_1 and f_2 being the focal length of L_2. The focusing condition (18) must still be satisfied.

6.4 Effect of the Bulge Caused by the Reference Beam

It is also of interest to study the effect of bulge levitation caused by the radiation pressure in the reference beam. Since the surface levitation satisfies a linear differential equation (for $h_s \ll \lambda_s$), the bulge due to the reference beam can be calculated independently of the bulge due to the intermodulation in the focused acoustic image.

The liquid surface is assumed to be subjected to a train of pulses of the form

$$p_{rb}(y) \sum_{m=0}^{M} \text{Rect} \left[\frac{\hat{t} - mt_1}{\Delta t} \right],$$

where t_1 is the reciprocal of the pulse repetition rate and P_{rb} is now given by $\rho_u |V_r|^2/4$. The transfer function (186) will be used to estimate the bulge levitation h_b. It was shown that, strictly speaking, (186) can be used only for $\hat{\eta} \geq O(10 \text{ rad/cm})$ and that h_b should be calculated from (208). Comparing (186) and (208) shows that the correct order of magnitude for h_b will be obtained, if not the exact value, for $\Delta P_r \leq O(P_r)$ and typical values

$$\nu \sim O(10^{-2} \text{ cm}^2/\text{s}),$$

$$\rho_M \sim O(\rho_u),$$

$$\rho_I \sim O(\rho_u),$$

$$\gamma \sim O(100 \mu \text{N/cm}),$$

$$T \sim O(10 \text{N/cm}),$$

and

$$d \geq O(10^{-2} \text{cm}).$$

Let $2y_b$ be the width of the reference beam. If $\bar{g}_1(\eta) \cong \bar{g}_1(\eta_r)$ for $\eta_r - 1/y_b \leq \eta \leq \eta_r + 1/y_b$, then

$$p_{rb} = \frac{1}{4} \rho_u |\bar{g}_1(\eta_r)|^2 A_r^2 \text{ Rect } (y/y_b) = P \text{ Rect } (y/y_b). \tag{252}$$

This can be expanded in the series

$$p_{rb} = \sum_{n=0}^{\infty} \bar{P}_{rb}(K_n) \cos K_n y, \tag{253}$$

where $K_n = n\pi/R_t$ and R_t is the minitank width. The Fourier coefficients $\bar{P}_{rb}(K_n)$ are given by

$$\bar{P}_{rb}(K_n) = P y_b / R_t, \qquad n = 0 \tag{254a}$$

$$= \frac{2y_b}{R_t} P \text{ sinc } \left[\frac{n\pi y_b}{R_t} \right], \quad n > 0. \tag{254b}$$

The expansion (253) represents p_{rb} in the interval $-R_t \leq y \leq R_t$ and repeats periodically outside the interval.

Hence, as pointed out by Pille [1], the bulge levitation can be calculated by assuming that the minitank is infinite in the y direction and is subjected to bounded pulses of radiation pressure of width $2y_b$ centered at $y = \pm 2nR_t$. Consider first the response to a single temporal

pulse Rect $(\hat{t}/\Delta t)$. An estimate of h_b can be made by applying (186) where $\hat{\eta}$ is not continuous but takes on the discrete values K_n:

$$h_b = \sum_{n=0}^{\infty} \bar{P}_{rb}(K_n) \ \bar{H}(K_n, \ t) \cos K_n y$$

$$= \sum_{n=0}^{\infty} G_n(t) \cos K_n y, \tag{255}$$

where

$$\bar{H}(K_n, \ t) = \frac{\omega_n e^{-q_n \omega_n t} \sin(\beta_n \omega_n t) \overset{t}{\oplus} \text{Rect}(\hat{t}/\Delta t)}{(\rho_u g + \gamma K_n^2)\beta_n} \tag{256}$$

and $G_n(t)$ is the generalized coordinate associated with mode shape $\cos K_n y$. Quantities such as ω_n and q_n are calculated by replacing $\hat{\eta}$ by K_n where appropriate.

Let

$$\bar{H}(K_n, \ t) = \frac{Q_n(t)}{(\rho_u g + \gamma K_n^2)\beta_n}, \tag{257}$$

so that $Q_n(t)$ is the time-dependent part of the generalized coordinate $G_n(t)$:

$$Q_n(t) = \omega_n e^{-q_n \omega_n t} \sin(\beta_n \omega_n t) \overset{t}{\oplus} \text{Rect}(\hat{t}/\Delta t). \tag{258}$$

Now

$$q_n = 2\mu K_n \sqrt{\frac{K_n}{\rho_u(\rho_u g + \gamma K_n^2)}} \ (\tanh K_n d)^E, \tag{259}$$

where $E = -2.3$ for $K_n d < \pi/2$ and $E = 0$ otherwise. Pille and Hildebrand [2] state that the formula for q_n is derived from a numerical analysis performed for $K_n \geqslant 0.04\pi/d$. It will be assumed here that to obtain an order of magnitude estimate of the bulge height, the preceding expression for q_n can be used for all K_n. When $n = 0$, $\omega_n = 0$ and the pulse response $Q_o(t)$ vanishes, as predicted by (258); the $n = 0$ mode corresponds to a uniform levitation of the liquid surface, and for a finite-depth minitank this clearly violates mass conservation.

Then, for $d \sim O(0.1 \text{ cm})$, $\Delta t \sim O(10^{-4} \text{ s})$, $K_n \leq O(10 \text{ rad/cm})$, and the values of ν, ρ_M, etc. quoted above,

$$Q_n(t) \cong 2\omega_n \Delta t \ e^{-q_n \omega_n t} \sin \beta_n \omega_n t, \qquad t > 2\Delta t. \tag{260}$$

Likewise, when $K_n \geqslant O(100 \text{ rad/cm})$, and $t > 2\Delta t$,

$$Q_n(t) \cong e^{-2K_n^2 \nu t} \left[\cos \beta_n \omega_n t - e^{2K_n^2 \nu \Delta t} \cos \beta_n \omega_n (t - \Delta t) \right]. \tag{261}$$

Using these values of $Q_n(t)$, it can be shown that

$$G_n(t_1)\big|_{K_n \leq O(10 \text{ rad/cm})} \gg G_n(t_1)\big|_{K_n \geq O(100 \text{ rad/cm})}. \tag{262}$$

That is, when a new pulse of radiation pressure reaches the liquid surface, the response associated with the mode shape $\cos K_n y$ is negligible for $K_n \geq O(100 \text{ rad/cm})$. The damping factor $e^{-2K_n^2 \nu t_1}$ associated with these high-frequency modes causes them to decay more rapidly than low-frequency modes $(K_n \leq O(10 \text{ rad/cm}))$, which have an approximate damping factor $e^{-2\nu t_1/d^2}$.

71

Consider next the response of the liquid surface to the pulse train

$$P_{rb} = p_{rb}(y) \sum_{m=0}^{M} \text{Rect}\left[\frac{\hat{t} - mt_1}{\Delta t}\right], \qquad (M+1)t_1 > t > Mt_1. \tag{263}$$

Since $G_n(t)$ has already been calculated for the case of a single pulse, it is simple to calculate the response due to a pulse train; the response is

$$h_b = \sum_{n=1}^{\infty} \left[\sum_{m=0}^{M} G_n(t - mt_1)\right] \cos K_n y. \tag{264}$$

Because $G_n(t_1)$ is negligible when $n \geq O(100 \, R_t/\pi)$, the above equation can be split into two summations:

$$h_b = \sum_{n=1}^{N} \left[\sum_{m=0}^{M} G_n(t - mt_1)\right] \cos K_n y + \sum_{n=N}^{\infty} G_n(t - Mt_1) \cos K_n y, \tag{265}$$

where $N \sim O(100 \, R_t/\pi)$. The first summation over n includes the low-frequency modes of vibration of the liquid surface. These low-frequency modes have natural frequencies which are at most of the order of $1/t_1$ and decay slightly during the interval between pulses. Hence the response of the low-frequency modes will increase with time, up to some upper bound. The high-frequency modes, represented by the second summation over n, have a response which becomes small when $t \to t_1$. Hence the high-frequency modes at time $t > Mt_1$ respond only to the previous pulse occurring at Mt_1.

Consider the summation

$$\sum_{m=0}^{M} G_n(t - mt_1) = P \frac{y_b}{R_t} \left[\frac{4\omega_n \Delta t}{\rho_u g + \gamma K_n^2}\right] \frac{\text{sinc } K_n y_b}{\beta_n}$$

$$\times \sum_{m=0}^{M} e^{-q_n \omega_n (t - mt_1)} \sin \beta_n \omega_n (t - mt_1) \, X(t - mt_1), \tag{266}$$

where M is large, and $X(t)$ is the Heaviside step function. Suppose that

$$e^{-q_n \omega_n (t - mt_1)} \sin \beta_n \omega_n (t - mt_1) \cong \text{constant} \tag{267}$$

over the interval $jt_1 \leq t \leq (j+1)t_1$ for any integer $j \geq m$. Then for large M

$$\sum_{m=0}^{M} e^{-q_n \omega_n (t - mt_1)} \sin \beta_n \omega_n (t - mt_1) \, X(t - mt_1)$$

$$= \left[\frac{1}{t_1}\right] \lim_{\substack{M \to \infty \\ t_1 \to 0}} \left\{\sum_{m=0}^{M} e^{-q_n \omega_n (t - mt_1)} \sin \beta_n \omega_n (t - mt_1) \, X(t - mt_1) t_1\right\}. \tag{268}$$

Performing the limiting process on the right-hand side of (268) leads to the convolution integral

$$\frac{1}{t_1} \int_{\tau=0}^{t} e^{-q_n \omega_n (t - \tau)} \sin \beta_n \, \omega_n (t - \tau) \, X(t - \tau) \, X(\tau) \, d\tau.$$

Hence the summation in (266) can be approximated by the convolution

$$\frac{1}{t_1} X(t) \overset{t}{\oplus} [e^{-q_n \omega_n t} \sin \beta_n \omega_n t \, X(t)],$$

provided that (267) is satisfied.

72

For typical depths $d \sim O(0.1 \text{ cm})$, a pulse repetiton rate of 60 Hz, and $K_n \lesssim O(1 \text{ rad/cm})$ it is found that $e^{-q_n \omega_n t}$ varies from a maximum of unity at $t = 0$ to a minimum of approximately 0.85 at $t = t_1$. Hence (267) is not satisfied and the summation in (266) cannot be replaced by the convolution without incurring an error of about 15% over each time increment t_1. At first glance it would seem that the error would accumulate and invalidate the calculation. However, sample calculations of the left-hand side of (266) show that the response of the corresponding mode tends to a steady-state value within a few percent of that predicted by performing the convolution.

Consequently

$$\sum_{m=0}^{M} G_n(t - mt_1) \cong \frac{4Py_b}{R_t} \left[\frac{\omega_n \Delta t}{\rho_u g + \gamma K_n^2} \right] \frac{\text{sinc } K_n y_b}{\beta_n t_1}$$
$$\times \int_{\tau=0}^{t} e^{-q_n \omega_n (t - \tau)} \sin \beta_n \omega_n (t - \tau) \, X(t - \tau) \, X(\tau) \, d\tau, \tag{269}$$

where $t > Mt_1$. The convolution is the response of a single-degree-of-freedom oscillator to a step function. The response time of the low-frequency modes is much longer than the time t_1 between pulses. Even though the surface is driven by a pulse train, the effect is that of an oscillator driven by a step function, weighted by the factor $\Delta t / t_1$. Evaluating the convolution in (269) and letting t be large gives

$$\sum_{m=0}^{M} G_n(t - mt_1) \cong \frac{\Delta t}{t_1} \left[\frac{\text{sinc } K_n y_b}{\rho_u g + \gamma K_n^2} \right] \frac{4Py_b}{R_t}, \tag{270}$$

showing that the low-frequency modes reach a steady-state value for $K_n \lesssim O(1 \text{ rad/cm})$.

As a first approximation (264) gives

$$h_b(y, t) \cong P \left[\frac{4y_b}{R_t} \right] \frac{\Delta t}{t_1} \sum_{n=1}^{N} \frac{(\text{sinc } K_n y_b) \cos K_n y}{\rho_u g + \gamma K_n^2}, \tag{271}$$

where the summation is over those modes for which $K_n \lesssim O(1 \text{ rad/cm})$.
Since $\gamma K_n^2 \ll \rho_u g$ in (271),

$$h_b(y, t) \cong \frac{2P \Delta t}{\rho_u g t_1} \left[\text{Rect} \left[\frac{y}{y_b} \right] - \frac{y_b}{R_t} \right], \tag{272}$$

where the expansion

$$\text{Rect} \left[\frac{y}{y_b} \right] = \frac{y_b}{R_t} + \sum_{n=1}^{\infty} \frac{2y_b}{R_t} (\text{sinc } K_n y_b) \cos K_n y \tag{273}$$

has been used. Recall that the response of the $n = 0$ mode vanishes to satisfy mass conservation. It is also assumed that the summation on the right-hand side of (273) can be truncated after N terms, where $K_N \sim O(1 \text{ rad/cm})$.

The approximation (272) predicts discontinuities in h_b at $|y| = y_b$, indicating that the effect of surface tension must be accounted for. Hence γK_n^2 must be retained and more terms must be used in summation (265).

Performing the summation (265) for $y_b = 4$ cm and retaining γK_n^2 shows that the bulge is flat to within a 15% variation for $|y| \leqslant 3.5$ cm. At $|y| = 4$ cm, h_b is about 10% of its average value in the region $|y| \leqslant 3.5$ cm. Here values of

$$M = 60,$$
$$N = 50,$$
$$R_I = 10 \text{ cm},$$
$$\rho_u = 1.8 \text{ g/cm}^3,$$

and

$$\gamma = 160 \ \mu\text{N/cm}$$

have been used in the calculations. It should be noted that $K_N \cong 15$ rad/cm. When $y_b = 7$ cm and the same system parameters are used, it is found that the departure from flatness of the surface is of the order of 10% for $|y| \leqslant 6.75$ cm. The maximum bulge response for both $y_b = 4$ cm and $y_b = 7$ cm is within a few percent of that predicted by the approximation (272).

In summary it would seem that there will be some nonuniformity in the bulge levitation in the region $|y| \leqslant y_b$. The exact departure from flatness is estimated to be of the order of 10 percent. This estimate is based on neglecting interaction of the liquid-surface displacement with membrane displacement, so that (186) can be used. It also assumes that the formula for q_n is valid for all spatial frequencies. Furthermore it assumes that there is no natural frequency of the liquid surface which is an integer multiple of the pulse repetition rate.

The bulge is seen to roll off at some value smaller than y_b. This indicates that the laser beam should illuminate an area somewhat smaller than the insonified area. Suppose that this is done, so that within the illuminated area, $h_b \cong h_o + \Delta h_b$ for $h_o = $ constant and $\Delta h_b < h_o$. Suppose also that Δh_b is approximated by

$$\Delta h_b = \sum_{n=0}^{N} B_n \cos K_n y. \tag{274}$$

The effect of Δh_b on the imaging process will now be considered.

For simplicity let $k_L^2 h_I^2$ and $k_L^2 (\Delta h_b)^2$ be much less than 1, so that $e^{-2ik_L h_I} \cong 1 - 2ik_L h_I$, etc. From (241) the field incident on the pinhole at $\hat{\eta} = \hat{\eta}_r$ in the back focal plane of L_3 is, ignoring a scanning by sinc $(\hat{\eta} y_B)$ and assuming $h_I \propto \psi_1 e^{i\hat{\eta}_r y}$,

$$\Psi \propto \bar{\psi}_1(\hat{\eta}_1) - 2ik_L \sum_{n=0}^{N} B_n \bar{\psi}_1(\hat{\eta}_1 \pm K_n); \tag{275}$$

recall that $\hat{\eta}_1 = \hat{\eta} - \hat{\eta}_r$. The light field is made up of the Fourier transform of $\bar{\psi}_1$ upshifted by $\hat{\eta}_r$, plus ghosts of $\bar{\psi}_1$ upshifted by $\hat{\eta}_1 \pm K_n$ and multiplied by B_n. For $\hat{\eta}_m >> K_n$ the pinhole will pass almost all components of $\bar{\psi}_1(\hat{\eta}_1 \pm K_n)$. Ignoring scaling factors, the light field in the back focal plane of L_4 is

$$\Psi \propto \psi_1(y'') [1 - 2ik_L \Delta h_b] e^{-i\hat{\eta}_r y''}. \tag{276}$$

It is assumed that $\psi_1 \overset{s}{\oplus} \mathrm{sinc}\ (y\hat{\eta}_m) \cong \psi_1$ in the above. The optical intensity is given by

$$|\Psi|^2 \propto |\psi_1|^2 [1 + 4k_L^2\ (\Delta h_b)^2]. \tag{277}$$

Consequently the optical intensity will be proportional to the acoustic image $|\psi_1|^2$ plus the image $|\psi_1|^2$ modulated by $4(k_L \Delta h_b)^2$.

For example, a reference transducer generating a typical peak intensity of the order of 10^{-2} W/cm^2 at the liquid surface gives rise to a Δh_b which is of the order of $10^{-2} \lambda_L$. This estimate is based on performing the summation (265) for $M = 50$ and using the previously cited values of ρ_u, γ, y_b, R_i, $\Delta t, \lambda_L$, etc. The magnitude P of the radiation pressure is calculated from $P = 2I/c$, where I is the intensity and c, the sound speed, is of the order of 1 km/s. For intensities which are of the order of $1 v^{-2}$ W/cm^2 the effect of bulge distortion is negligible; that is, $k_L^2(\Delta h_b)^2 << 1$. If either the ratio $\Delta t/t_1$ or the peak intensity is increased by an order of magnitude, then (272) predicts that $k_L \Delta h_b \sim O(1)$, so that bulge distortion may be objectionable in the optical reconstruction.

Bulge distortion may be objectionable in one class of imaging applications even if $(k_L \Delta h_b)^2 << 1$. Suppose that $\psi_1 = A - \Delta A$ Rect (y/y_o) with $\Delta A << A$. This would correspond, for example, to a weak debonding in a composite panel. Then (277) predicts that the image will be of the form

$$|\Psi|^2 \propto A^2[1 + 4k_L^2(\Delta h_b)^2] - 2A(\Delta A)\ \mathrm{Rect}\left[\frac{y}{y_o}\right]. \tag{278}$$

If $k_L(\Delta h_b)^2 \sim O(\Delta A/A)$ and $1/K_N^{-1} \lesssim O(y_o)$, then the weak object, which is represented by $-2A\Delta A$ Rect (y/y_o), becomes difficult to detect.

6.5. Beam Balance Ratio

It has been shown that h_i carries useful information about the acoustic image whereas h_b carries no information and can distort the optical reconstruction. One can think of h as signal and h_b as noise; it is desirable to maximize the signal-to-noise ratio h/h_b. This ratio can be maximized by adjusting the intensities in the reference beam and in the focused acoustic image.

As an illustration assume that the object fills the entire field of view of the acoustic lens system and let

$$\psi_1 = A\left[1 - \mathrm{Rect}\left[\frac{y - y_o}{y_1}\right]\right]. \tag{279}$$

This is an idealized representation of, for example, a composite panel with a debonding which causes a large change in acoustic impedance.

With the assumptions $\bar{g}_1(\eta) \cong \bar{g}_1(\eta_r)$ over $|\eta| \leqslant \eta_m$ and $\phi_r = A_r e^{-2\pi i \eta_r y}$, (100) gives

$$P_{rb} = \frac{1}{4}\ \rho_u |\bar{g}_1(\eta_r)|^2\ (|\psi_1|^2 + A_r^2). \tag{280}$$

75

The bulge height for $|y| < y_b$ is approximated by

$$h_b = 2 \frac{\Delta t}{t_1} \frac{P_{rb}}{\rho_u g} \left[1 - \frac{y_b}{R_t} \right]. \tag{281}$$

Likewise P_{ri} becomes $(1/4)\rho_u |\bar{g}_1(\eta_r)|^2 A_r \psi_1 e^{2\pi i \eta_r y}$, and if $\bar{H}(\eta, t_s) \cong \bar{H}(\eta_r, t_s)$ over the bandpass Rect $[(\eta - \eta_r)/\eta_m]$, then $h_i = \bar{H}(\eta_r, t_s) P_{ri}$.

It follows that the signal-to-noise ratio for $|y| < y_b$ is

$$\frac{h_i}{h_b} = \frac{\bar{H}(\eta_r, t_s) A_r \psi_1}{\dfrac{\Delta t}{t_1} \left\{ \dfrac{|\psi_1|^2 + A_r^2}{\rho_u g} \right\} (1 - y_b/R_t)}. \tag{282}$$

The ratio will vary with y, since ψ_1 is a function of y. Let A be a measure of ψ_1, since what is desired is to make the modulation h_i as large as possible and the "background" h_b as small as possible. Hence, in maximizing the ratio, ψ_1 will be replaced by A. The ratio becomes large as $y_b \rightarrow R_t$. As the insonified area of the surface becomes larger, less acoustic energy is converted into noise h_b.

Let $B = A/A_r$ be the beam balance ratio and $V = h_i/h_b$. Then (282) can be written as

$$V = K \left[\frac{B}{B^2 + 1} \right], \tag{283}$$

where $K = \bar{H}(\eta_r, t_s) (\rho_u g t_1)/\Delta t (1 - y_b/R_t)$. Now V will be maximized for the value of B which causes $\partial V/\partial B = 0$. This occurs for $B = 1$, or $A = A_r$. Now $A = S_m \phi_{inc}$ for a perfect acoustic lens system, where S_m is the maximum value of the object transmission function, and ϕ_{inc} is the velocity potential in the beam which insonifies the object. For a weakly transmitting object, $S_m \ll 1$, and, since $\phi_{inc} = A_r/S_m$ for maximum V, the object transducer must generate much more power than the reference transducer.

Suppose the intensities in the object and reference beams are adjusted so that $B = 1$, and consider the resulting value of V. For a typical system employing Freon E-5 as an imaging fluid and having $\hat{\eta}_r \sim O(150 \text{ rad/cm})$, Figs. 19 and 20 show that for $2\Delta t = 10^{-4}$ s,

$$10 \log_{10} \left[\frac{\bar{H}(\eta_r, t_s)}{H_N} \right] \cong -30, \tag{284}$$

with $H_N = 1/\rho_u g$. Let $y_b = 4$ cm, $R_t = 10$ cm, and $1/t_1 = 60$ Hz; for this example $V = 1/6$.

Suppose that

$$\psi_1 = A - \Delta A \text{ Rect} \left[\frac{y - y_o}{y_1} \right], \tag{285}$$

with $\Delta A \ll A$. Here the acoustic object has a slight reduction in transmission in the region $y_o - y_1 \leq y \leq y_o + y_1$. For this low-contrast object, it is desirable to adjust the reference and object transducer power levels to maximize the contrast in the optical reconstruction. This occurs for the value of $B = \Delta A/A_r$ which maximizes

$$V = \frac{KB}{(A/\Delta A)^2 B^2 + 1}. \tag{286}$$

76

It is found that $B = \Delta A / A$. Since B is defined as the ratio $\Delta A / A_r$, the optical contrast is optimized when $A = A_r$. Hence for both low- and high-contrast acoustic objects, it is desirable to have $\psi_1 = A_r$.

6.6. Detection of Phase Objects

It has been shown that when the $+1$ (or -1) order reflected light is used in the optical reconstruction, the optical image is ideally proportional to $|\psi_1|^2$. Any phase information contained in ψ_1 is lost.

Suppose the object is a composite panel which is being inspected for internal flaws. Some flaws, such as debonding between the layers making up the panel, change the amplitude of the sound passing through the panel and can be detected on optical reconstruction. Other flaws which only slightly reduce transmission may not be detectable by the usual method of optical reconstruction.

In a typical construction of a composite panel, sheets of composite material are glued together. Often these sheets are covered with thin layers which are peeled off prior to gluing. In any area where a layer (peel ply) is not completely removed, the glue forms a weak bond, which can lead to failure of the panel under loading. The acoustic impedance of the peel ply may be close to that of the panel. This, coupled with the thinness of the peel ply, makes its presence difficult to detect, since acoustic transmission is only slightly reduced.

However, any flaw which causes a modest phase change in the transmitted acoustic wave may be detectable by using more than one order of reflected light in the optical reconstruction. The various orders contain phase information about the acoustic object, and, by allowing them to interfere, this information is preserved.

To see how this may be done, consider a simple phase object on a uniform background: $\angle\psi_1 = \chi_o$ Rect (y/y_o) and $|\psi_1| = A$, where $\angle\psi_1$ is the phase angle of ψ_1. Recall that $\psi_1 \propto S_o\phi_{inc}$, with ϕ_{inc} being the velocity potential in the beam generated by the object transducer. For simplicity the levitation system is assumed to have perfect fidelity, so that $h_i \propto \psi_1 \, e^{2\pi i \eta_r y}$ and $h_c \propto \psi_1^* \, e^{-2\pi i \eta_r y}$. Suppose that the $+1$ and -1 orders are allowed to pass through the optics, by suitable spatial filtering in the back focal plane of lens L_3. The magnification is assumed to be unity. For $k_L h_i \ll 1$ and $1/\eta_m \ll y_B$, the optical intensity will be proportional to $k_L^2|h_i + h_c|^2$. For ψ_1 as given for the simple phase object being considered,

$$|\Psi|^2 \propto A^2\{1 + [1 - \text{Rect } (y/y_o)] \cos 4\pi\eta_r y + \text{Rect } (y/y_o) \cos (4\pi\eta_r y + 2\chi_o)\}. \quad (287)$$

The optical image for $|y| > y_o$ consists of fringes having spatial frequency $4\pi\eta_r$. When $|y| < y_o$, the fringes have the same spatial frequency but have a phase shift $2\chi_o$, which is twice the phase in the acoustic object. The nulls in this fringe pattern will be displaced by an amount $\Delta y = \chi_o/2\pi\eta_r$. Assuming that Δy is detectable by eye if it is greater than $1/10$ the wavelength of the fringe pattern, it is required that $\chi_o \geqslant 0.2\pi$ for detection of the phase object.

The phase change for an acoustic wave at normal incidence passing through the peel ply is

$$\chi_o = 2\pi (1/\lambda_1 - 1/\lambda_2) \tau \cong 2\pi\tau (\Delta\lambda)/\lambda^2. \quad (288)$$

where τ is the ply thickness, λ_1 is the wavelength in the ply, and λ_2 is the wavelength in the panel; it is assumed that $\lambda_1 \cong \lambda_2 = \lambda$. If $\Delta\lambda = 0.05\lambda$, for example, it is necessary for τ to be at least 2λ to make $|\chi_o| \geqslant 0.2\pi$. Suppose the sound speed in the panel is 3 km/s and the acoustic frequency is 5 MHz; then $2\lambda = 0.12$ cm.

If the thickness is such that $|\chi_o| < 0.2\pi$, then it may be possible to make the outline of the phase object visible by tipping the panel so that the acoustic wave is not at normal incidence. In this case the effective ply thickness is $\tau/\cos\theta$, where θ is the angle of incidence. Another possibility is to increase the transducer frequency, which decreases λ. This will also increase the fringe frequency, however, and it may be necessary to magnify the optical image so that the eye can resolve it.

It has been assumed here that χ_o is constant. If the phase object is such that $\chi_o = 2\pi\eta'y$, then in the region $|y| \leqslant y_o$ the spatial frequency of the fringe pattern will now be $4\pi(\eta_r + \eta')y$; for $|y| > y_o$ it remains $4\pi\eta_r y$.

It is possible to use orders other than the ± 1 orders. For example, if the 0 and $+1$ orders are used and ψ_1 is as given previously, then

$$|\Psi|^2 \propto 1 + 4k_L |h_i| \cos(2\pi\eta_r y + \chi_o \, \text{Rect} \, (y/y_0) - \pi/2) \qquad (289)$$

when $k_L h_i \ll 1$. The optical image consists of a bright background laced with fringes of amplitude $4k_L |h_i|$. The fringe pattern has an abrupt phase shift of χ_o at $|y| = y_o$. When the ± 1 orders are used, the corresponding phase shift, as was shown, is $2\chi_o$, but the fringe frequency was also doubled. Hence using the 0 and $+1$ orders neither increases nor decreases the sensitivity of this method of detecting phase objects. (This assumes that $\Delta y = 0.1/$(fringe frequency) is the governing criterion for detecting phase shifts by eye.) However, the modulation due to the fringe pattern is much less than when ± 1 orders are used.

If the $+1$ and $+2$ (or -1 and -2) orders are used, then

$$|\Psi|^2 \propto 4k_L^2 |h_i|^2 \{1 + 4k_L |h_i| \cos[2\pi\eta_r y + \chi_o \, \text{Rect} \, (y/y_o) - \pi/2]\}. \qquad (290)$$

For ψ_1 as given, this optical image is the same as that formed from the 0 and $+1$ orders, with a uniform reduction in intensity of $4k_L^2 |h_i|^2$.

In all of these cases the change in location of the local minima of the fringe pattern Δy is $\chi_o/2\pi\eta_r$. Suppose that, instead of the criterion $\Delta y > 0.1/\eta_r$, it is desired that $\Delta y > y'$, where y' is the smallest change in fringe location detectable by eye. Then for the case of $\lambda_1 \cong \lambda_2 = \lambda$ the thickness of the phase object must be such that

$$\tau \geqslant \lambda^2 y' \, (\sin\theta_r)/\lambda_i \Delta\lambda$$

to make its outline visible. As the acoustic frequency is varied, the ratio $\lambda^2/\lambda_i \Delta\lambda$ remains constant. The required thickness τ for detection of the phase object is invariant of frequency when this criterion is used. Hence it remains a matter of experiment to determine whether increasing the transducer frequency will increase the sensitivity of this method of detecting phase objects.

7. SUMMARY

The preceeding analysis has demonstrated that, subject to certain restrictions, the levita-
... system can produce an optical reconstruction of a focused acoustic image, which has been

recorded on the liquid surface. Some of these restrictions will be automatically satisfied by any imaging system of practical interest. This section will recapitulate only those restrictions which place constraints on the design and operation of a liquid surface levitation holography system.

In section 2 an aberration-free acoustic lens system of effective aperture a' (Fig. 3) was assumed to focus the acoustic image onto the liquid surface. The acoustic object was assumed insonified by a plane quasimonochromatic wave at normal incidence. The velocity potential in the focused image is

$$\bar{\psi}_1(\eta) = \bar{S}_o' \left[\frac{-\eta f_2}{f_1} \right] \text{Rect } (\eta/\eta_m) \, e^{\pi i \lambda_u \epsilon' \eta^2}, \tag{291}$$

where

$S_o' = A(y_o) \, S_o(y_o),$

$A(y_o) = $ amplitude of the wave which insonifies the object,

$S_o(y_o) = $ acoustic transmission function for the object being imaged,

$f_2 = $ focal length of the acoustic lens L_2,

$\eta_m = a'/\lambda_l f_2,$

$\lambda_l = $ acoustic wavelength in the object-tank fluid,

$\lambda_u = $ acoustic wavelength in the imaging fluid,
$\epsilon' = \epsilon (f_2/f_1)^2 (\lambda_l/\lambda_u),$

and

$\epsilon = $ distance to the object from the position of sharpest focus.

It was shown that the cutoff frequency η_m equals $a/\lambda_l D_2$ if the object is placed less than a distance f_1 from lens L_1; lens L_2 becomes the limiting aperture. The half-width of L_1 and L_2 is a. For an object farther than f_1 from L_1, $\eta_m = (a/D_1)(f_1/f_2)$ and L_1 is the limiting aperture. This aperture restricts the range of spatial frequencies passed by the lens system to $|\eta| \leqslant \eta_m$. Because of the magnification f_2/f_1 the range of spatial frequencies in $\bar{S}_o'$ increases as f_1/f_2. Hence magnifying the image will improve its quality.

The image will be degraded by the phase distortion $e^{\pi i \lambda_u \epsilon' \eta^2}$ due to defocusing. The effect of defocusing is negligible if $\epsilon \ll (f_1/a')^2(\lambda_l/\pi)$; the lens system is then diffraction limited. For a large-aperture lens system such that $a' \sim O(f_1)$, this inequality is satisfied when the object is placed within a few acoustic wavelengths of the plane of sharpest focus; that is, the depth of field of the lens system is of the order of λ_l. All the usual assumptions pertaining to linear acoustics must be satisfied.

The vertical velocity of the fluid particle at the liquid surface due to the velocity potential (291) was calculated in section 3. The velocity potential was assumed due to a temporal CW pulse; that is, (291) is to be multiplied by $e^{-i\omega_a t} \text{Rect } (\hat{t}/\Delta t)$, where ω_a is the transducer frequency and $2\Delta t$ is the pulse duration. Internal reflections in the minitank were accounted for, as well as the mechanical properties of the membrane at the bottom of the minitank. The membrane was assumed thin, with a thickness $2b$ such that

79

$$2b \ll \lambda_l,$$

$$2b \ll \lambda_u,$$

$$2b \ll \lambda_t,$$

and

$$2b \ll \lambda_p,$$

where λ_t is the wavelength of a shear wave in the membrane and λ_p is the wavelength of a dilatational wave in the membrane. The inequalities $2b \ll \lambda_t$ and $2b \ll \lambda_p$ allow thin-plate theory to be used in calculating transmission and reflection coefficients at the membrane. Furthermore it was assumed that

$$T \frac{\partial^2 w}{\partial y^2} \gg E(2b)^3 \frac{\partial^4 w}{\partial y^4} \,/\, (1 - \nu_p); \tag{292}$$

consequently, tensile forces in the plane of the membrane greatly exceed flexural forces. Here T is the tension per unit length in the membrane, E is Young's modulus in the membrane, and ν_p is Poisson's ratio in the membrane.

The analysis was restricted to two dimensions for simplicity, and the membrane displacement w was required to be much less than λ_a. It was found that the elastic restoring force in the membrane is negligible compared to the inertial force if

$$2\rho_M b \, \omega_a^2 \gg 4\pi^2 \eta^2 T,$$

where ρ_M is the membrane density. For spatial frequencies in the focused image, $\eta^2 \leqslant \eta_m^2$, so that this inequality is satisfied if

$$2\rho_M b c_l^2 \gg T(a'/f_2),$$

where c_l is the sound speed in the object tank. This is satisfied for typical values

$$c_l \sim O(1 \text{ km/s}),$$

$$\rho_M \sim O(1 \text{ g/cm}^3),$$

$$b \sim O(10^{-3} \text{ cm}),$$

$$T \sim O(10 \text{ N/cm}),$$

and

$$a'/f_2 \sim O(0.1).$$

The transmission and reflection coefficients at the membrane were calculated for an incident plane wave of infinite extent; Appendix B shows that the same results are obtained for a bounded wave whose width is much greater than λ_a.

It was found that the effect of the membrane on the coefficients is negligible if $4\pi\rho_M b \ll \rho_l \lambda_l + \rho_u \lambda_u$, with ρ_l being the density of the object-tank fluid and ρ_u being the density of the imaging fluid. These coefficients were substituted into the transfer function $\bar{g}_1(\eta)$ for the minitank, where $\bar{g}_1(\eta)$ relates the vertical particle velocity at the liquid surface to the acoustic velocity potential in the plane wave incident upon it; that is,

$$\bar{v}_{oz}(\eta, t) = 2ik_u \, \bar{g}_1(\eta) \, \bar{\psi}_1(\eta) \, \text{Rect} \, (\hat{t}/\Delta t) \, e^{-i\omega_a t} \tag{293}$$

and

$$\bar{v}_{rz}(\eta, t) = 2ik_u \, g_1(\eta) \, \bar{\phi}_r(\eta) \, \text{Rect} \, (\hat{t}/\Delta t) \, e^{-i\omega_a t}. \tag{294}$$

Here

$\bar{v}_{oz}$ = vertical velocity due to the object's focused image,

$\bar{v}_{rz}$ = vertical velocity due to the reference beam,

$k_u = 2\pi/\lambda_u$,

and

$\bar{\phi}_r$ = velocity potential in the reference beam.

In Figs. 10 and 11 $\bar{g}_1$ was plotted for various ratios of minitank depth to acoustic wavelength and for $\rho_M = 0$ or $\rho_M = 1.5$ g/cm^3. It was assumed that the imaging fluid is Freon E-5 and that the object-tank fluid is water. The membrane thickness was assumed to be 0.0025 cm, and the acoustic frequency was assumed to be 5 MHz. The plots show the following:

• As d/λ_u decreases, the range of spatial frequencies for which $\bar{g}_1(\eta) \cong$ constant increases.

• When $d/\lambda_u \cong 9$, the presence of the membrane causes the region $\bar{g}_1(\eta) \cong$ constant to shrink. Also, the effect of constructive and destructive interference (due to multiple internal reflections in the minitank) is enhanced, due to the membrane.

• For $d/\lambda_u \cong 9$, $\bar{g}_1(\eta)$ is sensitive to depth changes as small as 1/8 wavelength. If it is necessary to operate the system in this regime, care must be taken to control the depth.

• For both $d/\lambda_u \cong 2$ and $d/\lambda_u \cong 0.1$ the presence of the membrane is much less objectionable, since the region $\bar{g}_1(\eta) \cong$ constant is about the same for $\rho_M = 0$ and $\rho_M = 1.5$ g/cm^3.

These conclusions are based on an acoustic lens cutoff of $a'/f_2 \leqslant 0.5$.

Section 3 concluded with a discussion of the consequences of violating the requirement $w \ll \lambda_a$. It was shown that for $w \gtrsim O(\lambda_a)$ and $|\lambda_u - \lambda_l| \sim O(\lambda_l)$ an incident plane wave transmitted through the membrane will emerge as a superposition of plane waves with spatial frequencies given by $\eta = \eta_0 + nK$, with $n = 0, \pm 1, \pm 2$ etc., where η_0 is the spatial frequency of the original wave, and where the membrane displacement is assumed proportional to cos Ky. Since the membrane displacement is in general given by a superposition of sinusoids, the presence of side orders $\eta = \eta_0 + nK$ $(n \neq 0)$ can have objectionable effects on the imaging process.

When $|k_u - k_l| \ll 1/w$, the transmitted wave has the same spatial frequency as the incident wave. The only effect of the membrane then is to change the local transmission coefficient $\bar{T}_{12}$. It was assumed that the wavelength of the membrane displacement is much longer than λ_l or λ_u and that the slope of the membrane is much less than 1.

In section 4 it was shown that the momentum flux per unit area in the acoustic field will have a low temporal frequency component, called the radiation pressure vector. The vertical component of this vector, called the radiation pressure, was shown to consist of four terms at the liquid surface.

Two of these terms carry no information about the acoustic image; these terms are the radiation pressure in the reference beam and the radiation pressure in the focused acoustic image. The latter term is due to intermodulation of sound in the image.

Since the radiation pressure is a nonlinear quantity, there will be interference between sound in the image and sound in the reference beam. As a result of this interference the radiation pressure will have a component P_{ri} which carries information about the amplitude and phase of the object being imaged. Another component P_{rc} is the complex conjugate of P_{ri}; P_{rc} carries information about the amplitude and phase of the complex conjugate of the object.

Because the liquid surface levitates in response to the radiation pressure, it is necessary to have a reference beam to generate the interference terms P_{ri} and P_{rc} which preserve information about the acoustic object. If P_{ri} is used to record the acoustic image, then

$$\bar{P}_{ri}(\hat{\eta}) \text{ Rect } (\hat{t}/\Delta t) = \frac{1}{4} \rho_u \bar{g}_1^{\bullet}(\hat{\eta}_r) A_r \text{ [sinc}(\hat{\eta} - \hat{\eta}_r)y_b] \overset{\hat{\eta}}{\oplus} \bar{V}_{oz}(\hat{\eta}, t), \tag{295}$$

where a factor $2\pi i k_u$ has been absorbed in $\bar{g}_1^{\bullet}(\hat{\eta}_r)$. For a plane wave reference beam of constant amplitude A_r, spatial frequency $\hat{\eta}_r$, and beamwidth y_b, the spatial frequencies present in $\bar{P}_{ri}$ are upshifted by an amount $\hat{\eta}_r$, and those in $\bar{P}_{rc}$ are downshifted by the same amount. This shift should be large enough so that spatial frequency spectra of $\bar{P}_{ri}$ and $\bar{P}_{rc}$ do not overlap the spectrum of $\bar{P}_{rb}$. Recall that $\bar{P}_{rb}$ is that part of the radiation pressure carrying no useful information about the acoustic object; that is, $\bar{P}_{rb}$ is the sum of the radiation pressures in the reference beam and in the focused acoustic image.

Section 5 began with a brief review of nonlinear acoustics. The mass and momentum conservation equations were reduced to the usual first-order (linear) acoustic equations for small perturbations in pressure, density, and velocity. That is, with V_{1a} and ρ_{1a} as measures of the velocity and density perturbation, the first-order acoustic equations were recovered for

$$\frac{V_{1a}}{c} = M_a \sim O\left[\frac{\rho_{1a}}{\rho_0}\right], \qquad M_a << 1, \tag{296}$$

where M_a is the Mach number, c is the sound speed in the fluid, and ρ_0 is the equilibrium density in the fluid. Furthermore, viscosity was assumed small, so that the Reynolds number R_c is $>> 1$. The Reynolds number is the dimensionless ratio $c\lambda_a/\nu$, and ν is the coefficient of kinematic viscosity.

The second-order (in M_a) acoustic equations were then derived, which are nonlinear in the first-order quantities (velocity, density, etc.). Irrotational flow was also assumed, so that acoustic streaming was ignored. It was demonstrated that the nonlinear terms in the second-order acoustic equations cause a steady momentum flux per unit area, which is the radiation pressure vector.

The fluid was next considered to be semi-infinite, so that the effect of its surface must be taken into account. The momentum balance normal to the quiescent surface contains nonlinear terms due to the momentum flux per unit area in the acoustic field incident on the surface. The steady component of this momentum flux per unit area is the radiation pressure in the acoustic field; this will induce low temporal frequency motion of the liquid surface. The surface levitation will in turn generate changes in velocity, pressure, etc. in the fluid. For the surface to be capable of recording the acoustic image, the first- and second-order acoustic quantities must be unaffected by surface motions.

In the absence of the acoustic field (propagation of free waves on the liquid surface) the fluid behaves as if it is incompressible; the density perturbation ρ_s, due to motion of the surface, is of the order of $M_a^2 \rho_0$. Furthermore, both the momentum equation for the fluid and the boundary condition at the liquid surface are linear, if $|v_s| \ll C_s$, where v_s is the velocity induced by surface motion and C_s is the speed of propagation of a free wave on the surface.

For an acoustic field incident on the liquid surface, it was shown that the first- and second-order acoustic quantitites are unaffected by motion of the surface. The mass and momentum conservation equations for quantities such as ρ_s and v_s were likewise shown to be independent of the acoustic quantities. The coupling between the acoustic field and the surface-wave field occurs at the liquid surface, where levitation is induced by the presence of radiation pressure. The radiation pressure is balanced by forces per unit area due to surface tension, gravity, and inertia.

The transfer function $\bar{H}(\hat{\eta}, t)$, which relates the levitation of the surface to radiation pressure, was derived. The fluid was considered infinite in lateral extent but of finite depth. This models the behavior of the fluid in the minitank when the effects of its finite radius can be ignored. (The finite minitank was considered in Appendix D.) It was assumed that the membrane at the bottom of the minitank is stiffer than the liquid surface; that is, $h_s \gg w$. For typical values

$$T \sim O(10 \text{ N/cm}),$$

$$\gamma \sim O(100 \,\mu\text{N/cm}),$$

$$2b \sim O(10^{-3} \text{ cm}),$$

$$\rho_M, \rho_u, \rho_l \sim O(1 \text{ g/cm}^3),$$

$$d \gtrsim O(0.01 \text{ cm}),$$

and

$$\Delta t \sim O(10^{-4} \text{ s})$$

the inequality $h_s \gg w$ is satisfied for spatial frequencies at least of the order of 10 rad/cm. The imaging fluid is also assumed slightly viscous; as pointed out by Pille and Hildebrand [2], this requires the viscosity ν to be no greater than the order of $\omega_\eta/\hat{\eta}^2$. Here ω_η is the frequency of free vibration of the surface associated with spatial frequency $\hat{\eta}$.

The transfer function has the form [1,2]

$$\bar{H}(\hat{\eta}, t) = \frac{\omega_\eta \, e^{-q\omega_\eta t}(\sin \beta\omega_\eta t) \oplus \text{Rect} \, (\hat{t}/\Delta t)}{(\rho_u g + \gamma\hat{\eta}^2)\beta} \tag{297}$$

for a pulse of radiation of the form $\bar{P}_r(\hat{\eta})$ Rect $(\hat{t}/\Delta t)$. Here $\bar{P}_r(\hat{\eta})$ can be any of the four components of the radiation pressure that were mentioned in section 4 and

$$\beta = \sqrt{1 - q^2},$$

and

$$q = 2\mu\hat{\eta} \sqrt{\frac{\hat{\eta}}{\rho_u(\rho_u g + \gamma\hat{\eta}^2)}} \ (\tanh \hat{\eta}d)^E,$$

$$E = 0, \qquad d\hat{\eta} > \pi/2,$$

$$E = -2.3, \qquad d\hat{\eta} < \pi/2.$$

The corresponding levitation is then

$$\bar{h}_s(\hat{\eta}, t) = \bar{H}(\hat{\eta}, t) \ \bar{P}_r(\hat{\eta}). \tag{298}$$

The transfer function was calculated on the assumption that the relation between levitation and radiation pressure is linear, which requires that $|v_s| \ll C_s$, or $h_s \ll \lambda_s$. This allowed an estimate to be made of the permissible Mach numbers at the liquid surface. It was found that

$$M_a^2 \ll \frac{C_s}{c_u} \ \frac{4}{c_u\hat{\eta}\Delta t} \ \frac{1}{\tanh \hat{\eta}d} \tag{299}$$

for linearity; here a pulse of radiation pressure of spatial frequency $\hat{\eta}$ and duration $2\Delta t$ was assumed. Furthermore, the pulse duration is assumed such that $\omega_\eta\Delta t \leq O(1)$; otherwise the quantity $1/\Delta t$ in (299) is to be replaced by ω_η. When h_s is due to P_{ri}, then $M_a^2 = M_o M_r$; when h_s is due to P_{rb}, $M_a^2 = M_o^2 + M_r^2$.

The liquid surface was assumed to be subjected to a train of pulses occurring at regular intervals. The form of $\bar{H}(\hat{\eta}, t)$ for various minitank depths and pulse durations was calculated by the authors of Refs. 1 and 2 and reproduced here. There is a time t_s after the initiation of the pulse when $\bar{H}(\hat{\eta}, t_s)$ is approximately constant over a given bandwidth of spatial frequencies. Since P_{ri} contains information about the focused image, t_s should be selected such that $\bar{H}(\hat{\eta}, t_s)$ is constant over the bandwidth $\hat{\eta}_r - \hat{\eta}_m \leq \hat{\eta}_m \leq \hat{\eta}_r + \hat{\eta}_m$; then

$$\bar{h}_i'(\hat{\eta}, t_s) = \bar{H}(\hat{\eta}_r, t_s) \ \bar{P}_{ri}(\hat{\eta}). \tag{300}$$

Here $\hat{\eta}_r = 2\pi\eta_r$, and $\hat{\eta}_m = 2\pi\eta_m$; η_m is the maximum spatial frequency passed by the acoustic lens system.

When the pulse duration is infinitely long, the liquid surface reaches a steady-state levitation. The corresponding plot of $\bar{H}(\hat{\eta}, t)$ shows that the region where $\bar{H}(\hat{\eta}, t) \cong$ constant is confined to low spatial frequencies. $\bar{P}_{ri}(\hat{\eta})$ is upshifted to the region $\hat{\eta} \sim O(\hat{\eta}_r)$; in this region the liquid surface has poor fidelity—hence the need for pulsing the liquid surface.

It was assumed that the interval t_1 between pulses is long enough so that $\bar{h}_i(\hat{\eta}, t_1) \ll \bar{h}_i(\hat{\eta}, t_s)$. The levitation associated with $\bar{P}_{ri}(\hat{\eta})$ is then negligible when the next pulse of radiation pressure reaches the surface. However, a low spatial frequency bulge may build up as the surface responds to P_{rb}, the sum of the radiation pressures in the reference beam and in the focused image. These pressures constitute a source of noise in the imaging process.

The effect of coupling between the membrane and surface displacements at low spatial frequencies also was investigated. When the order of $\hat{\eta}$ is less than 10 rad/cm and the previously cited values of T, γ, d, etc. are used, the membrane displacement w_s is comparable in magnitude to h_s. This is true even if there is no discontinuity of radiation pressure at the membrane. The calculations of $\bar{H}(\hat{\eta}, t)$ in Refs. 1 and 2 were done on the assumption of a rigid membrane, or $h_s \gg w_s$; hence their results may be invalid at low spatial frequencies. However, the spectrum of $\bar{P}_{ri}(\hat{\eta})$, which carries information about the acoustic image, is usually upshifted by the order of 100 rad/cm, since typically $\hat{\eta}_r$ is of this order of magnitude. In this frequency range the calculations of $\bar{H}(\hat{\eta}, t)$ in Refs. 1 and 2 are rigorously correct.

It was pointed out in section 3 that unless $w \ll 1/|k_u - k_l|$, distortion in the acoustic image can result from diffraction of the acoustic field by the membrane. In a typical operating system with Freon E-5 used as the imaging fluid and water used as the object-tank fluid, $|\lambda_u - \lambda_l| \sim O(\lambda_l)$. Hence the membrane displacement must be a fraction of an acoustic wavelength. This places an upper bound on the radiation pressure; for the values of T, ρ_M, b, etc. used previously, it is required that

$$P_r \ll \frac{\rho_l \omega_m'}{\hat{\eta} \Delta t |k_u - k_l|} \tag{301}$$

at the membrane. Here ρ_l is the density of object-tank fluid, ω_m' is the frequency of free vibration of membrane (submerged), and P_r is due to a single plane wave (such as the reference beam), so that $P_r \sim O(\rho_u V_{la}^2/4)$. Recalling that $V_{1a} = c_u M_a$ allows the above inequality to be rewritten as

$$M_a^2 \ll \frac{\rho_l}{\rho_u} \frac{\omega_m'}{\omega_a} \frac{4}{c_u \hat{\eta} \Delta t}. \tag{302}$$

For a reference beam with a beamwidth of the order of 10 cm and an acoustic frequency of 5 MHz, it is required that

$$M_r^2 \ll 10^{-5}, \quad \hat{\eta} \sim O(0.1 \text{ rad/cm}). \tag{303}$$

It is assumed that w_s is due to only the reference beam in the preceding and that $\omega_m' \Delta t \ll 1$; otherwise, Δt is replaced by $1/\omega_m'$ in (302). If w_s is due to P_{ri}, and if P_{ri} has only one spatial frequency of the order of 100 rad/cm, then

$$M_o M_r \ll 10^{-1}, \quad \hat{\eta} \sim O(100 \text{ rad/cm}). \tag{304}$$

Another inequality must be satisfied by the Mach number. Linearity of the response of the liquid surface is obtained if $|\mathbf{v}_s| \ll C_s$, or

$$M_a^2 \ll \frac{C_s}{c_u} \frac{4}{c_u \hat{\eta} \Delta t} \frac{1}{\tanh \hat{\eta} d} \tag{299}$$

at the liquid surface. It is of interest to establish whether inequality (299) or (302) is the most stringent for a typical system. For the typical values

$\gamma \sim O(200 \ \mu\text{N/cm})$,

$\rho_u \sim O(1 \ \text{g/cm}^3)$,

$c_u \sim O(10^5 \ \text{cm/s})$,

and

$$d \sim O(.1 \text{ cm})$$

inequality (299) gives, at the liquid surface,

$$M_o^2 + M_r^2 \ll 10^{-2}, \quad \hat{\eta} \sim O(0.1 \text{ rad/cm}) \tag{305}$$

and

$$M_o M_r \ll 10^{-6}, \quad \hat{\eta} \sim O(100 \text{ rad/cm}). \tag{306}$$

Comparing (303) and (305) shows that for low spatial frequencies the requirement $w_s \ll 1/|k_u - k_l|$ is more stringent, with the assumption $|\lambda_u - \lambda_l| \sim O(\lambda_l)$. This is because $w_s \sim O(h_s)$ at low spatial frequencies, whereas $\lambda_s \gg \lambda_l$. Comparing (304) and (306) shows the requirement $h_s \ll \lambda_s$ to be more restrictive at high spatial frequencies. Now h_s is $\gg w_s$, but $\lambda_s \sim O(\lambda_l)$. It is assumed that P_{rb} and P_{ri} each have one dominant spatial frequency component.

Section 6 considered the optical reconstruction of the focused acoustic image, which is recorded as a phase hologram at the liquid surface. Laser light was assumed to illuminate the liquid surface at times $t = nt_s$, with $\overline{H}(\hat{\eta}, t_s)$ being approximately constant in the bandpass $-\hat{\eta}_m + \hat{\eta}_r \leq \hat{\eta} \leq \eta_m + \hat{\eta}_r$. For light at normal incidence to the surface the effect of surface levitation is to cause a phase change $-2ik_L h_s$ in the reflected light, where k_L is the optical wavenumber $2\pi/\lambda_L$.

For simplicity it is assumed that h_b, the bulge levitation, is constant over $|y| \leq y_B$, the illuminated area of the surface. The reflected light passes through an optical lens placed 1 focal length above the surface. The light field in the back focal plane of the lens consists of diffracted orders having spatial frequencies centered around $\hat{\eta} = n\hat{\eta}_r$; $\hat{\eta}_r$ is the spatial frequency of the reference beam and $n = 0, \pm 1, \pm 2$, etc. If most of the spatial frequencies present in the focused acoustic image are much greater than $1/y_B$, then the nth order is proportional to the Fourier transform of $\xi_n = J_n(2k_L|h_i|) e^{in\chi_o}$, where χ_o is the phase of h_i. Each order is centered at $y' = n\lambda_L f_3 \eta_r$, where f_3 is the focal length of the lens and y' is the coordinate in its back focal plane. If most of the spatial frequencies in the acoustic image are no greater than the order of $1/y_B$, then each order is given by $\overline{\xi}_n$, scanned by a sinc function.

The $+1$ order contains information about ψ_1, and the -1 order carries information about ψ_1^*. Let $k_L h_i$ be much less than 1; then, for a plane wave reference beam whose width is much greater than $1/\hat{\eta}_m$, the $+1$ order is proportional to $g_1 \overset{s}{\oplus} \psi_1$, as shown by (293) and (295). Likewise, the -1 order is proportional to $(g_1 \overset{s}{\oplus} \psi_1)^*$. If $\overline{g}_1(\eta) \cong$ constant over the bandwidth $|\eta| \leq \eta_m$, then $g_1 \overset{s}{\oplus} \psi_1 \propto \psi_1$ and $(g_1 \overset{s}{\oplus} \psi_1)^* \propto (\psi_1)^*$. Either the $+1$ or -1 order can be used to form the optical image, since it is the intensity in the light field that is viewed by the observer.

Assuming that the $+1$ order is to be used, a pinhole is centered at $y' = \lambda_L f_3 \eta_r$, in the back focal plane of the lens. The pinhole is large enough to pass the $+1$ order but blocks out all others. The light passed by the pinhole then passes through a second optical lens, which is placed a focal length f_4 away from the pinhole. A ground-glass viewing screen is placed in the back focal plane of this lens. The light field there is

$$\Psi(\bar{y}) \propto \{[k_L h_i(y_1) \text{ Rect } (y_1/y_B)] \overset{s}{\oplus} \text{ sinc } \hat{\eta}_m y_1\} \, e^{i\hat{\eta}_r y_1},\tag{307}$$

where $y_1 = -\bar{y} f_3/f_4$, $k_L h_i \ll 1$, and $\bar{y}$ is the coordinate in the back local plane of the second lens.

The input to the optical system is the levitation h_i; the output is the optical disturbance Ψ. In the Fourier-transform domain,

$$\overline{\Psi}(\hat{\eta}) \propto \left[\overline{h}_i\left(\frac{-f_4\hat{\eta}}{f_3}\right)\overset{\hat{\eta}_1}{\oplus} \text{ sinc}\left(\frac{f_4\hat{\eta}_1 y_B}{f_3}\right)\right] \text{Rect}\left(\frac{f_4\hat{\eta}_1}{f_3\hat{\eta}_m}\right),\tag{308}$$

where $\hat{\eta}_1 = \hat{\eta} - \hat{\eta}_r$. The optical system

● Degrades the image due to scanning by sinc $\hat{\eta}_1 y_B$. This arises because of the finite area illuminated by the laser and can be neglected if $\hat{\eta}_m \gg 1/y_B$ and $\overline{h}_i$ fills the bandwidth $|\hat{\eta}| \leqslant \hat{\eta}_m$.

● Blocks all spatial frequencies outside the bandwidth $-\hat{\eta}_m + \hat{\eta}_r \leqslant \hat{\eta} \leqslant \hat{\eta}_m + \hat{\eta}_r$. Recall that $\overline{h}_i$ occupies this portion of the spectrum due to upshifting by the reference beam.

● Increases the bandwidth of spatial frequencies in the optical image in the ratio f_3/f_4. As this ratio increases, the image becomes smaller and harder to see by eye.

When the scanning by sinc $\hat{\eta}_m y_1$ is negligible, the optical disturbance at the viewing screen is

$$\Psi \propto [k_L \rho_u A_r \overline{g}_1^{*}(\hat{\eta}_r)\overline{H}(\hat{\eta}_r, t_s)] \, [g_1 \overset{s}{\oplus} \psi_1] \, e^{i\hat{\eta}_r y_1}.\tag{309}$$

The reference beam is assumed to cause a particle velocity $\overline{g}_1^{*}(\hat{\eta}_r)A_r$ at the liquid surface, and have spatial frequency $\hat{\eta}_r$. If $g_1 \overset{s}{\oplus} \psi_1 \cong \overline{g}_1(\hat{\eta}_r)\psi_1$, then

$$\Psi(\bar{y}) \propto \psi_1(y_1) \, e^{i\hat{\eta}_r y_1}.\tag{310}$$

In this case the optical disturbance is proportional to the velocity potential in the focused acoustic image. The optical intensity $\Psi\Psi^{*}$ is viewed by the observer.

If $g_1 \overset{s}{\oplus} \psi_1 \cong \overline{g}_1(\hat{\eta}_r)\psi_1$ and $k_o h_i \sim O(1)$, then $\Psi\Psi^{*}$ is proportional to $J_1^2(\alpha|\psi_1|)$, where α is a constant. This gives an amplitude-distorted optical reconstruction of the acoustic image. When $g_1 \overset{s}{\oplus} \psi_1$ is not proportional to ψ_1, then

$$\Psi\Psi^{*} \propto J_1^2(\Lambda|V_o|),\tag{311}$$

where $\Lambda = k_L \rho_u A_r \overline{g}_1^{*}(\hat{\eta}_r) \, \overline{H}(\hat{\eta}_r, t_s)$ and $V_o = g_1 \overset{s}{\oplus} \psi_1$. This is an amplitude-distorted image of V_o, the first-order acoustic particle velocity at the surface. V_o in turn reflects degradation of the acoustic imaging process due to the lack of fidelity in the minitank transfer function.

All the above calculations have been done on the assumption that $e^{-2ik_L h_b} \cong$ constant over the illuminated portion of the surface. Since P_{rb} will in general cause a low spatial frequency bulge h_b, it is necessary to consider the effect of the bulge on the optical reconstruction.

The bulge was first assumed to be due to the radiation pressure in the acoustic image, which occupies a spectrum $|\hat{\eta}| \leqslant 2\hat{\eta}_m$. Unless $\hat{\eta}_r > 3\hat{\eta}_m$, some of the spectrum of $\bar{P}_{rb}(\hat{\eta})$ overlaps that of $\bar{P}_{ri}$. Consequently the high spatial frequency components of $\bar{h}_b$ will reflect some light which will be passed by the pinhole in the back focal plane of the first optical lens. This light will interfere with that in the optical reconstruction of the acoustic image and somewhat degrade the reconstruction. This can be avoided by

- Increasing θ_r, the angle made by the reference beam with the vertical. This in turn increases $\hat{\eta}_r$.

- Decreasing $\hat{\eta}_m$ by decreasing the aperture of the acoustic lens system. However, unless the acoustic image magnification is increased as fast as the aperture is decreased, the acoustic image will be degraded.

- Causing ψ_1 to be much less than the velocity potential A_r in the reference beam. This case often occurs in practice due to insertion loss caused by the acoustic object or by attenuation in the fluid. However, decreasing the ratio ψ_1/A_r also decreases the efficiency of the recording process at the surface, as more acoustic power goes into producing the noise h_b and less into signal h_i.

The effect of the bulge due to only the reference beam was next considered. It was found that, for typical system parameters, the bulge reaches a steady-state levitation as it responds to a train of pulses of radiation pressure. For typical system parameters each spatial frequency component $h_b(\hat{\eta})$ for $\hat{\eta} \leq O(1 \text{ rad/cm})$ has an associated response time which is longer than t_1, the reciprocal of the pulse repetition rate. To a first approximation $\bar{h}_b(\hat{\eta})$ responds as a lightly damped low-frequency oscillator subjected to a step function of radiation pressure. The magnitude of the step function is weighted by $\Delta t/t_1$. It was assumed that the pulse repetition rate is not an integer multiple of any of the ω_η. Recall that ω_η is the frequency of free vibration of the liquid surface associated with spatial frequency $\hat{\eta}$.

For a typical reference beam width of 4 cm and minitank width of 10 cm, it was found that h_b varies by less than 15% from its average value h_0 in the region $|y| \leq 3.5$ cm. At $|y| = 4$ cm h_b is is about 10% of its average value in the region $|y| \leq 3.5$ cm. This indicates that the laser should illuminate an area of the surface somewhat smaller than the insonified area.

If this is done, then in the illuminated region $h_b = h_0 + \Delta h_b$, with $h_0 \gg \Delta h_b$ and $h_0 =$ constant. The phase of the light reflected from the liquid surface is changed by an amount $-2ik_L(h_i + h_i^\bullet + \Delta h_b)$. With the assumptions $k_L h_i \ll 1$ and $g_1 \overset{s}{\oplus} \psi_1 \propto \psi_1$ the optical disturbance at the viewing screen will be of the form

$$\Psi \propto \psi_1[1 - 2ik_L\Delta h_b - 2k_L^2(\Delta h_b)^2 - ...]. \tag{312}$$

Each low spatial frequency component of Δh_b causes an additional set of orders to be reflected from the liquid surface. The spatial frequencies of these orders are so close to those of $\bar{h}_i(\hat{\eta})$ that they are passed by the pinhole and reach the viewing screen, where they interfere with the image term ψ_1.

Usually this interference will be negligible if $k_L\Delta h_b \ll 1$. This occurs for example for a reference transducer generating a peak intensity of the order of 0.01 W/cm^2 over a pulse dura-

tion $2\Delta t \sim O(10^{-4}$ s) with a pulse repetition rate of 60 Hz. The imaging fluid is assumed to be Freon E-5, with $\lambda_L = 0.6 \mu$ m.

There is a class of imaging applications for which the effect of the bulge may be objectionable even if $k_L \Delta h_b \ll 1$. This is the case of a low-contrast acoustic object. An example is a weak debonding in a composite panel, causing a slight local reduction in transmission of sound. The optical reconstruction consists of a background with a slight darkening corresponding to the presence of the debonding. If $\psi_1 = A$ represents the background and $\psi_1 = A - \Delta A$ corresponds to the debonding with $\Delta A \ll A$, then the effect of the bulge is objectionable if $\Delta A / A$ is the same order of magnitude as $k_L \Delta h_b$.

Since the bulge h_b contributes nothing to image formation and can even degrade the optical reconstruction, it can be thought of as noise. The levitation h_i records the acoustic image; hence h_i is signal. For maximum efficiency of the recording process at the surface, it is desirable to maximize the signal-to-noise ratio. For both low- and high-contrast acoustic objects the ratio reaches a maximum when ϕ_r, the velocity potential in the reference beam and ψ_1, the acoustic image velocity potential, are equal at the liquid surface. In general the acoustic path length from the object transducer to the surface is longer than that traveled by the reference beam; hence there will be more attenuation in ψ_1. The potential ψ_1 is also decreased due to insertion loss caused by the acoustic object. For ψ_1 to equal ϕ_r, it is generally necessary to have the object transducer more powerful than the reference transducer. Even when the signal-to-noise ratio is maximized, its value is only about 1/6 for typical system parameters.

Section 6 concluded with a discussion of the effect of using more than one order of reflected light for optical reconstruction. With the assumption $g_1 \overset{s}{\oplus} \psi_1 \propto \psi_1$, each reflected order carries phase information about the acoustic object. When either the $+1$ or -1 order only is used for reconstruction, this information is lost. By using multiple orders and allowing them to interfere at the viewing screen, the phase information is retained.

The effect of using pairs of orders was considered. For a phase object on a uniform background, this leads to a fringe pattern having spatial frequency $2\pi |m - n| \eta_r$ when the mth and nth orders are used. At the edge of the phase object the fringe pattern has a phase shift of $|m - n| \chi_o$. Here χ_o is the phase change which occurs as sound travels through the phase object. The phase shift is assumed detectable by eye if it causes a displacement of the fringe pattern greater than $0.10/\eta_r$; hence, χ_o must be at least 0.2π. If this measure of sensitivity is used, then any pair of orders can be used. However, the depth of modulation (contrast) in the fringe pattern is greatest when the ± 1 orders are used. One way of increasing χ_o is to increase the acoustic frequency, which decreases the acoustic wavelength. However, this also increases the spatial frequency of the fringe pattern, making it harder to resolve by eye.

Another possible criterion for detection of the phase object is that the displacement in the fringe pattern must be greater than some minimum value detectable by eye. This value may be independent of fringe spacing. If this criterion is used, then detection of the phase object is not related to the acoustic frequency.

8. REFERENCES

1. P. Pille, "Real Time Liquid Surface Acoustical Holography," Master's Thesis, University of British Columbia, 1972.

2. P. Pille and B.P. Hildebrand, "Rigorous Analysis of the Liquid-Surface Acoustical Holography System," pp 335-371 in *Acoustical Holography*, Vol. 5, Plenum Press, New York, 1974.

3. B.B. Brenden, "History and Present Status of Liquid Surface Acoustical Holography," J. Acoust. Soc. Am. **58** (No. 5), 951-955 (1975).

4. A. Papoulis, *Systems and Transforms With Applications in Optics*, McGraw-Hill, New York, 1968, Sec. 1 of Chap. 3 and Secs. 2, 3, and 5 of Chap. 9.

5. I.A. Viktorov, *Rayleigh and Lamb Waves*, Chapter II, Plenum Press, New York, 1967.

6. P. Bechmann and A. Spizzichino, *The Scattering of Electromagnetic Waves From Rough Surfaces*, Macmillan, New York, 1963, pp 28-29.

7. B.P. Hildebrand and B.B. Brenden, *An Introduction to Acoustical Holography*, Sections 6.4 and 3.36, Plenum Press, New York, 1972.

8. Z.A. Goldberg, "Acoustic Radiation Pressure," in *High Intensity Ultrasonic Fields*, L.D. Rozenberg, editor, Plenum Press, New York, 1971.

9. S. Hanish, "Nonlinear Acoustics," NRL Report 7772, Naval Research Laboratory, Washington, D.C., Dec. 1974.

10. H. Lamb, *Hydrodynamics*, Sections 229 and 266, Dover, New York, 1945.

11. H. Lamb, *Hydrodynamics*, Sections 326 and 349, Dover, New York, 1945.

12. E.G. Richardson, *Ultrasonic Physics*, Elsevier Publishing Company, Amsterdam, New York, 1962, pp 188.

13. A. Papoulis, *Systems and Transforms With Applications in Optics*, McGraw-Hill, New York, 1968, Sec. 1 of Chap. 3 and Sec. 3 of Chap. 9.

14. R.J. Collier, C.B. Burkhart, and L.H. Lin, *Optical Holography*, Academic Press, New York, 1971, pp 84-85.

Appendix A

Derivations of (14) and (19)

DERIVATION OF (14)

Suppose an object ψ_o is placed at a distance D_1 in front of a cylindrical acoustic lens and insonified with a plane wave at normal incidence. It will be shown that the field in the back focal plane of the lens is proportional to $\bar{\psi}_o(\eta)$.

The field in this plane (y_2 plane) is given by

$$\phi_o(y_2) \propto e^{ik(D_1+f_1)} e^{iky_1^2/2f_1} \overset{s}{\oplus} \{\text{Rect} (y_1/a) e^{-iky_1^2/2f_1} [\psi_o(y_o) \overset{s}{\oplus} e^{iky_o^2/2D_1}]\}. \tag{13}$$

Writing out the convolution integrals indicated in (13) gives

$$\phi_o(y_2) \propto e^{iky_2^2/2f_1} \int_{-\infty}^{\infty} \psi_o(y_o) e^{iky_o^2/2D_1} \left[\int_{-a}^{a} e^{iky_1^2/2D_1} e^{-2\pi iy_1(y_2/f_1 + y_o/D_1)/\lambda_a} dy_1 \right] dy_o. \tag{A1}$$

The y_1 integration will be performed first. If $y_1^2 \gg 2 D_1/k$ for $|y_1| \geqslant a$, then $e^{iky_1^2/2D_1}$ oscillates rapidly when y_1 is at least the same order of magnitude as the lens half-width a. Consequently there will be little contribution to the integral from the region $y_1 \geqslant a$ due to cancellations in the integrand caused by oscillation of this exponential function [4]. The quantity $e^{-2\pi iy_1(y_2/f_1+y_o/D_1)/\lambda_a}$ will vary much more slowly than $e^{iky_1^2/2D_1}$ for $y_1 \geqslant a$. These considerations allow the limits of the y_1 integration to be extended to $\pm\infty$.

If the quantity $-(y_2/f_1 + y_o/D_1)/\lambda_a$ is denoted as $\bar{\eta}$, which has units of spatial frequency, the y_1 integration becomes [4]

$$\int_{-\infty}^{\infty} e^{iky_1^2/2D_1} e^{2\pi iy_1\bar{\eta}} dy_1 \propto e^{-\pi i\lambda_a D_1\bar{\eta}^2}. \tag{A2}$$

When the quantity $e^{-\pi i\lambda_a D_1\bar{\eta}^2}$ is substituted into (A1), quadratic phase factors involving y_o^2 cancel, leaving

$$\phi_o(y_2) \propto e^{iky_2^2(1-D_1/f_1)/2f_1} e^{ik(D_1+f_1)} \int_{-\infty}^{\infty} \psi_o(y_o) e^{-2\pi iy_o y_2/\lambda_a f_1} dy_o. \tag{A3}$$

The integral is the Fourier transform $\bar{\psi}_o(\eta)$ for $\eta = y_2/\lambda_a f_1$, so that (A3) becomes (14). Hence the field in the back focal plane of a lens is proportional to the Fourier transform of the object distribution. Note the constant phase factor, which gives the phase change of a plane wave traveling from the y_o to the y_2 plane.

DERIVATION OF (19)

The calculations leading to (19), the field in the image plane, will also be performed. The field $\phi_o^-(y_3)$ incident on L_2 is (see (15))

$$\phi_o^-(y_3) \propto e^{ikf_2} \int_{-\infty}^{\infty} e^{ik(y_3-y_2)^2/2f_2} \, \text{Rect} \, (y_2/a') \, \phi_o(y_2) \, dy_2, \tag{A4}$$

and $\phi_o^+(y_3)$ is the field emerging from acoustic lens L_2:

$$\phi_o^+(y_3) = \text{Rect} \, (y_3/a) \, \phi_o^-(y_3) \, e^{-iky_3^2/2f_2}. \tag{A5}$$

The lens has a width $2a$ and focal length f_2. The field in the y_4 plane is, from (17),

$$\phi_o(y_4) \propto e^{ikD_2} \int_{-\infty}^{\infty} e^{ik(y_4-y_3)^2/2D_2} \, \phi_o^+(y_3) \, dy_3. \tag{A6}$$

Combining the preceding equations gives, with $L = D_1 + f_1 + f_2 + D_2$,

$$\phi_o(y_4) \propto e^{ikL} \left\{ e^{iky_4^2/2D_2} \int_{y_2=-\infty}^{\infty} \left[\int_{y_3=-a}^{a} e^{iky_3^2/2D_2} \, e^{-2\pi i y_3(y_4/\lambda D_2 + y_2/\lambda f_2)} \, dy_3 \right] \right.$$

$$\left. \times \bar{\psi}_o(\eta) \, \text{Rect} \, (y_2/a') \, e^{iky_2^2(1/f_1+1/f_2-D_1/f_1^2)/2} \, dy_2 \right\}. \tag{A7}$$

The y_3 integration will be performed first. Since $ka^2/2D_1 \gg 1$, the limits of integration can be extended to $\pm\infty$. Let $\eta_1 = y_4/\lambda D_2 + y_2/\lambda f_2$, so that [4]

$$\int_{-\infty}^{\infty} e^{iky_3^2/2D_2} \, e^{-2\pi i y_3 \eta_1} \, dy_3 \propto e^{-\pi i \eta_1^2 \lambda_a D_2}. \tag{A8}$$

When this expression is substituted into (A7), quadratic phase factors involving y_4^2 will cancel. Furthermore quadratic phase factors in y_2^2 will cancel if

$$1/f_1 + 1/f_2 = D_1/f_1^2 + D_2/f_2^2. \tag{A9}$$

If the above is satisfied, then (A7) reduces to

$$\phi_o(y_4) \propto e^{ikL} \int_{-\infty}^{\infty} \text{Rect} \, (y_2/a') \, \bar{\psi}_o(\eta) \, e^{-2\pi i y_2 y_4/\lambda f_2} \, dy_2. \tag{A10}$$

Since

$$\bar{\psi}_o(\eta) = \int_{-\infty}^{\infty} \psi_o(y_o) \, e^{-2\pi i y_o y_2/\lambda f_1} \, dy_o, \tag{A11}$$

then

$$\phi_o(y_4) \propto e^{ikL} \int_{-\infty}^{\infty} \psi_o(y_o) \left[\int_{-\infty}^{\infty} \text{Rect} \, (y_2/a') \, e^{-2\pi i y_2(y_o/\lambda f_1 + y_4/\lambda f_2)} \, dy_2 \right] dy_o. \tag{A12}$$

The y_2 integration is performed first. Let $\eta_2 = y_o/\lambda f_1 + y_4/\lambda f_2$; then

$$\int_{-\infty}^{\infty} \text{Rect} \, (y_2/a') \, e^{-2\pi i \eta_2 y_2} \, dy_2 \propto \text{sinc} \, (2\pi \eta_2 a'). \tag{A13}$$

Substitution of (A13) into (A12) gives

$$\phi_o(y_4) \propto e^{ikL} \int_{-\infty}^{\infty} \psi_o(y_o) \, \text{sinc} \left[\frac{2\pi a'}{\lambda} \left(\frac{y_o}{f_1} + \frac{y_4}{f_2} \right) \right] dy_o. \tag{A14}$$

Let $\bar{y}_o = -y_o \, f_2/f_1$, so that (A14) can be rewritten in the form of a convolution integral

$$\phi_o(y_4) \propto e^{ikL}(f_1/f_2) \int_{-\infty}^{\infty} \psi_o \left(\frac{-\bar{y}_o \, f_1}{f_2} \right) \, \text{sinc} \left[\frac{2\pi a'}{\lambda f_2} (y_4 - \bar{y}_o) \right] d\bar{y}_o, \tag{A15}$$

which is the same as (19).

If (A9) is not satisfied, then quadratic phase factors would appear in (A15). These factors would cause a phase distortion: the system would be out of focus. This justifies the use of the terminology "focusing condition" in referring to (A9) and (18).

Appendix B

Bounded Acoustic Beam Incident on a Finite Membrane

In the analysis of section 3, (70) shows that an infinite plane wave incident on the membrane separating the imaging fluid from the object tank fluid gives rise to a traveling wave on the membrane. Since the minitank is finite, such a wave would reach the minitank wall and be reflected, a circumstance not considered in section 3. Hence it is necessary to consider the effect of the finite size of the minitank to see if it causes any corrections to be made to the transmission and reflection coefficients $\bar{T}_{12}$ and $\bar{R}_{21}$.

The finite size of the acoustic lens system limits the size of the incident beam in the focused acoustic image; also, the reference transducer emits a collimated beam of finite size. Hence the problem to be considered is illustrated in Fig. B1, where a beam of width r_b falls on a membrane of width R_t at an angle θ_1.
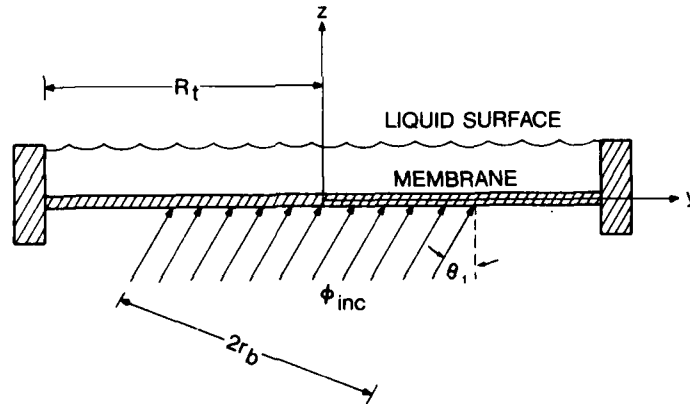

Fig. B1 — Bounded beam incident on a finite minitank

For simplicity the beam striking the membrane will be assumed symmetric about the center of the membrane. The problem is assumed two-dimensional, with variations in only the y and z directions allowed. Furthermore the fluids above and below the membrane are assumed identical and extend to infinity in the $-z$ direction. To conform with the analysis of section 3, the membrane is subjected to uniform tension and is thin enough so that in-plane stretching forces are much larger than flexural forces. The membrane is initially at rest.

The equations governing the behavior of the system consisting of membrane plus fluid are the wave equation

$$\nabla^2 \phi = \left(\frac{1}{c^2}\right) \ddot{\phi} \tag{B1}$$

for the fluid and the equation of motion

$$-T \frac{\partial^2 w}{\partial y^2} + 2\rho_M b \ddot{w} = -\rho_0 (\dot{\phi}_l - \dot{\phi}_u) \Big|_{z=0} \qquad \text{(B2)}$$

for the membrane. Here ϕ_u is the velocity potential for the upper ($z > 0$) fluid, ϕ_l is the velocity potential for the lower ($z < 0$) fluid, and ρ_0 is the equilibrium density of the fluid. The boundary condition at the membrane is

$$\dot{w} = \frac{\partial \phi_u}{\partial z} = \frac{\partial \phi_l}{\partial z}, \qquad \text{(B3)}$$

and the boundary condition at $y = \pm R_l$ is

$$w = 0. \qquad \text{(B4)}$$

In the lower fluid let

$$\phi_l = \phi_{inc} + \phi_{refl} + \phi_{lr}, \qquad \text{(B5)}$$

where the velocity potentials in the incident and specularly reflected acoustic beams are ϕ_{inc} and ϕ_{refl} respectively, with ϕ_{refl} satisfying the boundary condition

$$\frac{\partial \phi_{refl}}{\partial z} = -\frac{\partial \phi_{inc}}{\partial z} \qquad \text{(B6)}$$

at the membrane. ϕ_{lr} is the velocity potential in the acoustic field generated by motion of the membrane and satisfies

$$\frac{\partial \phi_{lr}}{\partial z} = \dot{w} \qquad \text{(B7)}$$

at the membrane. Taking

$$\phi_{inc} = A \; e^{2\pi i \eta_o y} \; e^{2\pi i \zeta_o z} \; e^{-i\omega_a t} \; \text{Rect} \left[\frac{\hat{t} - z/c}{\Delta t} \right] \text{Rect} \left[\frac{y \cos \theta_1 - z \sin \theta_1}{r_b} \right] \qquad \text{(B8)}$$

gives

$$\phi_{refl} = A \; e^{2\pi i \eta_o y} \; e^{-2\pi i \zeta_o z} \; e^{-i\omega_a t} \; \text{Rect} \left[\frac{\hat{t} + z/c}{\Delta t} \right] \text{Rect} \left[\frac{y \cos \theta_1 + z \sin \theta_1}{r_b} \right] \qquad \text{(B9)}$$

to satisfy the boundary condition (B6) and the scalar wave equation. Small angles of incidence are assumed.

Let the membrane displacement w be expanded in a series of the membrane eigenfunctions:

$$w = \int_{-\infty}^{\infty} \left[\sum_n \overline{W}_n(\omega) \cos K_n y \right] e^{-i\omega t} \, d\omega. \qquad \text{(B10)}$$

where $K_n = (2n + 1)\pi/2R_l$, so that $w = 0$ at $y = \pm R_l$. Note that the $\cos K_n y$ form an orthogonal set:

$$\frac{1}{R_l} \int_{-R_l}^{R_l} \cos K_n y \; \cos K_q y \; dy = 0, \quad n \neq q \qquad \text{(B11a)}$$

$$= 1, \quad n = q. \qquad \text{(B11b)}$$

The natural frequencies of free vibration of the membrane (with no fluid present) are

$$\omega_n^2 = \frac{TK_n^2}{2\rho_M b}.$$ (B12)

To satisfy the wave equation and the boundary condition (B3), let

$$\phi_u = \int_{-\infty}^{\infty} \left[\sum_n \overline{\Phi}_n(\omega) \cos K_n y \, e^{2\pi i \zeta_n z} \right] e^{-i\omega t} \, d\omega$$ (B13)

and

$$\phi_{lr} = -\int_{-\infty}^{\infty} \left[\sum_n \overline{\Phi}_n(\omega) \cos K_n y \, e^{-2\pi i \zeta_n z} \right] e^{-i\omega t} \, d\omega,$$ (B14)

where $2\pi\zeta_n = \sqrt{(\omega/c)^2 - K_n^2}$. Also, from boundary condition (B7),

$$\overline{\Phi}_n(\omega) = \frac{-\omega \, \overline{W}_n(\omega)}{2\pi \, \zeta_n},$$ (B15)

where the orthogonality property (B11) has been used.

The net pressure acting on the membrane is

$$-\rho_o \left(\dot{\phi}_{inc} + \dot{\phi}_{refl} + \dot{\phi}_{lr} - \dot{\phi}_u \right) \big|_{z=0}.$$

Expanding $\phi_{inc} + \phi_{refl}$ at $z = 0$ gives

$$2Ae^{i(2\pi\eta_o y - \omega_a t)} \text{ Rect } (y/y_b) \text{ Rect } (\hat{t}/\Delta t)$$

$$\propto 2A \left\{ \int_{-\infty}^{\infty} \text{sinc}((\omega - \omega_a)\Delta t) \, e^{i(\omega - \omega_a)\Delta t} \, e^{-i\omega t} \, d\omega \right\}$$

$$\times \sum_n \left\{ \text{sinc } ((K_n - 2\pi\eta_o)y_b) + \text{sinc } ((K_n + 2\pi\eta_o)y_b) \right\} \cos K_n y.$$ (B16)

Here $y_b = r_b/\cos\theta_1$. For simplicity the notation sinc $(K_n \pm 2\pi\eta_o)y_b \equiv$ sinc $(K_n - 2\pi\eta_o)y_b +$ sinc $(K_n + 2\pi\eta_o)y_b$ will be introduced. Using this notation plus (B10), (B13), (B14), and (B15) in the equation of the motion of the membrane leads to

$$\overline{W}_n(\omega) = \frac{-8\Delta t \, y_b \pi \zeta_n A \omega \rho_0 \, [\text{sinc } (\omega - \omega_a)\Delta t] \, e^{i(\omega - \omega_a)\Delta t} \, \text{sinc } (K_n \pm 2\pi\eta_o)y_b}{[-2\rho_M b(-\omega^2 + \omega_n^2)2\pi\zeta_n + 2i\omega^2\rho_0]R_t}.$$ (B17)

This fairly complicated expression can be simplified. Consider the term sinc $(\omega - \omega_a)\Delta t$ for typical values $\omega_a \sim O(10^7 \text{ rad/s})$ and $\Delta t \sim O(10^{-4} \text{ s})$. Since $\omega_a \gg 1/\Delta t$, then sinc $(\omega - \omega_a)\Delta t \rightarrow 0$ unless $\omega \sim 0(\omega_a)$ in (B17). Likewise, considering sinc $(K_n \pm 2\pi\eta_o)y_b$ for $r_b \sim O(20 \text{ cm})$, $\cos\theta_1 \sim O(1)$, and $c \sim O(1 \text{ km/s})$, it is seen that $K_n \cong 2\pi\eta_o$. Hence $2\pi\zeta_n = \sqrt{(\omega_a/c)^2 - (2\pi\eta_o)^2} = 2\pi\zeta_0$. Furthermore for $K_n \sim O(2\pi\eta_o)$ the natural frequencies of the membrane are much less than the operating frequency ω_a of the transducers; that is, $TK_n^2/(2\rho_M b) \ll \omega_a^2$. Here typical values of

$$T \sim O(10 \text{ N/cm}),$$

$$\rho_M \sim O(1 \text{ g/cm}^3),$$

and

$$b \sim O(10^{-3} \text{ cm})$$

have been used. Using these results gives the simpler expression

$$\overline{W}_n(\omega) = \frac{-8\Delta t \; y_b \; \pi i \zeta_0 A \omega \rho_0 \; [\text{sinc} \; (\omega - \omega_a) \Delta t] e^{i(\omega - \omega_a)\Delta t} \; \text{sinc} \; (K_n \pm 2\pi \eta_o) y_b}{[2\rho_M b \; (2\pi\zeta_o\omega^2) + 2i\omega^2\rho_o] R_t}. \quad (B18)$$

This can be given a physical interpretation. Recall that the incident pressure P_{inc} equals $-\rho_0\phi_{inc}$, which gives

$$\overline{P}_{inc}(K_n, \omega) = 2\Delta t \; y_b \; i\omega\rho_0 A \; [\text{sinc} \; (\omega - \omega_a)\Delta t] \; e^{i(\omega - \omega_a)\Delta t} \; [\text{sinc} \; (K_n \pm 2\pi\eta_o)y_b]/R_t. \quad (B19)$$

Furthermore the velocity of the membrane is

$$\dot{w} = \int_{-\infty}^{\infty} \left[\sum_n -i\omega \overline{W}_n(\omega) \cos K_n y \right] e^{-i\omega t} \, d\omega, \quad (B20)$$

where from (B18) and (B-19)

$$-i\omega \overline{W}_n(\omega) = \frac{2\overline{P}_{inc}(K_n, \; \omega)}{-i\omega(2\rho_M b) + 2\rho_0 c/\cos \theta_1} \quad (B21)$$

for $2\pi\zeta_o = (\omega_a/c) \cos \theta_1$. Note that $-i\omega \, \overline{W}_n(\omega)$ is the (Fourier-transformed) generalized velocity associated with the nth mode of motion of the membrane. Consequently the denominator in (B21) is the impedance $\overline{Z}_n(\omega)$ presented to the nth mode by the membrane inertia force and also by a resisitive force due to the fluid. Writing

$$\overline{Z}_n(\omega) = -i\omega(2\rho_M b) + 2\rho_0 c/\cos \theta_1 \quad (B22)$$

shows that the reactive component is due to membrane inertia. The resistive component damps membrane motion because sound is radiated to infinity. The quantity $2\rho_0 c/\cos \theta_1$ is analogous to the characteristic impedance presented by an acoustic fluid to passage of a plane wave. The factor $1/\cos \theta_1$ appears because the plane wave propagates at an angle θ_1 to the direction of membrane velocity (z direction).

Recall that the membrane displacement is given by (B10), repeated here for convenience:

$$w = \int_{-\infty}^{\infty} \left[\sum_n \overline{W}_n(\omega) \cos K_n y \right] e^{-i\omega t} \, d\omega. \quad (B10)$$

The summation will be performed first, followed by the integration. From (B18),

$$\sum_n \overline{W}_n(\omega) \cos K_n y \propto \frac{2y_b}{R_t} \sum_n \left\{ [\text{sinc} \; (K_n \pm 2\pi\eta_o)y_b] \cos K_n y \right\}, \quad (B23)$$

where the right-hand side is recognized as the series expansion for $e^{2\pi i \eta_o y}$ Rect (y/y_b). Consequently

$$w = A \; e^{2\pi i \eta_o y} \text{Rect} \; (y/y_b)$$

$$\times \int_{-\infty}^{\infty} \frac{-4\Delta t \; \pi i \zeta_o \omega \rho_0 \; [\text{sinc} \; (\omega - \omega_a) \; \Delta t] \; e^{i(\omega - \omega_a)\Delta t} \; e^{-i\omega t} \, d\omega}{2\pi\zeta_o(2\rho_M b) \; \omega^2 + 2i\omega^2\rho_0}. \quad (B24)$$

Note that the response of the membrane is in the form of traveling waves of finite lateral extent, due to the factor Rect (y/y_b). Hence for $y_b < R_l$ there will be no reflection of these waves from the minitank walls.

Furthermore, since $w \propto$ Rect (y/y_b), the boundary conditions $w = 0$ at $y = \pm R_l$ are automatically satisfied, and it is possible to express w as the double Fourier integral

$$w = \int\!\!\int_{-\infty}^{\infty} \bar{\bar{w}}(\eta, \omega) \, e^{2\pi i \eta y} e^{-i\omega t} \, d\eta d\omega, \tag{B25}$$

where

$$\bar{\bar{w}}(\eta, \omega) = \frac{-8\Delta t \, y_b \pi i \zeta_o A \omega \rho_0 \, [\text{sinc } (\omega - \omega_a)\Delta t] \, e^{i(\omega - \omega_a)\Delta t} \, \text{sinc } 2\pi (\eta - \eta_o)y_b}{2\rho_M b (2\pi \zeta_o)\omega^2 + 2i\omega^2 \rho_0}. \tag{B26}$$

In like fashion let the velocity potential ϕ_u in the upper fluid be given by

$$\phi_u = \int\!\!\int_{-\infty}^{\infty} \bar{\bar{\phi}}_u(\eta, \omega) \, e^{2\pi i \eta y} e^{2\pi i \zeta z} e^{-i\omega t} \, d\eta d\omega. \tag{B27}$$

The boundary condition $\phi_{u,z} = \dot{w}$ at $z = 0$ gives

$$\bar{\bar{\phi}}_u = \frac{4\Delta t \, y_b i \omega^2 \rho_0 A \, [\text{sinc } (\omega - \omega_a)\Delta t] \, e^{i(\omega - \omega_a)\Delta t} \, \text{sinc } 2\pi (\eta - \eta_o)y_b}{[2i\omega^2 \rho_0 + 2\pi \zeta_o (2\rho_M b) \, \omega^2]}. \tag{B28}$$

For reasons of image fidelity, it is desirable that $\bar{\bar{\phi}}_u \propto \bar{\bar{\phi}}_{inc}$; then ϕ_u will have the same form as ϕ_{inc} but with a constant change in amplitude and phase. The result (B28) will now be applied to determine whether this can be achieved with values of ω_a, ρ_M, etc. used in typical levitation systems.

Consider the case of a membrane of density 2 g/cm^3 and thickness $2b = 2.5(10^{-3})$ cm submerged in water and insonified by an acoustic beam having a frequency of 1 MHz. Then $\rho_0/\rho_M \gg 2\pi \zeta_o b$, so that

$$\bar{\bar{\phi}}_u \cong 2A\Delta t \, y_b \, [\text{sinc } (\omega - \omega_a) \, \Delta t] \, e^{i(\omega - \omega_a)\Delta t} \, \text{sinc } 2\pi (\eta - \eta_o)y_b. \tag{B29}$$

When the incident beam is expressed as

$$\phi_{inc} = \int\!\!\int_{\infty}^{-\infty} \bar{\bar{\phi}}_{inc}(\eta, \omega) \, e^{2\pi i \eta y} e^{2\pi i \zeta z} e^{-i\omega t} \, d\eta d\omega, \tag{B30}$$

it is discovered that $\bar{\bar{\phi}}_{inc}$ is also given by (B29). Consequently ϕ_u is just ϕ_{inc} continued into the upper $(z > 0)$ fluid; the transmission coefficient is now unity. This is be expected, since any effect of the membrane on ϕ_{inc} is insignificant when $\rho_0 \gg 2\pi \zeta_o \rho_M b$.

Suppose the acoustic frequency is increased to 5 MHz; then the inequality no longer holds for the values of ρ_0, ρ_M, etc. used previously. Since

$$\bar{\bar{\phi}}_{inc} = 2A\Delta t \, y_b \, [\text{sinc } (\omega - \omega_a) \, \Delta t] \, e^{i(\omega - \omega_a)\Delta t} \, \text{sinc } 2\pi (\eta - \eta_o)y_b, \tag{B31}$$

(B28) shows that the transmission coefficient $\bar{T}_{12}(\eta)$, defined as the ratio $\bar{\bar{\phi}}_u / \bar{\bar{\phi}}_{inc}$, becomes

$$\bar{T}_{12}(\eta) = \frac{2\rho_0}{2\rho_0 - 4\pi i \rho_M b \zeta}, \tag{B32}$$

which is just the form assumed by (73) for $\rho_u = \rho_l$ and $\lambda_u = \lambda_l$.

98

If the membrane is not to distort the acoustic field, then ϕ_u must be a bounded beam traveling the same direction as ϕ_{inc} when the imaging and object-tank fluids are identical. Hence $\bar{T}_{12}(\eta)$ must be essentially constant over the bandwidth of spatial frequencies corresonding to the dominant frequencies in the spectrum of $\bar{\phi}_{inc}$. The only variable in $\bar{T}_{12}(\eta)$ is $2\pi\zeta$, so it is necessary for ζ to be constant in this region. Now $\bar{\phi}_{inc} \propto$ sinc $2\pi(\eta - \eta_o)y_b$, which has its dominant spatial frequencies in the region $-y_b/2 + \eta_o \leqslant \eta \leqslant y_b/2 + \eta_o$. Then $\eta = \eta_o + \Delta\eta$, where $\Delta\eta \sim O(y_b/2)$. Recall that for a quasimonochromatic pulse

$$2\pi\zeta \cong \sqrt{(\omega_a/c)^2 - 2\pi\eta^2} \tag{B33}$$

or

$$2\pi\zeta \cong \sqrt{(\omega_a/c)^2 \cos^2\theta_1 - 2\pi\eta\Delta\eta - (\Delta\eta)^2}. \tag{B34}$$

Obviously, for $2\pi\eta\Delta\eta + (\Delta\eta)^2 << (\omega_a/c)^2 \cos^2\theta_1$, $2\pi\zeta$ is essentially constant. At (or near) normal incidence this requires $(1/y_b)^2 << (\omega_a/c)^2$. For a typical beamwidth y_b of 5 cm in water at 5 MHz, the inequality is easily satisfied. The utility of this inequality is that it acts as a lower bound on the beamwidth.

The velocity potential in the upper fluid is now calculated from

$$\phi_u = \int\!\!\!\int_{-\infty}^{\infty} \bar{T}_{12}(\eta) \, \bar{\phi}_{inc}(\eta, \omega) \, e^{2\pi i\eta y} \, e^{2\pi i\zeta z} \, e^{-i\omega t} \, d\eta d\omega. \tag{B35}$$

Since $\bar{T}_{12}(\eta)$ is constant, ϕ_u will just be ϕ_{inc} continued into the region $z = 0$ but with a constant change in amplitude and phase.

Appendix C

Proof that $\Delta \bar{P}_r \leq O(\bar{P}_r)$

In reducing equation (208) to the simpler form (166), it has been assumed that

$$\Delta \bar{P}_r \leq O(\bar{P}_r).$$

$\Delta \bar{P}_r(\eta)$ represents one spatial frequency component of ΔP_r, with ΔP_r being the radiation pressure at the membrane. P_r is the radiation pressure at the surface. The above relationship will now be verified for $|\rho_u - \rho_l| \sim O(\rho_u)$.

From (90) and continuity of velocity in the vertical (z) direction at the membrane,

$$-\Delta P_r = (\Delta \rho <v_z^2> + <P_{l2}> - <P_{u2}>) \ \text{Rect} \ (\hat{t}/\Delta t), \tag{C1}$$

where $\Delta \rho = \rho_l - \rho_u$ $v_z = v_{1a} \cdot e_z$, P_{l2} is the second-order acoustic pressure in the object-tank fluid, and P_{u2} is the second-order acoustic pressure in the imaging fluid. From (118)

$$<P_{l2}> = \frac{c_l^2}{2\rho_l} <\rho_{l1}^2> - \frac{\rho_l}{2} <v_{l1} \cdot v_{l1}>, \tag{C2}$$

where c_l is the sound speed in the object-tank, ρ_{l1} is the first-order density perturbation in the object-tank, and v_{l1} is the first-order acoustic particle velocity in the object-tank. Use of the relations $\rho_{l1} = P_{l1}/c_l^2$ and $P_{l1} = -\rho_l \dot{\phi}_{l1}$ and of similar relations for ρ_{u1}, P_{u2}, etc. leads to

$$-\Delta P_r = \frac{\Delta \rho}{2} <v_z^2> - \frac{1}{2}\rho_l <v_{ly}^2> + \frac{1}{2} \rho_u <v_{uy}^2>$$

$$- \frac{\rho_u}{2c_u^2} <\dot{\phi}_{u1}^2> + \frac{\rho_l}{2c_l^2} <\dot{\phi}_{l1}^2>, \tag{C3}$$

where $v_{ly} = v_{l1} \cdot e_y$, etc.

Suppose an acoustic wave is incident on the membrane, as shown in Fig 5. Due to reflection from the membrane as well as multiple internal reflections in the minitank, the velocity potential ϕ_{l1} in the object-tank is

$$\phi_{l1} = \phi_{inc} + \left[\bar{R}_{12} - \bar{T}_{12} \bar{T}_{21} e^{4\pi i \zeta_u d} \sum_{n=0}^{\infty} (-\bar{R}_{21} e^{4\pi i \zeta_u d})^n \right] e^{-2\pi i \zeta z} \phi_{inc} \Big|_{z=0}. \tag{C4}$$

Here $\phi_{inc} = Ae^{2\pi i(\eta y + \zeta z)}$ is the velocity potential in the incident wave, and the membrane is at $z = 0$. The factor Rect $(\hat{t}/\Delta t)$ has been omitted for simplicity. $\bar{R}_{21}$ is the reflection coefficient for a wave incident on the membrane from the minitank side (Fig. 9); $\bar{T}_{12}$ is the transmission coefficient for the case of a wave incident on the membrane from the object-tank side. These were calculated in section 3.2. $\bar{T}_{21}$ can be obtained by interchanging the roles of ρ_u and ρ_l, c_u and c_l, etc. in (73). It is assumed that $w \ll \lambda_a$.

Since

$$\sum_{n=0}^{\infty} (-\bar{R}_{21})^n e^{4\pi i \zeta_u n d} = \frac{1}{1 + \bar{R}_{21} e^{4\pi i \zeta_u d}} \tag{C5}$$

and $v_z = \phi_{I1,z}$ at the membrane,

$$v_z = 2\pi i \zeta \phi_{inc}\big|_{z=0}\left[1 - \bar{R}_{12} + \left(\frac{\bar{T}_{12}\bar{T}_{21}e^{4\pi i\zeta_u d}}{1 + \bar{R}_{21}e^{4\pi i\zeta_u d}}\right)\right]. \tag{C6}$$

It is easy to show that the right-hand side is of the order of $2\pi\zeta\phi_{inc}\big|_{z=0}$. Then the term $\Delta\rho\langle v_z^2\rangle$ in (C3) is of the order of $\rho_u(2\pi\zeta\phi_{inc})^2$, if $\Delta\rho \sim O(\rho_u)$, as it is for a water-Freon E-5 interface. This is to be compared with the order of magnitude of P_r, the radiation pressure at the liquid surface. Recall that $P_r = (1/2)\,\rho_u\langle v_{1a} \cdot e_z^2\rangle$; from (58) and (59)

$$v_{1a} \cdot e_z = 4\pi i\zeta_u \bar{T}_{12}\phi_{inc}(z = 0)e^{2\pi i\zeta_u d}/(1 + \bar{R}_{21}e^{4\pi i\zeta_u d}), \tag{C7}$$

so that $\bar{P}_r \sim O[\rho_u(2\pi\zeta_u\bar{T}_{12}\phi_{inc})^2]$. For $\zeta_u \sim O(\zeta)$ and $\bar{T}_{12} \sim O(1)$ it is seen that $\bar{P}_r$ and $\Delta\rho\langle v_z^2\rangle$ are the same order of magnitude. It is desirable to have $\bar{T}_{12} \sim O(1)$ in order to transmit sound energy into the minitank.

Consider the remaining terms on the right-hand side of (C3). For example, the term $(\rho_u/c_u^2)\langle\dot{\phi}_{u1}^2\rangle$ becomes

$$\rho_u\left[(\omega_a/c_u)\,\bar{T}_{12}\left(1 - e^{4\pi i\zeta_u d}\frac{1 + \bar{R}_{21}}{1 + \bar{R}_{21}e^{4\pi i\zeta_u d}}\right)\right]^2 [\phi_{inc}\,(z = 0)]^2,$$

where multiple internal reflections in the minitank are accounted for. For moderate angles of incidence, $2\pi\zeta_u \sim O(\omega_a/c_u)$, and it is seen that the above is of the order of $\bar{P}_r$. In this fashion it can be shown that $\Delta\bar{P}_r \sim O(\bar{P}_r)$, for $\Delta\rho \sim O(\rho_u)$, $\zeta_u \sim O(\zeta)$, and $\bar{T}_{12} \sim O(1)$.

If the minitank and object-tank fluids are the same, then

$$\Delta\bar{P}_r = -\frac{\rho_u}{c_u^2}\left[\langle\dot{\phi}_{u1}^2\rangle - \langle\dot{\phi}_{I1}^2\rangle\right] = \frac{\langle P_{I1}^2\rangle - \langle P_{u1}^2\rangle}{\rho_u c_u^2}, \tag{C8}$$

since $v_{Iy} = v_{uy}$ by Snell's law. If $\bar{T}_{12} = 1$, then $\phi_{u1} = \phi_{I1}$ at the membrane and $\Delta\bar{P}_r = 0$. From (73) $\rho_u\lambda_u$ must be much greater than $4\pi\rho_M b$ for this to occur; otherwise there will be a discontinuity in first-order acoustic pressure at the membrane and $\Delta\bar{P}_r$ will not vanish. For any case of practical interest, $4\pi\rho_M b \leq O(\rho_u\lambda_u)$. Hence, even if $\Delta\bar{P}_r \neq 0$, $\Delta\bar{P}_r$ will at most be of the order of $\bar{P}_r$.

If $|\Delta\rho| \gg \rho_u$, then $\Delta\bar{P}_r \gg \bar{P}_r$, since most of the incident acoustic waves are reflected at the membrane. However, this would be an exceedingly poor design of the levitation system, since most of the acoustic power would be wasted.

101

Appendix D

Response of the Liquid Surface to a Finite Pulse of Radiation Pressure

In section 5, the minitank, the reference beam, and the focused acoustic image have been assumed infinite in lateral extent. Actually, the reference transducer is of finite diameter $2r_b$, and, if the liquid surface is in the near field of the transducer, the reference beam is also of the same finite diameter. The lateral extent of the focused acoustic image is limited by the field of view of the acoustic lens system. If the acoustic object to be imaged is placed in the near field of the object transducer, only an area of radius r_a of the object will be insonified. Due to magnification by the acoustic lenses, the focused image occupies an area of radius $(f_2/f_1)r_a$ on the liquid surface. To record the entire field of view in the image, it is necessary that $r_b \geqslant (f_2/f_1)r_a$.

Hence it is of interest to consider the case of a bounded pulse of radiation pressure incident on the liquid surface of a finite minitank of radius R_t. It was shown in section 5.6 that the response of the infinite liquid surface can be calculated, for $\hat{\eta} \geq O(10 \text{ rad/cm})$, on the assumption that the membrane at the minitank bottom is rigid. It will be assumed that this is true also for the finite minitank. Consider the response of the liquid surface to a bounded pulse of radiation pressure having spatial frequency $\hat{\eta}$:

$$P_r(y, t) = P \, e^{i\hat{\eta}y} \, \text{Rect}(y/y_b) \, \text{Rect}(\hat{t}/\Delta t), \qquad (D1)$$

where for simplicity a two-dimensional problem is assumed.

To calculate this response, it is necessary to solve

$$\nabla^2 \phi_s = 0 \qquad (D2)$$

in the minitank for the velocity potential ϕ_s. Viscosity is neglected for simplicity. The boundary condition which governs the motion of the liquid surface will be

$$-\rho_u \dot{\phi}_s - \rho_u g h_s + \gamma \frac{\partial^2 h_s}{\partial y^2} = -P_r, \qquad z' = d. \qquad (D3)$$

If the minitank walls are assumed to be rigid, the normal velocity must vanish at $y = \pm R_t$:

$$\frac{\partial \phi_s}{\partial y} = 0, \qquad y = \pm R_t. \qquad (D4)$$

At the bottom of the minitank

$$\frac{\partial \phi_s}{\partial z'} = 0, \qquad z' = 0. \qquad (D5)$$

It is assumed that P_r is centered about the z' axis. Let ϕ_s be expanded in terms of the symmetric eigenfunctions ϕ_n:

$$\phi_s(y, z', t) = \sum_n A_n(t)\phi_n(y, z'). \qquad (D6)$$

The ϕ_n are solutions to $\nabla^2\phi_n = 0$ that satisfy the rigid-wall boundary conditions and are the normal modes of free vibration for the fluid in the minitank. It is straightforward to show that

$$\phi_n = \cosh K_n z' \cos K_n y \tag{D7}$$

for $K_n = n\pi/R_t$ and $n = 0, 1, 2$, etc. In like fashion let

$$h_s = \sum_{n=0}^{\infty} h_n(t) \cos K_n y. \tag{D8}$$

Satisfying the relation $\dot{h}_s = \phi_{s,z'}$ at the liquid surface requires that

$$A_n(t) = \frac{\dot{h}_n(t)}{K_n \sinh K_n d}. \tag{D9}$$

It remains to satisfy boundary condition (D3). To do so, P_r is expanded in the series

$$P_r(y, \ z' = d, \ t) = P \left\{ 2(y_b/R_t) \sum_{n=0}^{\infty} \left[\text{sinc } (K_n + \hat{\eta}) y_b \right. \right.$$

$$\left. \left. + \text{sinc } (K_n - \hat{\eta}) y_b \right] \cos K_n x \right\} \text{Rect } (\hat{t}/\Delta t). \tag{D10}$$

Substitution of the above into (D3) and invoking orthogonality of the cos $K_n x$ leads to

$$\ddot{h}_n(t) + \left[(\rho_u g + \gamma K_n^2) \frac{K_n}{\rho_u} \tanh K_n d \right] h_n(t) = P \ (2y_b/R_t) [\text{sinc } (K_n - \hat{\eta}) y_b + \text{sinc } (K_n + \hat{\eta}) \ y_b]$$

$$\times \frac{K_n}{\rho_u} \tanh K_n d \ \text{Rect}(t/\Delta t). \tag{D11}$$

Let $\omega_n^2 = (\rho_u g + \gamma K_n^2)(K_n/\rho_u) \tanh K_n d$, where ω_n is the nth natural frequency of the fluid in the minitank. Then (D11) has the solution

$$h_n(t) = \frac{P[\text{sinc } (K_n - \hat{\eta})y_b + \text{sinc } (K_n + \hat{\eta})y_b] \ \omega_n \sin \omega_n t \oplus \text{Rect } (\hat{t}/\Delta t)}{\rho_u \ g + \gamma K_n^2}. \tag{D12}$$

Consider the behavior of sinc $((K_n - \hat{\eta})y_b)$ as a function of the eigenvalues K_n. This function is centered at $K_n = \hat{\eta}$, and becomes negligible when K_n differs by more than the order of π/y_b from $\hat{\eta}$. For a typical value of $y_b \cong 10$ cm (corresponding to a 10 cm diameter reference beam incident at an angle of $60°$), the significant values of K_n are given by $K_n = \hat{\eta} + \Delta K_n$, and $\Delta K_n \lesssim O(\pi/10)$. The quantity K_n^2 can be approximated by $\hat{\eta}^2$ with 6% error when $\hat{\eta} = 10$ rad/cm and 0.6% error when $\hat{\eta} = 100$ rad/cm.

This allows the approximation

$$\frac{\omega_n \text{ sinc } [(K_n - \hat{\eta})y_b] \sin \omega_n t}{\rho_u g + \gamma K_n^2} \cong \frac{\omega_\eta \text{ sinc } [(K_n - \hat{\eta})y_b] \sin \omega_\eta t}{\rho_u g + \gamma \hat{\eta}^2}, \tag{D13}$$

where $\omega_\eta^2 = (\rho_u g + \gamma \hat{\eta}^2)(\hat{\eta}/\rho_u) \tanh \hat{\eta} d$. Applying the same reasoning to terms in (D12) multiplied by sinc $(K_n + \hat{\eta})y_b$ and substituting into (D8) gives

103

$$h_s(y, t) = \frac{P[\omega_\eta \sin \omega_\eta t \oplus \overset{\prime}{\text{Rect}} (\hat{t}/\Delta t)] \sum_n [\text{sinc}\, (K_n - \hat{\eta})y_b + \text{sinc}\, (K_n + \hat{\eta})y_b] \cos K_n y}{\rho_u g + \gamma \hat{\eta}^2}. \qquad \text{(D14)}$$

The summation is $e^{i\hat{\eta}y}$ Rect (y/y_b), so h_s reduces to the form calculated for an unbounded pulse of radiation pressure. This occurs because $K_n = \hat{\eta}$, for $\hat{\eta} \gg (\pi/y_b)$. The fact that the wavelength λ_s of the surface levitation equals $2\pi/\hat{\eta}$ gives the requirement $\lambda_s \gg 2y_b$. As long as the insonified area of the liquid surface greatly exceeds λ_s, effects of finite lateral size are negligible. If the inequality $\lambda_s \gg 2y_b$ is not satisfied, (D8) and (D12) predict that h_s will be given by a superposition of normal modes of vibration of the liquid surface.